The Organisation of Afferent Input to the Basal Ganglia.

Maria Dalzell

New College

Supervisor: Prof. J.P. Bolam

Co-Supervisor: Dr. P. Magill

MRC Anatomical Neuropharmacology Unit

University of Oxford

Thesis submitted for the degree of Masters by Research at the University of Oxford

TRINITY TERM 2014

The Organisation of Afferent Input to the Basal Ganglia

Maria Dalzell, New College.

Thesis submitted for the degree of Masters by Research at the University of Oxford.

Trinity Term 2014.

ABSTRACT

The basal ganglia are a collection of interconnected subcortical nuclei involved in movement, association, motivation and reward processing. Two populations of neurons that play critical roles in the basal ganglia are dopaminergic neurons of the substantia nigra (SN) and neurons of the subthalamic nucleus (STN). To define the afferent input to these neurons, which ultimately controls their activity, quantitative immunocytochemical analyses of afferent synaptic terminals was carried out at the electron microscopic level in rat. Glutamatergic afferents from cortical and subcortical sources were identified using antibodies against vesicular glutamate transporters (VGluT1 and 2 respectively). In the SN, dopaminergic neurons were labelled using antibodies against tyrosine hydroxylase (TH). In the analysis of the STN, additional populations of afferent terminals were labelled using antibodies against vesicular GABA transporter (VGAT), vesicular acetylcholine transporter (VAChT) and TH. Synapses were also categorised on the basis of their membrane specializations into type-1 (putatively excitatory) and type-2 (putatively inhibitory).

In the SN, differences in the ratio of type-1 and 2 synapses were seen between two functional sub-regions (pars compacta: SNc and pars reticulata: SNr). Dopaminergic dendrites in the SNc receive equal innervation from boutons forming type-1 and 2 synapses (53% vs 47%), whereas dopaminergic dendrites in the SNr receive mainly type-2 synapses (73% vs 27%). Type-1 synaptic boutons included both VGluT1- and VGluT2-positive boutons in the SNc, meaning cortical and sub-cortical glutamatergic neurons directly innervate dopaminergic neurons of the SNc. In the SNr only VGluT2-positive boutons were detected suggesting that SNr dendrites only receive sub-cortical glutamate. However, a large proportion of boutons forming type-1 synapses were not labelled (~40% of type-1 synaptic boutons) suggesting other transmitters provide a large amount of innervation to these neurons.

In the STN type-1 and 2 synapses provided roughly equal innervation of dendrites. The boutons forming type-1 synapses were almost entirely either VGluT1- or VGluT2-positive boutons (98%) indicating that STN neurons receive input from both cortical and subcortical glutamatergic neurons. Significantly more boutons were immunolabelled with VGluT2 compared to VGluT1 (31% vs 18%), showing that subcortical sources provide the majority of glutamatergic input to STN neurons. VGAT-positive synaptic boutons were exclusively type-2 and made up ~89% of type-2 synapses, TH-positive boutons comprised only ~4% of total synapses and VAChT-positive boutons were more varied producing both type-1 and 2 synapses. Type-1 synapse forming VAChT-positive boutons comprised 4% of total synapses and type-2 synapse forming VAChT-positive boutons 6% of the total innervation. Together this totals over 100% suggesting at least two of these markers are co-localised within a subgroup of boutons.

In conclusion, this study demonstrates that both dopaminergic neurons of the SN and neurons of the STN are under the afferent synaptic control of both cortical and sub-cortical glutamatergic neurons as well as GABAergic and other populations of terminals. The quantitative analyses demonstrate differences in the innervation of the different types or sub-types of neurons that likely underlie their functional properties.

FOR MY HUSBAND STEPHEN.

WITHOUT YOUR LOVE AND SUPPORT, NONE OF THIS WOULD HAVE BEEN POSSIBLE.

Acknowledgements

I would like to thank my supervisor, Paul Bolam for his training, support and advice throughout my time in the lab. I would also like to thank my co-supervisor, Pete Magill, for his additional input and advice.

A massive thanks is also due to all the members of the lab, who have supported me in so many ways: teaching me the skills necessary to conduct my research, engaging me during interesting discussions and generally being a fantastic bunch of people to work with. Thank you for making my time in Oxford so memorable. A special mention goes to Federica for supplying friendship, wine and an ear for venting - you will be sorely missed.

I would like to thank the Medical Research Council for providing the funding for my research and attendance at conferences at home and abroad, and all the staff at the MRC anatomical neuropharmacology unit for the fantastic facilities and smooth day to day running of the unit. I am most grateful to the technicians Gareth, Chad, Liz and Lisa who have supported me and my work and kept the lab stocked up and in one piece.

Finally, I thank my friends and family, in Oxford and beyond. You have kept me sane on a long and difficult journey and I will always remember it with fondness and a smile. To the world's best housemate Puck (and Susie): thank you for the chocolate, wine and laughter. House sharing turned to true friendship and you shall always be part of my life (sorry about that…). To Eleanor: sharing the experience of Oxford with you has been a pleasure; I can't wait for our next adventure. To my rowing crews, new college and blue: thank you for the distraction and for teaching me to push harder toward my goals. And finally, to my husband, Stephen, your love and support are unending and I can never thank you enough – but I will spend the rest of my life trying.

TABLE OF CONTENTS

CHAPTER ONE

GENERAL INTRODUCTION

1.1. Anatomical Organisation of the Basal Ganglia

1.1.1. Overview of the basal ganglia 2

1.1.2. Striatum 7

1.1.3. Globus pallidus external segment (GPe) 14

1.1.4. Subthalamic nucleus (STN) 18

1.1.5. Output nuclei 18

1.2. Substantia Nigra and Dopamine

1.2.1. Anatomy of the substantia nigra (SN) 21

1.2.2. The function of dopamine in the basal ganglia 24

1.2.3. Dopamine and movement disorders 25

1.2.4. Dopamine and associative/limbic disorders 27

1.3. The Subthalamic Nucleus

1.3.1. Anatomy of subthalamic nucleus (STN) 28

1.3.2. The role of the STN in basal ganglia information processing 30

1.4. Glutamate vesicular transporters 34

1.5. Aims of the Thesis 37

CHAPTER TWO

INNERVATION OF DOPAMINE NEURONS WITHIN THE SUBSTANTIA NIGRA

2.1. Introduction 39

2.2. Materials and Methods

2.2.1. Animals 41

2.2.2. Tissue preparation 41

2.2.3. Double label immunohistochemistry 41

2.2.4. Single-immunolabelling 44

2.2.5. Electron microscopic analysis 44

2.2.6. Statistical analysis 45

2.3. Results

2.3.1. Distribution of immunolabelling at the light microscopic level 46

2.3.2. Immunolabelling in the electron microscope 47

2.3.3. TH-immunopositive structures within the SN 51

2.3.4. Glutamatergic inputs to TH-immunopositive structures in the SNc 52

2.3.5. Glutamatergic inputs to TH-immunopositive structures in the SNr 60

2.3.6. Statistical analyses 62

2.4. Discussion

2.4.1. Summary of results 63

2.4.2. Comparisons to previous studies 64

2.4.3. Functional significance of glutamate in the SNc 68

CHAPTER THREE

INNERVATION OF THE SUBTHALAMIC NUCLEUS

3.1. Introduction 73

3.2. Materials and Methods

3.2.1. Animals 75

3.2.2. Tissue preparation 75

3.2.3. Immunohistochemistry 75

3.2.4. Controls for immunolabelling 77

3.2.5. Electron microscopic analysis 78

3.2.6. Statistical analysis 79

3.3. Results

3.3.1. Light microscopic observations 80

3.3.2. Synapses formed by VGluT1-, VGluT2- and VGAT-positive boutons in the STN 81

3.3.3. Synapses formed by VAChT- and TH-positive boutons in the STN 90

3.3.4. Morphological characteristics of VGluT1- and VGluT2-positive synaptic boutons 94

3.3.5. Morphological characteristics of VGAT-positive synaptic boutons 100

3.3.6. Morphological characteristics of TH- and VAChT-positive synaptic boutons 100

3.4. Discussion

3.4.1. Summary of results 108

3.4.2. Dopamine and acetylcholine release in the STN 109

3.4.3. Glutamatergic control of STN firing 110

3.4.4. Deep brain stimulation of the STN 112

3.4.5. Conclusions 114

CHAPTER FOUR

GENERAL DISCUSSION

4.1. Summary and Conclusions

4.3.1. Synaptic weight 117

4.3.1. Chapter two: innervation of dopamine neurons within the substantia nigra 119

4.3.2. Chapter three: innervation of the subthalamic nucleus 120

4.3.3. Conclusions of the thesis 121

4.2. Technical considerations 124

4.3. Future Directions

4.3.1. Elucidating the source of type-1 synaptic boutons in the SNc 126

4.3.2. Differences in afferent input between dopamine neurons 127

4.3.3. Studying the input/output profile of non-dopaminergic SNc neurons 127

4.3.4. Defining the anatomical nature of STN neurons 128

4.3.5. Determining the source of ACh in STN and any co-localisation of transmitters 128

4.3.6. The electrophysiological response to individual afferent stimulation 129

4.4. Final statement 129

Bibliography 131

LIST OF FIGURES

Chapter 1: General Introduction

1.1. Coronal view of the human brain, showing the basal ganglia and related nuclei 3

1.2. Diagram showing a coronal view of the human brain, showing the basal ganglia 4

1.3. A simplified flow diagram showing the main connections of the basal ganglia 5

1.4. A revised circuit diagram showing the GPe as the main integrative hub of the basal ganglia 17

Chapter 2: Innervation of Dopamine Neurons within the Substantia Nigra

2.1. A light micrograph showing the area of substantia nigra used in analysis 48

2.2. Examples of conjugated immunogold labelling 49

2.3. Micrographs showing DAB immunolabelling 50

2.4. Examples of types of synapses formed with a TH-immunopositive dendrite 54

2.5. Glutamatergic synapses with TH-immunopositive dendrites 55

2.6. Summary of the proportion of immunolabelled synaptic boutons 56

2.7. A more complete diagram of basal ganglia circuitry 66

2.8. Comparison of current data to published work 67

2.9. Cortical information flow though the basal ganglia 70

Chapter 3: Innervation of the Subthalamic Nucleus

3.1. The location of the sub-region of subthalamic nucleus used in this experiment 82

3.2. Examples of DAB immunolabelling 83

3.3. Examples of types of identified synapses 84

3.4. Micrographs showing synaptic boutons providing cortical and subcortical glutamatergic innervation of the STN 85

3.5. Plot of the percentage of synaptic boutons labelled by each antibody 88

3.6. Micrograph showing inhibitory input to STN dendrites 89

3.7. Micrographs showing TH- and VAChT-immunopositive terminals in the STN 91

3.8. Micrograph showing the difficulty of classifying synapses formed by TH-positive boutons in single sections 92

3.9. Percentage of immunopositive boutons forming synapses in VAChT- and TH-immunolabelled tissue 95

3.10. Micrographs showing serial section analysis 96

3.11. Micrographs showing the differences between spines and dendrites 97

3.12. Micrograph showing cortical input to an STN neuron somata 98

3.13. Example micrographs showing axo-axonic synapses 107

3.14. An updated diagram showing the connectivity of the basal ganglia circuit 115

Chapter 4: General Discussion

4.1. A revised circuit diagram showing the connectivity of the basal ganglia 123

LIST OF TABLES

Chapter 2

2.1. Summary of the morphological characteristics of synaptic boutons and their targets 58

Chapter 3

3.1. Summary of the terminal size, target size and type and active zone size of VGluT1-, VGluT2- and VGAT-immunopositive synaptic boutons in the STN 103

3.2. Summary of the terminal size, target size and type and active zone size of VAChT and TH boutons 104

ABBREVIATIONS

6-OHDA	6-hydroxydopamine
ABC	avidin-biotin-peroxidase complex
ACh	acetylcholine
ADHD	attention deficit hyperactivity disorder
AMPA	α-Amino-3-hydroxy-5-methyl-4-isoxazolepropionic acid
BG	basal ganglia
C	cortex
cAMP	cyclic adenosine monophosphate
CB	calbindin
ChAT	choline acetyltransferase
CM	central median nucleus
CR	calretinin
Cx	cortex
DA	dopamine
DAB	3,3'-diaminobenzidine
DBS	deep brain stimulation
dH2O	distilled water
DR	dorsal raphe nucleus
DStr	dorsal striatum
EP	entopeduncular nucleus
EPSP	excitatory post-synaptic potentials
GABA	gamma-aminobutyric acid
GP	globus pallidus
GPe	globus pallidus external segment
GPi	globus pallidus internal segment

HBN	habenula
IgG	immunoglobulin G
IPSP	inhibitory post-synaptic potentials
L-DOPA	L-3,4-dihydroxyphenylalanine
MSN	medium spiny neuron
NAC	nucleus accumbens core
NAS	nucleus accumbens shell
NGS	normal goat serum
NMDA	N-methyl-D-aspartate
NO	nitric oxide
NOS	nitric oxide synthase
OCD	obsessive compulsive disorder
PB	phosphate buffer
PBS	phosphate buffered saline
Pf	parafascicular nucleus
PPN	pedunculopontine nucleus
PV	parvalbumin
RF	reticular formation
SC	superior colliculus
SN	substantia nigra
SNc	substantia nigra pars compacta
SNr	substantia nigra pars reticulata
STN	subthalamic nucleus
STR	striatum
TAN	tonically active neuron
Th	thalamus
TH	tyrosine hydroxylase

TRIS	tris(hydroxymethyl)aminomethane
VA	ventral anterior thalamus
VAChT	vesicular acetylcholine transporter
VGAT	vesicular GABA transporter
VGluT1	vesicular glutamate transporter 1
VGluT2	vesicular glutamate transporter 2
VL	ventral lateral thalamus
VP	ventral pallidus

Chapter One

General Introduction

1.1. Anatomical Organisation of the Basal Ganglia

1.1.1. Overview of the basal ganglia

The basal ganglia (BG) are a collection of interconnected subcortical nuclei in the base of the forebrain (Figures 1.1 and 1.2). Understanding the complex architecture underlying the connectivity of these nuclei (Figure 1.3) and the way information is integrated and transmitted is the subject of many active research groups. This chapter aims to summarise the main anatomical aspects of basal ganglia circuitry, with each major nucleus explored in detail.

The BG are implicated in many functional roles, primarily motor control such as action selection, initiation and termination, but also in many limbic functions such as motivation, association and reward processing (Graybiel, 1995; Espinosa-Parrilla *et al.*, 2013; van Schouwenburg *et al.*, 2013; Hikosaka *et al.*, 2014). The dorsal BG is generally considered to process motor and associative information, receiving information from the cortex in a topographical manner which is maintained throughout the BG. The ventral BG is considered to process limbic information. The maintained topographical organisation of functional information throughout the BG has led to the proposal of functionally segregated loops within the BG, and the resulting basal ganglia-thalamocortical pathway, which are processed in parallel (Alexander & Crutcher, 1990), however it should be noted that due to large dendritic trees of individual neurons within each nucleus convergence may occur, particularly in rodents where topographical regions are less defined (Mink, 1996).

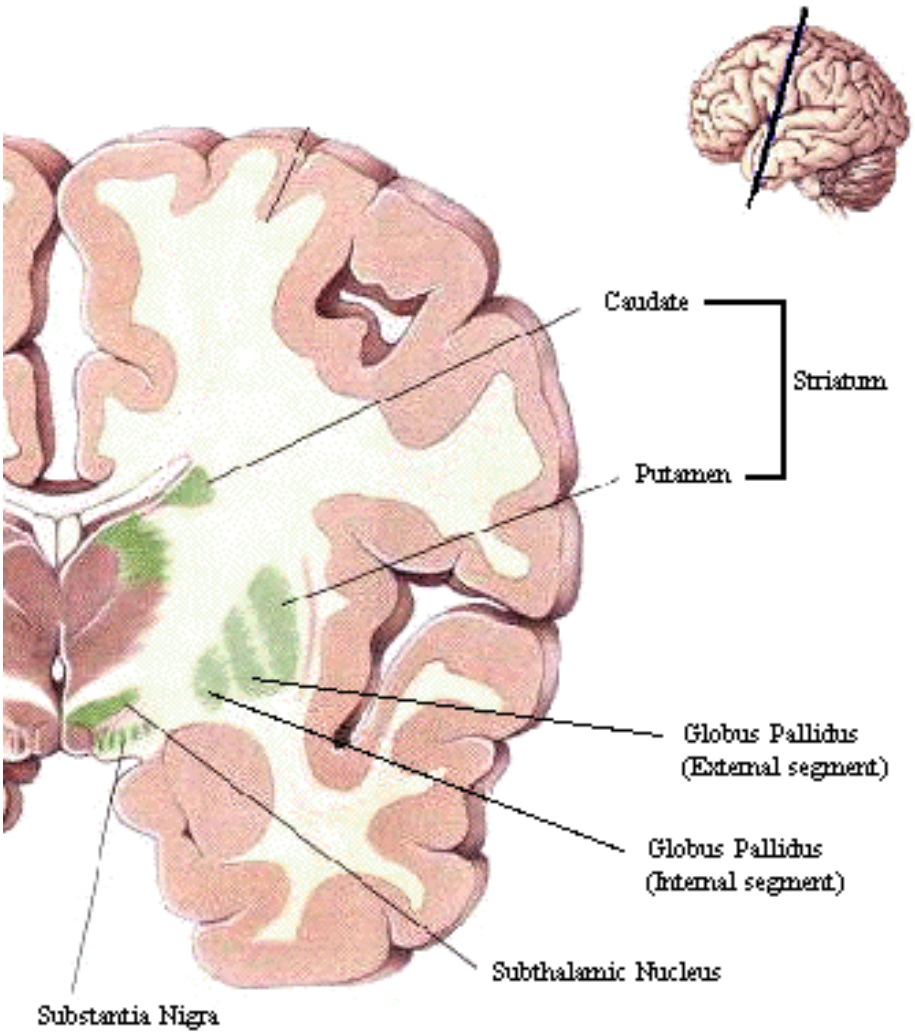


Figure 1.1: Diagram showing a coronal view of the human brain, showing the basal ganglia.

The section is angled rostrocaudally (shown top right) to encounter most of the BG nuclei in a single section. Figure taken from (Bear *et al.*, 2007).

Caudate and putamen are analogous to the striatum in rodents. Globus pallidus external segment (GPe) is analogous to globus pallidus in rodents (GP). Globus pallidus internal segment (GPi) is analogous to the entopeduncular nucleus (EP) in rodents.

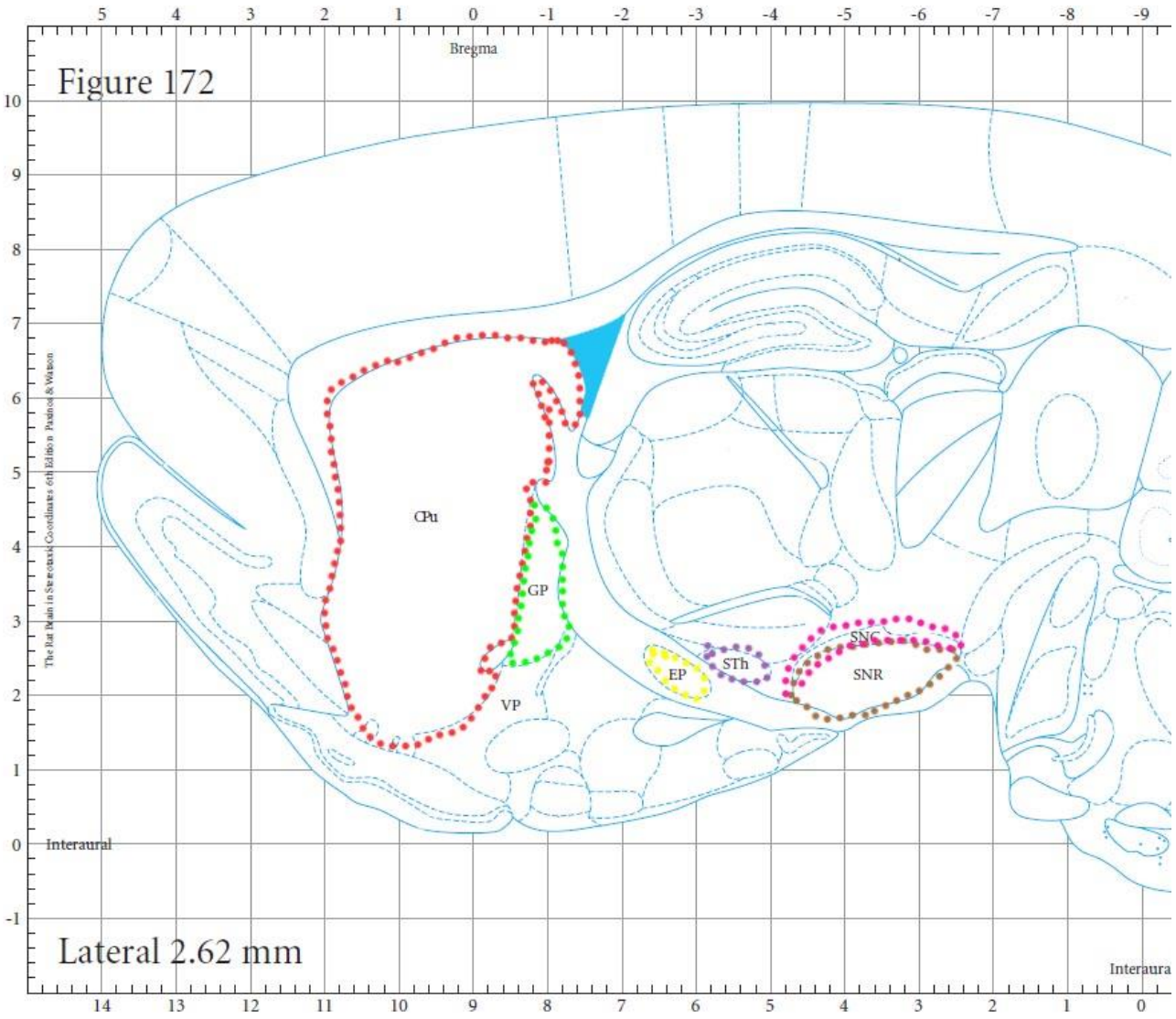


Figure 1.2: A schematic diagram showing the basal ganglia nuclei within the rat brain. A diagram showing the locations of each basal ganglia nuclei within the rat brain. The brain is shown in a parasagittal section. Adapted from 'The rat brain in stereotaxic coordinates' (Paxinos & Watson, 2007)

CPu (red), Striatum; GP (green), Globus Pallidus (analogous to GPe); VP, Ventral Pallidus; EP (yellow); Endopeduncular nucleus (analogous to GPi); STh (purple), Subthalamic nucleus; SNc (pink), Substantia Nigra pas compacta; SNr (brown), Substantia Nigra pas reticulata. Scale bars in mm.

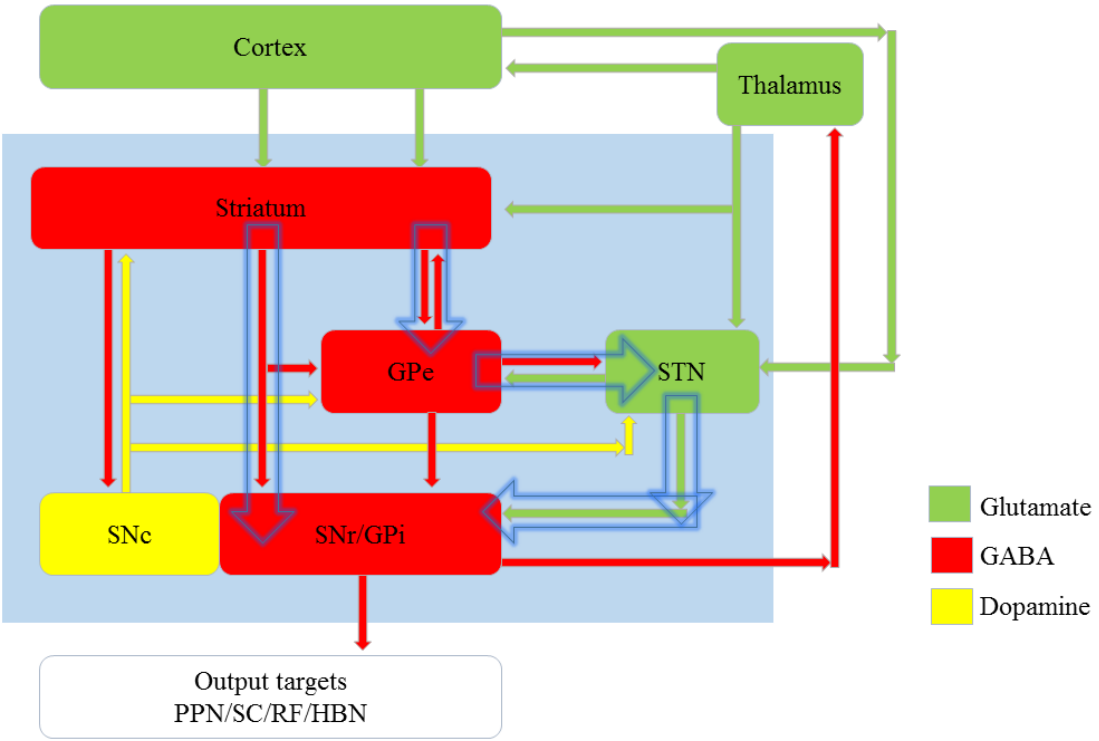


Figure 1.3: A simplified flow diagram showing the main connections of the basal ganglia.

The originally proposed model of information flow through the basal ganglia (DeLong, 1990) showed cortical and thalamic information entering via the striatum, where information is then processed via one of two pathways; the direct and indirect pathways (marked with blue arrows) with direct pathway neurons projecting onto output structures GPi/SNr and indirect pathway neurons reaching the output via the GPe and STN. The entire network is modulated by dopaminergic neurons arising in the SNc. Output neurons either project directly to brainstem nuclei or back to the cortex via the thalamus.

GPe, globus pallidus external segment; GPi, globus pallidus internal segment; HBN, habenula; SC, superior colliculus; SNc, substantia nigra pars compacta; SNr, substantia nigra pars reticulata; *STN, subthalamic nucleus; PPN, pendunculopontine nucleus; RF, reticular formation.*

Whilst the ventral BG holds a vital role in information processing and is implicated in many neurological disorders such as impulse control disorders, Tourette's and ADHD (Leisman *et al.*, 2014), the dorsal BG is the main area studied within this thesis and thus all further reference to the BG is confined only to the dorsal segment. In the rodent (the subject of study within this thesis) the principal input structure is the striatum (caudate and putamen in humans), which receives a vast innervation from almost the entire neocortex, many thalamic nuclei and the substantia nigra pas compacta (SNc). The striatum then transmits information via one of two pathways, the 'direct' pathway monosynaptically connected to the output nuclei, or the 'indirect' pathway which reaches the output nuclei via several relay nuclei (Figure 1.3) (Smith *et al.*, 1998). Other BG nuclei, principally the subthalamic nucleus (STN), are known to receive direct input from cortex and thalamus (Nambu *et al.*, 2000) and understanding the organisation of this afferent input to the BG is the primary focus of this thesis.

Neurons in the main output nuclei of the BG, the substantia nigra pars reticulata (SNr) and globus pallidus internal segment (GPi), maintain a high resting firing rate (Squire, 2009). The neurons within the output nuclei are GABAergic having an inhibitory action on their targets, principally the thalamus, inhibiting movement. During movement afferents provide excitatory glutamatergic input to the striatum increasing the activity of striatal neurons (Mink, 1996) and leading to SNr/GPi inhibition via the direct pathway, or increased firing via the indirect pathway (Groenewegen, 2003). Direct pathway activation inhibits output nuclei directly as it is a GABAergic projection, indirect pathway activation results in increased firing of output nuclei by disinhibiting a tonic glutamatergic projection from STN to GPi/SNr (Figure 1.3). The precise balance between these antagonising pathways results in a change in output firing and the resulting movement. A loss of balance between these two pathways, caused either by

drugs, neurodegeneration or physical damage, can result in many debilitating movement disorders. An imbalance in favour of direct pathway activity is linked to hyperkinetic disorders such as Huntington's disease, whereas imbalance in favour of indirect pathway activity results in hypokinetic disorders such as Parkinson's disease (Albin *et al.*, 1989; 1995). A critical determinant of balance between these pathways is dopamine. The source of striatal dopamine is neurons located in the substantia nigra (SN), which have immense axons densely innervating the striatum (Moss & Bolam, 2008). Increased dopamine levels within the striatum result in the facilitation of movement; increasing direct pathway activity and decreasing indirect pathway activity. The dopaminergic modulation of firing activity of BG neurons is a key part of many models of BG activity in health and disease, therefore it will be discussed in greater detail in Section 1.3.

1.1.2. Striatum

The striatum is the main input structure of the BG, containing approximately 2.8 million neurons per hemisphere in the rat (Oorschot, 1996). The principal neuron type is the medium spiny neuron (MSN), a GABAergic projection neuron which comprises ~95% of the striatal population. The remaining ~5% of neurons are a variety of interneurons, each subtype characterised by distinct innervation patterns and molecular markers (Wu & Parent, 2000). Classically four subtypes have been described, although many more small populations are being uncovered, there are three GABAergic subtypes: the parvalbumin-expressing (PV) interneuron, the calretinin-expressing (CR) interneuron and the nitric oxide synthase-expressing (NOS) interneuron, and one cholinergic interneuron (Phelps *et al.*, 1985; Tepper *et al.*, 2010).

In addition to interneurons, the activity of MSNs is modulated by dopamine release from a dense innervation arising from the dopaminergic neurons of the SNc (Moss & Bolam, 2008) and release of histamine from terminals arising from the hypothalamic tuberomammillary nucleus (Ellender *et al.*, 2011). Other nuclei currently being investigated for their role in modulating striatal neuron activity include an acetylcholine-releasing projection originating in the pedunculopontine nucleus (PPN) (Dautan *et al.*, 2014) and a serotonin-releasing projection arising in the dorsal raphe nucleus (DR) (van der Kooy & Hattori, 1980a; Politis *et al.*, 2014) both of which have been shown to innervate the striatum.

MSNs can be separated into two classes depending on both their projection pattern, the expression of dopamine receptor subtypes and other molecular markers. MSNs comprising the direct pathway express the D1 subclass of dopamine receptors; a G protein coupled receptor which activates adenylyl cyclase, increasing the intracellular concentration of the second messenger cyclic adenosine monophosphate (cAMP) leading to increased excitability. The second class of MSNs project to the output nuclei via the external segment of the globus pallidus (GPe) and subthalamic nucleus (STN) and are referred to as giving rise to the "indirect" pathway. Indirect pathway MSNs express the D2 subclass of dopamine receptors; a G protein coupled receptor which inhibits adenylyl cyclase, decreasing cAMP and leading to supressed excitability (Groenewegen, 2003; Beaulieu & Gainetdinov, 2011).

Dopamine release in the striatum has a facilitatory effect on direct pathway neurons which in turn ultimately leads to reduced inhibition of the thalamus, and an 'inhibitory' effect on indirect pathway neurons which ultimately leads to greater thalamic inhibition. In the absence of dopamine, such as in Parkinson's disease where a selectively

vulnerable population of dopaminergic neurons of the SNc degenerate, the activity of indirect pathway neurons increases and direct neurons decreases. This leads to excessive inhibition of the thalamus from basal ganglia output nuclei resulting in hypokinesia, difficulty with initiation of movement and rigidity (Albin *et al.*, 1995; Groenewegen, 2003).

The reverse is the case in Huntington's disease, a hyperkinetic disorder. MSNs forming the indirect pathway preferentially degenerate, resulting in imbalance of information flow in favour of the direct pathway. This leads to sudden, uncontrolled movements suggesting that a precise balance between the two pathways is required to ensure smooth, controlled movements (Albin *et al.*, 1995; Groenewegen, 2003).

In addition to the two classes of MSNs and the topography of afferent inputs, there is an additional layer of organisation within the striatum. Small compartments of striatum express high levels of opioid μ receptors (patches), the remainder of the striatum, which expresses relatively high levels of choline acetyltransferase (ChAT) and calbindin, is referred to as the matrix (Gerfen, 1992). Neurons localised within patches have a distinct innervation pattern, receiving input from specific cortical areas and projecting directly to the dopaminergic neurons of the SNc. The cortical areas innervating patch neurons are associated with limbic information, meaning that patch neurons, including MSNs, are proposed be involved in limbic information processing - despite being found in dorsal striatum, and may also contribute to the overall excitability of the striatum by influencing dopamine release (Gerfen, 1992).

MSNs receive information from virtually all of the cerebral cortex. Cortical innervation is excitatory, glutamatergic and almost exclusively targets the heads of spines in MSNs (Bolam *et al.*, 2000). The thalamus also provides a large projection to the striatum,

principally from the parafascicular nucleus (Pf) and the centre median nucleus (CM; central lateral nucleus is rodents: CL) (Smith *et al.*, 2004; Raju *et al.*, 2006; Smith *et al.*, 2014). Thalamic glutamatergic afferents also target the spines of MSNs, although synapses are also formed with dendritic shafts, particularly within the matrix (Bolam *et al.*, 2000; Raju *et al.*, 2006; Doig *et al.*, 2010). Electrophysiological data show that cortical and thalamic afferents exhibit different physiological properties with different types of synaptic plasticity produced with MSNs to a given stimulus pattern (Ding *et al.*, 2008). The synaptic properties also differ between the different thalamic afferents. Terminals derived from neurons in the CL form synapses with a high proportion of fast-responding ionotropic receptors (AMPA receptors) whereas terminals derived from neurons in the Pf form synapses with a higher proportion of slower, longer lasting, metabotropic receptors and NMDA receptors. Synapses formed by Pf terminals show plastic changes in response to repeated activation, whereas synapses formed by CL and cortical terminals do not (Ellender *et al.*, 2013). This suggests that the cortex and CL nucleus drive MSNs to respond in a reproducible, reliable manner, while Pf nucleus afferents response depends on prior activity states of the neurons and are thus likely to be more modulatory.

Interneurons of the striatum

The interneurons of the striatum comprise a small but influential population of the striatal neurons. Each interneuron subtype is distributed throughout the three-dimensional space of the striatum in a distinct manner, and each have characteristic firing patterns, afferent innervation patterns and axon branching patterns. This indicates that each class of interneuron holds a functionally unique role.

The most abundant, and well-studied, of the striatal GABAergic interneurons in the rat is the PV-expressing neuron. PV-expressing neurons account for about 1% of striatal neurons and are defined by the presence of the calcium binding protein parvalbumin (Wu & Parent, 2000; Tepper *et al.*, 2010). They are a heterogeneous population with a range of anatomical properties, suggesting there may be sub-classes within this group (Bennett & Bolam, 1994a). Generally PV-expressing neurons can be identified by a fast-spiking activity with short duration action potentials. They generally fire in high frequency stutters, often as high as 400 Hz, separated by periods of silence (Tepper *et al.*, 2010; Sharott *et al.*, 2012).

PV-expressing neurons receive innervation from distinct cortical afferents, some thalamic nuclei, and other striatal PV-expressing interneurons (Kita *et al.*, 1990; Bennett & Bolam, 1994b; Sidibe & Smith, 1999; Ramanathan *et al.*, 2002). Dopaminergic projections from the SNc also synapse with PV-expressing neurons (Kita *et al.*, 1990), as do pallidal projections from the globus pallidus external segment (Bevan *et al.*, 1998). The main efferent targets of PV-expressing neurons are MSNs, with both direct and indirect pathway MSNs targeted (Kita *et al.*, 1990; Bennett & Bolam, 1994b).

In-vivo, PV-expressing interneurons evoke powerful inhibitory post synaptic potentials (IPSPs) in MSNs. These IPSPs are strong enough to delay or completely block MSN firing. PV-expressing neurons therefore have the potential to significantly alter MSN firing, indeed increases in cortical activity have been shown to induce a strong inhibition of MSNs via PV-expressing interneuron firing. PV-expressing neurons have a modest effect upon other PV-expressing interneurons and so their main role appears to be the feed-forward inhibition of MSNs from the cortex (Tepper *et al.*, 2010).

Whilst PV-expressing neurons are the most abundant interneuron in rats, in humans and other primates the largest population of GABAergic interneurons is the CR-expressing interneuron (Wu & Parent, 2000). CR-expressing interneurons make up 0.5% of striatal neurons in rats, although this count is significantly higher in monkeys and humans (Wu & Parent, 2000). Despite their prevalence, relatively little is known about the CR-expressing interneuron. Prior attempts to define them electrophysiologically have failed (Tepper *et al.*, 2010) and limited studies have been performed on their anatomy (Bennett & Bolam, 1993). CR-expressing interneurons have been shown to have a range of sizes and morphologies, suggesting at least two subpopulations (Bennett & Bolam, 1993; Petryszyn *et al.*, 2014) and all are immunopositive for the calcium binding protein, calretinin, but negative for the other biomarkers found in striatal interneurons such as PV and NOS in rodents. A small population of CR-expressing interneurons express ChAT in primates (Bennett & Bolam, 1993; Petryszyn *et al.*, 2014). Unfortunately, attempts to uncover the afferent and efferent projections have not yet been successful, although at least three sources of afferent innervation have been implicated and efferent output has been suggested to form both symmetric and asymmetric synapses (putatively excitatory and inhibitory synapses respectively) again suggesting a range of subtypes (Bennett & Bolam, 1993). It is hoped that new transgenic models will increase our knowledge of these illusive interneurons, with regards not only to their firing pattern and anatomy, but also their functional significance within the striatum.

The third class of GABAergic interneuron are the NOS-expressing interneurons. These neurons are defined by the presence of nitric oxide synthase, an enzyme involved in the synthesis of nitric oxide (NO). NOS-expressing neurons have long duration action potentials and can show spontaneous tonic activity (Tepper *et al.*, 2010). In addition to GABA these neurons produce and release NO, a potent signalling molecule, in response

to cortical afferent input, although the regulation of this process is poorly understood in the striatum (Sammut *et al.*, 2007). NOS-expressing neurons receive afferent input from cholinergic and dopaminergic axons and GABAergic innervation from the globus pallidus and PV-expressing interneurons (Kubota *et al.*, 1988; Vuillet *et al.*, 1992; Bevan *et al.*, 1998). The main target of NOS-expressing neurons are MSNs, although ChAT interneurons can also be targeted. They are also immunopositive for the neuropeptides somatostatin and neuropeptide Y (Tepper *et al.*, 2010), leading to the suggestion that the main role of NOS-expressing neurons is modulation of MSN firing via the release of neuroactive peptides.

The main class of non-GABAergic interneuron is the choline acetyltransferase- (ChAT) expressing interneuron. They primarily receive afferent input from the thalamus, other local interneurons, from cortical areas and from MSN collaterals; they also express a high density of dopamine receptors (Lapper & Bolam, 1992; Berlanga *et al.*, 2005; Gonzales *et al.*, 2013; Doig *et al.*, 2014). They are large neurons which have been reported to trigger potent IPSPs in targeted MSNs, although the mechanism behind this is poorly understood it has been suggested that acetylcholine (ACh) release from ChAT-expressing interneurons drive the release of GABA from dopamine terminals in the striatum (Nelson *et al.*, 2014). However, caution should be taken when interpreting these results as they were performed *in vitro* using transgenic rodents and have not been shown *in vivo* or in genetically normal rodents. It is also known that ACh can trigger the release of dopamine from terminals locally, independently of action potentials within the dopaminergic neuron (Threlfell *et al.*, 2012) and that ChAT-expressing neurons have close anatomical relationships with the striatal dopaminergic axons (Dimova *et al.*, 1993) although again caution should be exercised when considering *in vitro* data. ChAT-expressing neurons fire autonomously at slow rates, and so are often referred to as

tonically active neurons (TANs). TANs have been recorded in a range of behavioural experiments, showing a pause in tonic firing during a wide range of reward paradigms (Apicella *et al.*, 2009; Goldberg & Reynolds, 2011; Benhamou *et al.*, 2014) and have been proposed to amplify dopamine signals to MSNs (Cragg, 2006). It is therefore proposed that ChAT-expressing neurons hold pivotal roles in reward signalling and learning, with a strong link suggested between acetylcholine and dopamine release probability in the striatum (Threlfell & Cragg, 2011).

In addition to the four main classes of interneuron described above, new subtypes are being found – including a TH-expressing GABAergic interneuron (Unal *et al.*, 2011) and a functionally distinct neuropeptide Y-expressing GABAergic interneuron (Ibanez-Sandoval *et al.*, 2011), meaning our understanding of the complexity of the striatal network is growing (Tepper *et al.*, 2010). The diversity and interconnectivity of neurons within the striatum mean that our understanding of this key site of information processing is still relatively primitive. Increasing our understanding of the connections and projections of the various neural populations, and furthering our understanding of how they fire, is critical for us to be able to improve computational models of normal function and predict disease state changes.

1.1.3. Globus pallidus external segment (Globus pallidus in rodents)

The external segment of the globus pallidus (GPe) is the first relay nucleus of the indirect pathway (Figure 1.3). The principal afferent innervation arises in the striatum, although there are also strong glutamatergic feedback projections from the STN (Shink *et al.*, 1996; Jaeger & Kita, 2011) and extensive local axon collaterals between GPe neurons (Kita & Kitai, 1994; Sadek *et al.*, 2007).

The main projection neurons of the GPe send axons to the STN, the next nucleus in the classical model of basal ganglia circuitry (DeLong, 1990), and also directly to the output nuclei, GPi and SNr (Smith & Bolam, 1989; Kita & Kitai, 1994). However, it is now known that GPe projection neurons can be separated into two main classes; the prototypic projection neuron, sending collaterals to downstream targets, and a second class the arkypallidal projection neuron, which sends projections exclusively upstream to the striatum, each with distinct electrophysiological profiles (Mallet *et al.*, 2012). This fits with the anatomical data shown by Kita & Kitai (1994) as they found a sub-population of GPe neurons sent axons rostrally, most likely to striatum. At least two subtypes of neurons have also been shown genetically, again with distinct projection patterns and electrophysiology, showing that this nucleus is not a simple homogeneous structure (Mastro *et al.*, 2014).

Due to the extensive network of connections and multiple subtypes, GPe neurons can no longer be thought of as simply relay neurons within the indirect pathway. It is clear that the role played by these neurons is far more complex than previously appreciated. The GPe is perhaps better considered as the integrative hub of the basal ganglia (Figure 1.4), receiving innervation from the two nuclei that act as the main input structures, striatum and STN, and in turn sending projections to the entire basal ganglia (Jaeger & Kita, 2011). Pallidal neurons are densely innervated, with synapses covering the entirety of their dendrites (DiFiglia & Rafols, 1988), allowing the summation of a wide range of inputs. The GPe may well be the central processing nucleus of the basal ganglia, making information processing an integrative and complex network rather than linear pathways such as that shown by the traditional basal ganglia model (DeLong, 1990; Jaeger & Kita, 2011).

In healthy animals GPe neurons exhibit high firing rates with little synchrony. However, in disease models such as 6-OHDA treated rats, an experimental model of Parkinson's disease, firing becomes rhythmic and synchronous resulting in a strong beta wave generation throughout the basal ganglia and indeed cortex (Jaeger & Kita, 2011). Strong reciprocal connections between the GPe and STN have been implicated in the generation of this oscillation (Plenz & Kital, 1999; Kumar *et al.,* 2011; Tachibana *et al.*, 2011), yet again showing the importance of anatomy in understanding the function, or dysfunction, of neural networks.

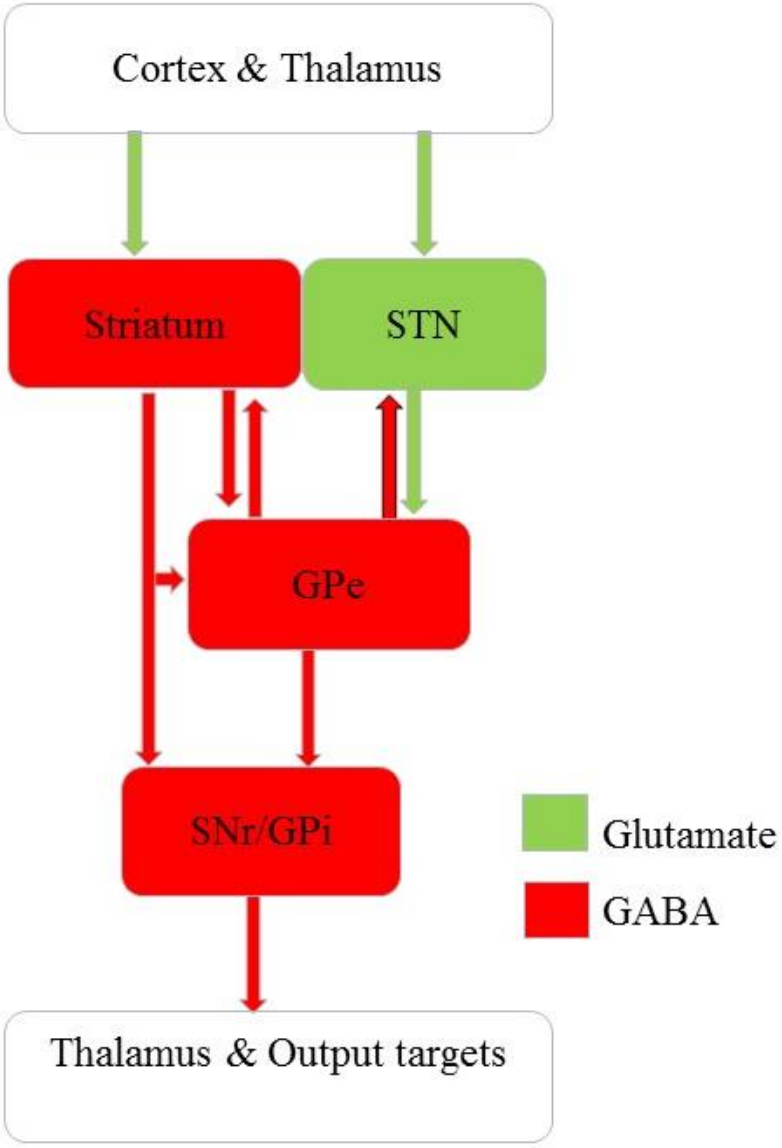


Figure 1.4: A revised circuit diagram showing the GPe as the main integrative hub of the basal ganglia.

In this model the STN and striatum act as the main input pathways, sending reciprocal projections to the GPe. The GPe then collates the information sending to all aspects of the basal ganglia.

STN, subthalamic nucleus; GPe, globus pallidus external segment; GPi, globus pallidus internal segment; SNr, substantia nigra pars reticulata.

1.1.4. Subthalamic nucleus (STN)

The STN is unique among basal ganglia nuclei as it is the only nucleus to utilise excitatory glutamate as its neurotransmitter. It is also a second point of entry for cortical and thalamic information to enter the basal ganglia network. The STN forms part of the indirect pathway although in light of the many advances in our knowledge of connectivity it may be advantageous to consider the STN as forming part of the principal input structure (Figure 1.4) instead of simply a relay structure as shown in Figure 1.3. The afferent innervation of STN neurons is the main topic of Chapter 3 and as such a more detailed discussion on STN connectivity and function will be covered in section 1.3.

1.1.5. Output nuclei

The main output from the BG is the internal segment of the globus pallidus (GPi; entopeduncular nucleus – EP – in rodents) and the SNr. Together these two nuclei transmit the information processed throughout the BG to the target structures: principally thalamic nuclei (Bolam *et al.*, 2000).

Globus pallidus internal segment (entopeduncular nucleus – EP – in rodents)

The GPi is the smallest structure within the BG in the rat, comprising only 3200 neurons per hemisphere (Oorschot, 1996). It is targeted by MSNs of the direct pathway and neurons of the GPe (Smith *et al.*, 1998). These afferent inputs are inhibitory GABAergic inputs, which reduce the high intrinsic firing rate of GPi neurons in response to activation. There are also glutamatergic inputs from the STN to GPi, which have opposing effects to the GABAergic inputs (Smith *et al.*, 1998). The majority of GPi

neurons project to thalamic nuclei and PPN (Parent & De Bellefeuille, 1982; Sidibe *et al.*, 1997). Despite its small size, information flow appears to remain roughly segregated by primary function, in both input and output, although some convergence has been identified (Parent & De Bellefeuille, 1982; Bevan *et al.*, 1997). In non-human primates, ventrolateral GPi receives afferents from striatal regions receiving sensory motor information, dorsal GPi receives afferents from associative striatal regions and the rostromedial pole receives information from limbic striatal areas (Sidibe *et al.*, 1997). This segregation remains in the GPi efferent projection, with sensory-motor areas of GPi innervating separate regions of thalamus to associative and limbic areas. The sensory-motor GPi also targets the CM region of thalamus and PPN, whilst associative and limbic regions tend to target the Pf and ventral anterior/ventrolateral (VA/VL) thalamic nuclei, and the hypothalamus (Parent & De Bellefeuille, 1982; Sidibe *et al.*, 1997).

Substantia nigra pas reticulata (SNr)

In addition to the GPi, the non-dopaminergic neurons of the SNr are also output neurons of the BG (Deniau *et al.*, 1978). The SNr receives input in a similar manner to the GPi, from striatal MSNs of the direct pathway, GPe neurons and STN. Like GPi neurons, most SNr neurons are GABAergic neurons, although a small population of dopaminergic neurons are present (Yung *et al.*, 1998). The efferent targets of SNr projection neurons are more diverse than GPi projection neurons, targeting various thalamic structures including Pf, VL, ventral medial, paracentral and mediodorsal nuclei. Additionally, SNr projection neurons make synaptic contact with neurons in the PPN, superior colliculus (SC), periaqueductal gray, and the deep mesencephalic nucleus (Hopkins & Niessen, 1976; Bentivoglio *et al.*, 1979; Cebrian *et al.*, 2005).

Like the GPi, SNr projection neurons are GABAergic with a high resting firing rate, likely elicited from the STN in the same manner that gives rise to GPi firing, resulting in a strong inhibition of movement at rest which is released during BG activity (Freeze *et al.*, 2013). However, there does appear to be some heterogeneity within SNr projection neurons, with subtypes determined by the expression of calcium binding proteins PV or CR (Lee & Tepper, 2007). Again, topographical organisation has been shown in the arrangement of afferent and efferent projections within the SNr (Deniau *et al.*, 1996) and a partial functional topography has been seen experimentally (Takakusaki *et al.*, 2003), although robust local axon collaterals are present between SNr projection neurons allowing convergence of information (Lee & Tepper, 2007). Additionally, the axons of SNr neurons branch giving rise to innervation of multiple regions (Deniau *et al.*, 1978).

The efferent projections of both GPi and SNr suggest that the BG is primarily sending information back to the cortex via the thalamus, or to sub-cortical structures involved in the control of movement. Projections are also present to most of the nuclei which send afferent information to one or more BG nuclei, such as the PPN, SC, DR and Pf/CM thalamic nuclei, covering brain regions involved in reward, movement, association, motor control and sensory processing. This results in multiple loops of information feeding back into the BG and allows a constant adaptation and reaction to a wide range of information, in addition to influencing premotor cortex (via thalamus) and sub-cortical structures to control movements.

1.2. Substantia Nigra and Dopamine

1.2.1. Anatomy of the substantia nigra (SN)

The SN can be separated into two main functionally and biochemically different compartments; the substantia nigra pas compacta (SNc) and substantia nigra pas reticulata (SNr). As discussed previously (Section 1.1.5.) the SNr is part of the output nuclei of the basal ganglia, receiving information from BG nuclei and sending GABAergic projections to thalamic and brain stem targets. The SNc, on the other hand, is heavily interconnected with the BG, receiving afferent input from striatum and sending projection neurons to all BG nuclei (Gauthier *et al.*, 1999). The SNc projection neurons utilise dopamine as a transmitter, although a smaller population of GABAergic neurons are also present (Nair-Roberts *et al.,* 2008). There have been suggestions that co-localisation of GABA and dopamine may occur within one neuron but the synthesis of this GABA is proposed to be local to the release site, and taken up via the plasma membrane of dopaminergic boutons. Additionally, the function of this GABA release is poorly understood and has only been shown in genetically modified animals, or *in vitro* (Gonzalez-Hernandez *et al.*, 2001; Nelson *et al.*, 2014; Tritsch *et al.*, 2014).

The dopaminergic neurons of the SNc have been separated into two subgroups dependent on the expression of a calcium binding protein, calbindin, and connectivity patterns (Liang *et al.,* 1996). Calbindin-positive dopaminergic neurons are typically found in the dorsal SNc and have dendrites which arborise within the SNc (Liang *et al.*, 1996). The dendrites of calbindin-negative dopaminergic neurons, found within the ventral tier of the SNc, on the other hand have been shown to extend into the SNr to varying degrees (Liang *et al.*, 1996), resulting in a different ratio of afferent inputs (Henny *et al.*, 2012). In addition to being calbindin-negative, dopaminergic neurons of

the ventral tier are enriched with the pigment neuromelanin in humans and non-human primates (Zucca *et al.*, 2014). This results in dark coloured cell bodies, producing a black band within the brain and is the reasoning behind the name (Latin translation: substantia = substance, nigra = black).

Afferent connectivity of SNc dopaminergic neurons

Uncovering the brain regions sending projections to the dopaminergic neurons of SNc has been an active area of research for many years. Early studies performed using antro- and retrograde tracers were able to show regions sending projections to the SNc. It was established that a strong inhibitory projection from striatal MSNs located within patches made contacts with SNc neurons, MSNs within the nucleus accumbens and also that the GPe sends prominent inhibitory input to SNc neurons (Hattori *et al.*, 1975; Smith & Bolam, 1990). In addition to inhibitory innervation, excitatory inputs from SC, STN and PPN have been shown (Kanazawa *et al.*, 1976; Futami *et al.*, 1995; Comoli *et al.*, 2003) and several early studies reported a direct cortical projection (Kornhuber *et al.*, 1984; Naito & Kita, 1994).

More recent studies have used advanced immunohistochemistry or genetic tools to elucidate the inputs to only dopaminergic neurons, as the SNc also contains non-dopaminergic cells. These studies have supported our knowledge of afferent innervation and revealed the differences in innervation pattern of dendrites within the SNr and SNc. For example: a study of the innervation of single dopaminergic neurons shows that dendrites within the SNr receive large amounts of inhibitory input (over 70% of synaptic input) compared to a more balanced input to SNc dendrites (50% inhibitory, 50% excitatory) (Henny *et al.*, 2012). Another key study used a modified rabies virus to identify all brain areas giving rise to monosynaptic projections with dopaminergic

neurons within the SNc (Watabe-Uchida *et al.*, 2012). This study found that key areas projecting to SNc dopaminergic neurons were: striatum, GPe, SNr, STN, PPN, SC, and small areas of cortex and thalamus. This fully agrees with the earlier tracer studies and allows us to continue researching to elucidate the quantity of innervation arising from each of these regions.

Efferent connectivity of SNc dopaminergic neurons

Ventral tier (calbindin-negative) dopaminergic neurons have two projection patterns, they either send axons almost exclusively to the striatum or innervate all BG nuclei and provide little arborisation in the striatum (Gauthier *et al.*, 1999). Their axons are long and branch extensively, producing a lattice of dopaminergic terminals throughout the striatum, innervating primarily the patch areas of striatum (Gerfen *et al.*, 1987; Prensa & Parent, 2001). Dorsal tier (calbindin-positive) dopaminergic neurons have a broader range of targets. Again, they project to striatum, although generally to the matrix regions (Gerfen *et al.*, 1987; Prensa & Parent, 2001).

However, recent research has called into question the specificity of patch/matrix segregation of dopaminergic terminals. Single cell labelling of dopamine neurons resulted in axonal terminals in both regions of striatum, although each individual neuron did show a preference to one region (Matsuda *et al.*, 2009). Another study (Moss & Bolam, 2008) found that dopamine neurons provide an equally spread lattice of terminals throughout the striatum, suggesting that dopamine non-specifically innervates the entire striatum, providing a constant supply of dopamine transmission to the area, although the distribution between patch and matrix was not examined.

1.2.2. The function of dopamine in the basal ganglia

Dopamine is implicated in a wide range of roles in the basal ganglia and the brain as a whole. This section shall only review several of the key roles that dopamine plays, more in-depth reviews are available here (Schultz, 1998; Wise, 2004; Schultz, 2007a; Retailleau *et al.*, 2012). Dopamine neuron firing has long been linked to reward, with dopaminergic neurons showing reproducible bursts of firing when a reward is unexpectedly presented (Mirenowicz & Schultz, 1996). However, dopamine neuron firing may not result in dopamine release due to a wide range of local factors within the striatum. This has been expanded on over the years, and we now know that dopamine neuron firing also results with the expectation of reward, and is supressed if an expected reward is withheld (Schultz, 2013). However, reward prediction is not the only role assigned to dopamine neuron firing in the BG. Dopamine neuron firing is implicated in learning, motivation, action control and decision making. It is proposed that dopamine neuron firing is involved in selection of behaviours which are more likely to result in reward, acting in line with memory, motor pathways and driving motivation.

The striatum integrates information about motor and sensory cues from cortical and thalamic neurons. The membrane potential of MSNs within the striatum have been shown to oscillate between an ‘up’ state and a ‘down’ state, depending on the prior stimulation (Zold *et al.*, 2012). If dopamine is released in striatum, signalling unexpected reward, while the MSN is both in ‘up’ state and receiving excitatory inputs, potentiation, and therefore learning [see (Lovinger, 2010) for review], will occur between the excitatory input and the MSNs, favouring the outcome which led to a reward (Surmeier *et al.*, 2009). This system allows associations to be made between a wide variety of modalities, such as sound, touch, taste, vision, location and many more.

As well as dopamine release caused by action potentials from dopaminergic cell bodies within the SNc, local striatal dopamine release has been shown independent of action potentials in response to acetylcholine or cortical glutamate release (Threlfell *et al.*, 2012; Cachope & Cheer, 2014). Clearly the role of dopamine is not yet fully understood, especially in light of the multiple ways dopamine can be released. However, there are a few areas of research where the role of dopamine is quite well studied, namely in disease states.

1.2.3. Dopamine and movement disorders

Dopamine is also implicated in many disease states and disorders, most famously involving motor control. The classic example is Parkinson's disease. Parkinson's disease is a neurodegenerative disease, typically affecting the elderly with age being the highest risk factor (Pringsheim *et al.*, 2014). It is characterised by slow movements, difficulty initiating movements and rigidity. It is also regularly accompanied by a resting tremor. Dopaminergic neurons within the ventral tier of the SNc (calbindin-negative and neuromelanin-enriched) are selectively vulnerable, resulting in a degeneration of nigro-striatal pathways (Hornykiewicz, 1973; Hirsch *et al.*, 1989). The severity of the motor symptoms of Parkinson's disease are correlated with the degree of loss of dopamine at the level of the striatum and indeed, this can be replicated in animals by chemically lesioning dopaminergic neurons in SNc using the neurotoxin, 6-hydroxydopamine (6-OHDA) (Zigmond & Stricker, 1984). In fact the main drug treatments for Parkinson's disease aim to increase activity at dopamine receptors, either directly with dopamine agonists or indirectly by administering L-DOPA, a pre-curser of dopamine, to increase production in the surviving dopaminergic neurons (Connolly & Lang, 2014).

Despite knowing the cause of motor symptoms for many decades, the trigger leading to initial neurodegeneration and the reason for ventral tier dopaminergic neurons vulnerability is still not known. Several theories have been proposed to explain the selectivity between the dopaminergic neurons, ranging from a protective role of calbindin (Kim *et al.*, 2000), a toxic accumulation of neuromelanin (Zucca *et al.*, 2014) or morphological differences which increase the energy demand on ventral tier neurons (Bolam & Pissadaki, 2012).

Increasing our understanding of the differences between dopamine neurons prone to degeneration and those which are selectively resistant can help increase our potential to uncover what causes Parkinson's disease, and potentially lead to preventive treatments in future.

At the other end of the spectrum, excessive dopamine signalling within the BG leads to dyskinesia. Dyskinesia is classified as a collection of uncontrolled and random movements, such as limb jerks or muscle spasms (Aquino & Lang, 2014). Sometimes more complicated movement patterns can be displayed, such as chewing and lip smacking (Aquino & Lang, 2014). Dyskinesia can be caused by long-term use of medications which change dopamine signalling globally throughout the brain (Cerasa *et al.*, 2014), however many spontaneous cases have been uncovered with genes involved in the striatal response to dopamine generally considered to be at fault (Goodchild *et al.*, 2013).

1.2.4. Dopamine and associative/limbic disorders

In addition to motor disorders, dopamine dysfunction has been implicated in a range of psychiatric disorders including obsessive compulsive disorder (OCD), attention deficit hyperactivity disorder, anxiety, addiction (including alcohol, drugs, gambling and more), anorexia, obesity, schizophrenia and depression to name a few (Nikolaus *et al.*, 2010; Del Campo *et al.*, 2011; Kontis & Theochari, 2012; Brunelin *et al.*, 2013; Kenny *et al.*, 2013; Marinelli & McCutcheon, 2014; Pauls *et al.*, 2014; Trifilieff & Martinez, 2014). It is therefore clear that dopamine has a wider role in the striatum than simply facilitating motor control and signalling reward.

Our understanding of dopamine in associative and limbic disorders is not as clear as motor disorders, it is known that either high levels or low levels of dopamine can result in varied and debilitating effects. An exact balance of dopamine, dopamine receptors and other modulatory transmitters within the striatum is required for information processing. Understanding the anatomical connectivity of dopamine neurons can help develop our models of dopamine firing, release and postulate at mechanisms underlying the development of a wide range of disorders

1.3. The Subthalamic Nucleus

1.3.1 Anatomy of the subthalamic nucleus (STN)

The STN is a small nucleus, located anterior to the SN. It contains approximately 13,600 neurons per hemisphere in the rat (Oorschot, 1996) and is the only BG nucleus which primarily utilises glutamate as a neurotransmitter. Whilst it has been suggested that the STN contains only glutamatergic neurons (Afsharpour, 1985; Smith & Parent, 1988), a single study in human brain tissue found GABAergic interneurons (Levesque & Parent, 2005) and others have suggested the presence of unidentified interneurons in non-human primates (Rafols & Fox, 1976; Pearson *et al.*, 1985) although it should be noted no recent studies have been published to clarify the presence or not of any STN interneurons.

At present, the STN is considered to be a homogeneous nucleus receiving input in a roughly topographical manner, with all neurons exhibiting similar firing activity (Bevan *et al.*, 1995). Neurons fire spontaneously, with three different patterns of activity: bursty, irregular or rhythmic (Wilson & Bevan, 2011). It is has been shown that STN neurons fire autonomously, with afferent input changing the pattern or rate of firing (Wilson & Bevan, 2011).

Afferent inputs to the STN

The afferent inputs to the STN have been well studied using a range of tracer and degeneration techniques, with some newer studies using immunohistological methods.

Excitatory input is glutamatergic and arises from the frontal cortex, CM/Pf thalamic nuclei and PPN (Sugimoto *et al.*, 1983; Sadikot *et al.*, 1992; Bevan *et al.*, 1995; Nambu *et al.*, 2000). Both sources provide input in a topographical manner, supporting the

theory of segregated circuits within the basal ganglia for limbic and motor/associative information (Bevan *et al.,* 1995). Cortical areas projecting to the STN have also been shown to overlap with areas projecting to the striatum, suggesting convergence of information flow (Feger *et al.*, 1994). Thalamic areas on the contrary project either to STN or striatum, showing that separate information is sent to each BG area in rats (Feger *et al.*, 1994). With regards to excitatory inputs, cortical inputs are considered to provide the main source of glutamate to the STN, although direct comparisons between cortical and thalamic inputs have not been made (Nambu *et al.*, 2000).

STN neurons receive a strong inhibitory input from the GPe (Smith *et al.*, 1990a), which is classically recognised as the main source of input to the STN. Additionally, the mesopontine tegmentum is known to send glutamatergic, GABAergic and cholinergic inputs to the STN (Bevan & Bolam, 1995) and there have been suggestions that glutamate and acetylcholine may co-localise within the same terminals (Clarke *et al.*, 1997).

Finally, small projections from the SNc have been shown to the STN (Cragg *et al.*, 2004) and a serotonin projection has been proposed (Mori *et al.*, 1985) although tracer studies have had little success in demonstrating the source of this projection (Canteras *et al.*, 1990).

Efferent outputs of the STN

The main targets of STN neurons are the output nuclei of the BG; the GPi and SNr, and the GPe (Ricardo, 1980; Van Der Kooy & Hattori, 1980b; Kita & Kitai, 1987; Shink *et al.*, 1996). More detailed analysis has revealed that single STN neurons can send projections to the GPe, striatum and the both output nuclei, and that at least 94% of STN neurons project to at least one of these areas in rats (Van Der Kooy & Hattori, 1980b;

Koshimizu *et al.*, 2013). GPe neurons receive the largest proportion of STN boutons (Koshimizu *et al.*, 2013) suggesting the reciprocal connection between GPe and STN is of high importance in STN function.

Smaller projections to PPN, periaqueductal gray, hypothalamus and ventral thalamus (Smith *et al.*, 1990b; Rico *et al.*, 2010) have been shown, although there has been suggestions that the smaller projections may originate within the neighbouring zona incerta and be shown due to technical limitations of the tracing method (Ricardo, 1980).

1.3.2 The role of the STN in basal ganglia information processing

Due to the excitatory nature of STN projection neurons, their role in BG information processing has been the subject of much research. Initially, researchers believed STN neurons to drive activity of the entire BG due to the absence of excitatory inputs within the BG network (Kitai & Kita, 1987). However, it is now known that many BG nuclei – including the output nuclei, are autonomously active allowing firing in the absence of excitatory inputs, and so this theory has been dismissed. There are three main areas of thought with regard to STN function: as an integral part of the centre-surround model of action selection (Nambu *et al.*, 2002), as an inhibitory controller in conflicting situations (Alegre *et al.*, 2013) and as an oscillation generator in combination with the GPe (Zavala *et al.*, 2014).

Centre-surround theory

An essential role of any movement generator is to prevent unwanted movements whilst selecting specific motor patterns. In other brain regions, such as the retina, a centre-surround model creates blanket inhibition over an area (surround), with a focused point

of activity in the desired area of action (centre). This prevents unwanted activation of surrounding neurons, producing a highly specific pattern of firing. It has been suggested that the cortical innervation of STN, due to its faster conduction, creates a blanket inhibition of thalamus by increasing excitatory drive to output neurons (Mink, 1996; Nambu *et al.*, 2002). This increased BG output inhibits all movement prior to the cortical information selecting the appropriate motor pattern (Mink, 1996; Nambu *et al.*, 2002). However, this model does little to explain the strong links between GPe and STN, and the wide ranging afferent connectivity of STN and so the full picture of STN function is likely to be far more complex.

Inhibitory control theory

In more recent years the idea of inhibiting unwanted movements has been developed, with the BG being central to inhibitory control of impulsive, compulsive and unwanted actions. Clearly, many disorders attributed to the BG are disorders where inhibitory control is dysfunctional, resulting in increased impulsive or compulsive behaviour (such as addiction or OCD) or excessive inhibition preventing wanted actions (such as Parkinson's disease). To further understand the role of the STN in inhibitory control a range of experimental paradigms have been created, testing the ability of participants (animal or human) to stop behaviours, after cortical initiation.

The main experimental test used to measure inhibitory control is the stop-signal task (measuring the speed to inhibit an already-engaged response) (Eagle & Baunez, 2010). Together, these tests have revealed that information flow through the faster cortico-subthalamic pathway can inhibit responses already engaged through the direct/indirect pathways, inhibiting motor responses (Aron & Poldrack, 2006). This is a vital requirement during periods of conflicting information, when behaviour patterns may

need to change rapidly to achieve the best outcome. Increasing STN activity results in more successful inhibition after initiation (Aron & Poldrack, 2006), likewise decreased STN connectivity (such as in aging) results in less successful inhibition (Coxon *et al.*, 2012), although after a set time point no inhibition is possible (thought to be the minimum amount of time required for information to reach output nuclei from the STN). In this way the STN could act as an emergency brake, to prevent unwanted behaviours during times of conflict. However, as in the centre-surround model, many of the STNs connections are not taken into account in this model, critically the GPe-STN loop, therefore inhibitory control is potentially just one of several roles of STN neurons in BG activity.

Oscillation generation

Finally, work has been ongoing to explain the functional role of the GPe-STN loop. Both nuclei have strong reciprocal connections, which maintain a topography between the two brain regions (Shink *et al.,* 1996). Computational studies have shown that the GPe-STN network, in combination with the autonomic properties of these neurons, are sufficient to generate oscillations of activity (Holt & Netoff, 2014; Nevado-Holgado *et al.*, 2014). Indeed, in disease states such as Parkinson's disease, increased indirect pathway activity results in strong beta-rhythm oscillations, not just within the BG but throughout the thalamus and cortex. It has been proposed that the GPe-STN network may generate these oscillations (Holt & Netoff, 2014), and then by virtue of their extensive connectivity with the entire BG, entrain BG nuclei, output nuclei and their targets.

Understanding the role of BG oscillations in normal behaviour is still in its infancy. Oscillations have been found in the GPe-STN network in healthy animals, and may

potentially result in shorts bursts of oscillatory activity (Plenz & Kital, 1999; Wichmann *et al.*, 2002; Marceglia *et al.*, 2011). Due to the presence of oscillations within the BG network in healthy and Parkinsonian animals and the potential for GPe-STN activity to generate this, understanding the functional role of this network is a high priory in BG research. Disrupting activity in either GPe or STN, through the use of lesions (Tseng *et al.*, 2007) or stimulation with electrodes (deep brain stimulation; DBS), has been shown to result in relief of parkinsonian symptoms (McConnell *et al.*, 2012). In addition, reduction of oscillatory activity has been shown in Parkinson's patients during a motor task, prior to movement onset (Williams *et al.*, 2005) reinforcing the idea that oscillations within the STN can prevent movement.

The mechanism behind the symptomatic relief of DBS is still controversial with several conflicting theories (McIntyre *et al.*, 2004). Therefore, increasing our knowledge of STN connectivity and the control of STN neuron firing is critical to improve computational models, generate accurate theories regarding BG processing, and potentially refine treatment methods in the future – not only for Parkinson's disease but for a whole range of BG disorders.

1.4 Glutamate vesicular transporters

One of the key results presented within this study is identifying the source of afferent innervation to each nucleus, particularly identifying glutamatergic projections as originating from either cortical or subcortical regions. This was done using immunohistochemistry with antibodies against sub-types of glutamate vesicular transporters.

Prior research has uncovered three glutamate vesicular transporters (VGluTs); VGluT1, VGluT2 and VGluT3 (Takamori *et al.*, 2000; 2001; Gras *et al.*, 2002). These proteins are found predominantly localised in the membrane of vesicles, with only a small fraction present on the presynaptic membrane (Hagiwara *et al.*, 2005), and the presence of VGluTs within vesicle membranes of a neuron is sufficient to define the neuron as glutamatergic (Takamori *et al.*, 2000). VGluTs within the vesicle membrane act as transporters, packing glutamate into the vesicles, VGluTs on the presynaptic membrane are proposed to indirectly increase local glutamate production by co-transporting phosphate into the terminal, which in turn activates phosphate-activated glutaminase (an enzyme that converts glutamine to glutamate) and increases production of glutamate, ensuring vesicles are surrounded by high concentrations of neurotransmitter (Takamori, 2006).

The three isoforms of VGluT are very similar on molecular and biochemical levels, and understanding the role of each isoform is currently an active area of research. Each isoform shows a distinct expression pattern, with limited co-expression (Herzog *et al.*, 2001; Kaneko & Fujiyama, 2002; Herzog *et al.*, 2004). Indeed, this complementary expression has been exploited in a range of anatomical studies to uncover likely sources of glutamate (Moss & Bolam, 2008; Doig *et al.*, 2010; Villalba & Smith, 2011). Briefly,

VGluT1 and 2 are associated with typical glutamate neurons with terminals forming excitatory type-1 (asymmetric) synapses, whilst the VGluT3 subtype is more likely to be expressed by non-neuronal cells such as astrocytes or within terminals identified by another neurotransmitter such as GABA or 5-HT (Takamori, 2006). It should also be noted that at this time, unlike VGluT1 and 2, the presence of VGluT3 has not been shown to be sufficient to result in glutamate release.

Previously, the different isoforms of VGluTs were proposed to confer different properties to the synapse, with VGluT1 producing low release probability and LTP, and VGluT2 producing high release probability and LTD (Fremeau *et al.*, 2001; Takamori, 2006). However, recent evidence has called this hypothesis into question as both isoforms are now found to be expressed in single neurons during development, with no change in the synaptic properties of the neurons during maturation (Takamori, 2006). Recent studies have found some functional roles, with VGluT1 being implicated in vesicle clustering and stability (Siksou *et al.*, 2013) and both VGluT1 and 2 being implicated in controlling the quantal size of vesicles (Moechars *et al.*, 2006; Takamori, 2006).

Cerebral cortex, hippocampus and cerebellar cortex express mRNA for VGluT1. However, neurons located within layer IV of the cortex are the exception as they express mRNA for VGluT2 (Fremeau *et al.*, 2004). The brainstem and deep cerebellar nuclei express almost exclusively VGluT2 mRNA transcripts (Fremeau *et al.*, 2004). All thalamic nuclei express high levels of VGluT2 transcript, although some thalamic nuclei do express VGluT1 mRNA at low levels the thalamus is generally considered to be exclusively produce VGluT2 expressing terminals (Barroso-Chinea *et al.*, 2007). Overall, this can allow us to propose that terminals expressing VGluT1 are likely to be

cortical in nature and VGluT2 are likely to arise from subcortical sources such as the thalamus or PPN, particularly as the layer IV neurons are not currently known to project to the STN or SN.

1.5 Aims of the Thesis

The anatomical organisation of the basal ganglia has been repeatedly linked to the various functional roles assigned to this complex yet important collection of nuclei. This thesis aims to expand our current knowledge of the afferent innervation of the basal ganglia, and update the functional models of information flow accordingly.

The organisation of glutamatergic afferent input to dopaminergic neurons of the SN is discussed in Chapter two. Each compartment of the SN will be considered separately, as prior reports have shown that dopamine neurons with dendrites in the SNr receive more inhibitory inputs than those in the SNc (Henny *et al.*, 2012).

Chapter three is concerned with the characterisation of afferent input to the STN, which sends prominent glutamatergic projections to the SN (and other regions). Excitatory glutamatergic input will be examined, as will inhibitory GABAergic input. Additionally, the proportion of input utilising dopamine and acetylcholine as transmitters shall be examined.

Together the data aims to expand the current understanding of connectivity within the BG and the link these findings to possible functional roles in health and disease.

Chapter Two

Innervation of Dopamine Neurons within the Substantia Nigra

2.1 Introduction

The activity of dopaminergic neurons of the substantia nigra is critical in a variety of behaviours, from voluntary movement to reward processing (Schultz, 2007b; Wise, 2009). Changes in dopamine neuron activity are implicated in a wide range of disorders, from movement disorders such as Parkinson's disease and restless leg syndrome, through to psychiatric disorders including OCD and addiction (Kapur & Mann, 1992; Nisell *et al.*, 1995; Chesselet & Delfs, 1996; Turjanski *et al.*, 1999; Denys *et al.*, 2004). The dopamine neurons of the substantia nigra have wide ranging axons, synapsing onto the entire basal ganglia and selected areas of cortex and thalamus (Moss & Bolam, 2008; Yetnikoff *et al.*, 2014), and therefore placing them in a strong position to influence brain function and behaviour.

Dopaminergic neurons have an intrinsic pacemaker firing pattern, which is modified by afferent stimulation (Grace & Bunney, 1984b). Excitatory glutamatergic input causes burst firing of dopamine neurons and therefore increased dopamine release within the target structures (Grace & Bunney, 1984a; Zhang *et al.*, 2009). Likewise, inhibitory inputs cause pauses in firing, a key element of reward prediction error (Schultz, 1998). Understanding the sources of these afferents will help to build and improve current models of basal ganglia circuitry and the brain regions which can influence reward and movement based behaviour.

Understanding the signals that lead to dopamine release may also advance our understanding of Parkinson's disease, where dopamine levels become depleted following the death of these neurons. Some theories hypothesize that excessive excitatory drive leads to excitotoxicity and cell death of a selectively vulnerable population of dopamine neurons (Ambrosi *et al.*, 2014). By determining the sources of

excitatory drive these brain regions can be manipulated experimentally to test models of excitotoxicity and potentially create more realistic animal models of dopamine neuron degeneration than the current industry standard of chemically lesioning.

The main aim of this study was to quantify the glutamatergic innervation of the dopaminergic neurons of the substantia nigra, noting the source of the projection (cortical vs. subcortical). The dendrites of DA neurons have been shown to have different innervation profiles dependent on their location within functionally separate compartments of the SN, the SNc and SNr, and so these compartments will be analysed separately (Henny *et al.*, 2012). To achieve this, a quantitative analysis of synapses formed with dopaminergic dendrites in the SNc and SNr will be conducted on tissue immunolabelled to reveal markers of cortical glutamatergic (vesicular glutamate transporter 1; VGluT1) or subcortical glutamatergic (vesicular glutamate transporter 2; VGluT2) terminals. To visualise dopaminergic dendrites, tissue will also be immunolabelled to reveal tyrosine hydroxylase (TH), the rate-limiting enzyme in the synthesis of catecholamines such as dopamine.

Additionally, the methodology used will be compared to previously used, but labour-intensive, methods performed by Henny and colleagues (Henny *et al.*, 2012). This is to confirm the accuracy of this method for quantifying known afferents; synapses formed by VGluT2-immunopositive boutons, and to test the efficacy of the technique for future experiments.

2.2 Materials and Methods

2.2.1 Animals

All experiments were conducted in accordance with the Animals (Scientific Procedures) Act 1986 (UK). Procedures were performed on adult male Sprague Dawley rats (350-480g).

2.2.2 Tissue preparation

Rats were anaesthetised with sodium pentobarbitone (200 mg/kg, Rhône Mérieux) then perfused through the heart with ~ 50 ml of phosphate buffered saline (PBS; 0.01 M phosphate buffer, pH 7.4, 0.876% NaCl, 0.02% KCl) followed by 300 ml of fixative (0.1 M phosphate buffer, pH 7.4, 3% paraformaldehyde, 0.1% glutaraldehyde) over ~20 min. Free fixative was removed by post-perfusion with PBS. The brain was removed and stored in PBS until cut into 60 µm parasagittal sections using a vibrating blade microtome (VT1000S; Leica).

2.2.3 Double label immunohistochemistry

All methods were conducted as previously described (Moss & Bolam, 2008; Henny *et al.*, 2012; Doig *et al.*, 2014).

All sections were washed three times in PBS and placed into a cryoprotectant (0.05 M PB, 25% sucrose, 10% glycerol) overnight (~15 h) before freeze-thawing. Each section was placed in separate wells of a 6-well plate and excess cryoprotectant removed. The plate was then placed into liquid nitrogen for approximately 30 s, removed and warmed cryoprotectant was immediately added to the well. Sections were then stored in cryoprotectant for at least one hour before the freeze-thaw process was repeated, thawing with warmed PBS. Sections were then washed three times with PBS.

Sections were double-immunolabelled to reveal: vesicular glutamate transporter 1 (VGluT1; marker of cortical boutons), vesicular glutamate transporter 2 (VGluT2; marker of thalamic boutons) or tyrosine hydroxylase (TH; rate-limiting enzyme in the synthesis of catecholamines, a marker of dopaminergic and noradrenergic neurons) in one of two patterns: 1) VGluT1 (visualised using 3,3'-diaminobenzidine [DAB]) and TH (visualised using gold-conjugated antibodies enhanced with silver [immunogold]), or 2) VGluT2 (DAB) and TH (immunogold). Several sections were single-stained for either VGluT1 or VGluT2 revealed with DAB or double-immunolabelled for VGluT1 (DAB) and VGluT2 (immunogold).

Normal goat serum in PBS (NGS-PBS; Vector Laboratories) was used as a blocking buffer (10% NGS) on sections before the addition of primary antibodies. This step coats the section in a non-reactive protein to prevent non-specific antibody binding. Primary antibodies for the double-immunolabelling experiments were added sequentially. Antibodies against TH (mouse monoclonal antibody, Sigma T2928, 1:1000 dilution) were added to sections in 2% NGS-PBS and left overnight, shaking at room temperature. They are then washed three times in PBS and left for 2 h at room temperature on a shaker with goat anti-mouse IgG gold-conjugated antibody (1.4 nm colloidal gold, Nanoprobes, 1:100 dilution). This was followed by three PBS washes, 2 distilled water washes (dH_2O; 5 min and 3 min) and 2 acetate buffer washes (0.1 M sodium acetate 3-hydrate; pH 7.4; 5 min and 3 min) in preparation for silver intensification. Silver reagent (1-2 ml; HQ Silver kit, Nanoprobes) was added to each section and allowed to react for 5 min in the dark, then given a 1 min acetate buffer wash, 2 dH_2O washes (3 min each) and finally washed 3 times in PBS. Sections were then incubated in either the VGluT2 (raised in rabbit, Synaptic Systems 135-403, 1:2000 dilution) or VGluT1 antibody (raised in guinea pig, gift 1:1000; 2% NGS-PBS) and left

overnight shaking at room temperature. Sections were washed three times in PBS and then incubated in a biotin-conjugated goat antibody against either rabbit or guinea pig IgG (rabbit: BA1000, Vector Laboratories, diluted 1:200 in PBS; guinea pig: BA7000, Vector Laboratories, diluted 1:200 in PBS) for 2 h at room temperature on a shaker. Sections were then washed three times in PBS and incubated in avidin-biotin-peroxidase complex (ABC; Vector Laboratories, prepared according to the manufacturers' instructions) for 90 min with shaking at room temperature.

After the ABC incubation, sections were washed three times in PBS and twice in TRIS buffer (0.05 M, pH 7.4). Diaminobenzidine (DAB; 2 ml of 0.025% in TRIS buffer; Sigma) was added to sections and left for 20 min at room temperature with regular shaking. H_2O_2 (final concentration: 0.002%; BDH) was added and the reaction was allowed to continue for 5-6 min until staining was revealed. The reaction was stopped by removal of the DAB solution and addition of TRIS buffer and sections were then washed 3 times in TRIS buffer and three times with 0.1 M phosphate buffer (PB; pH 7.4).

The sections were then placed flat in glass Petri dishes and osmium tetroxide (1% in PB; Oxkem) was applied for 7 min. They were then washed three times with 0.1 M PB and dehydrated in a series of ethanol dilutions (twice for 10 min in 50% ethanol, 45 min in 70% ethanol that included 1% uranyl acetate (TAAB), 15 min in 95% ethanol, and twice for 10 min in dry absolute ethanol). Sections were then washed twice in propylene oxide (Sigma) for 10 min, placed into resin (Durcupan ACM; Fluka) using modified forceps and left overnight at room temperature. The resin was then warmed to reduce its viscosity, sections were placed on greased microscope slides, a greased coverslip was applied, and the resin was cured at 65°C for 48 h.

2.2.4 Single-immunolabelling

Selected sections were labelled for either VGluT1 or VGluT2 using only the immunoperoxidase procedure above. These sections were treated as above except they were incubated in the osmium tetroxide solution for ~20 min. To test specificity of each antibody reaction each experiment was performed with either primary or secondary antibodies omitted.

The primary antibodies were raised against rat VGluT1, VGluT2 and TH. The distribution of immunolabelling at light and electron microscopic levels was distinct for each antibody and was consistent with previous observations (Moss & Bolam, 2008; Doig *et al.*, 2010; Henny *et al.*, 2012).

2.2.5 Electron microscopic analysis

All sections were examined in the light microscope, the glass cover slip was removed and then areas of the substantia nigra were cut from the slide, glued to the top of a resin block and trimmed with razor blades. Two blocks were taken from each animal, one from substantia nigra pas compacta (SNc) and one from substantia nigra pars reticulata (SNr). Serial sections, 50 nm thick (silver/grey), were then cut using an ultramicrotome (EM UC6; Leica Microsystems), and were collected on pioloform-coated, single-slot copper grids (Agar Scientific). The sections were then lead stained to improve contrast for electron microscopic examination. A Philips CM10 electron microscope was used to examine sections of tissue. All analyses were performed at a minimum of 5 μm from the tissue–resin border (i.e., the surface of the section). The maximum distance from the tissue–resin border examined was determined by the penetration of the gold-conjugated

antibody together with the angle at which the tissue–resin was sectioned and was therefore variable.

Sections on the grid were numbered from left to right, and a section was selected using a random number generator. Low magnification micrographs were recorded (indicated magnification: 5,800x) and all immunogold-positive post-synaptic elements in frame were recorded. Once 30-35 structures had been identified each structure was then examined in 5 serial sections at higher magnification (indicated magnification: 25,000x), using the low magnification micrograph as a map of the grid. Micrographs were taken of each structure in each of the 5 serial sections. Once collected, the micrographs were analysed in Fiji (Fiji: an open-source platform for biological-image analysis), to record the area of the structure, any synapses made onto the structures, length of the active zone of the synapse, area of the bouton producing synapses, the type of structure targeted (e.g. spine or dendrite) and if boutons were immunolabelled.

2.2.6 Statistical analysis

All statistical calculations were performed using the programme SigmaPlot (Version Systat Software, San Jose, CA). All data was tested for normality and Student's t-test was used if data passed. If data were not normal then the Wilcoxon Mann-Whitney test was used. All p-values are two tailed. Differences were considered significant when $p < 0.05$.

2.3. Results

2.3.1 Distribution of immunolabelling at the light microscopic level

The patterns of immunolabelling for each antibody were consistent with previously published data (Kaneko & Fujiyama, 2002; Doig *et al.*, 2010; Henny *et al.*, 2012) and consistent with prior observations within the basal ganglia laboratories of the MRC Unit.

VGluT1 and VGluT2 immunoreactivity was observed within bouton-like structures with no co-localisation observed in double-labelled control tissue at either the light or electron microscopic levels. TH immunolabelling showed no co-localisation with VGluT1 or VGluT2 immunolabelling, again this was confirmed at the electron microscope level.

A strong band of TH immunolabelling was present in the area expected to contain SNc dopaminergic cell bodies. At high magnification darkly labelled cell bodies and emerging dendrites were clearly visible. Dendrites were also visible in the area below the SNc, consistent with known extension of the dendrites of some dopaminergic SNc neurons into the SNr. Rare examples of cell bodies were seen within the SNr.

Small, punctate, labelled structures were observed within both the SNc and SNr in VGluT2-immunolabelled tissue. These were presumed to be synaptic boutons. Immunolabelling was not clearly visible within either SNc or SNr in the VGluT1-immunolabelled tissue, although this does not rule out the presence of synaptic boutons which may only be identifiable at the electron microscopic level.

Due to the close proximity of the ventral tegmental area, another region rich in dopaminergic neuron within the midbrain, and the known differences between dorsal

and ventral dopaminergic neurons within the SN, namely the relative protection from degeneration of dorsal dopaminergic neurons in Parkinson's disease and the presence of calcium binding proteins (Fearnley & Lees, 1991), it was important to ensure all samples for analysis at the electron microscopic level were from a comparable place. The SNc sample was taken from the centre of the strong band of TH immunolabelling (in the sagittal plane), and the SNr sample directly ventral to this (Figure 2.1).

2.3.2 Immunolabelling in the electron microscope.

In double-labelled tissue, cortical or subcortical glutamatergic boutons were identified by immunoperoxidase (DAB) labelling for VGluT1 or VGluT2, respectively and dopaminergic structures were identified by immunogold labelling for TH. Immunogold labelling appears as electron-dense gold particles of irregular size. A structure was deemed immunopositive if it contained at least 5 gold particles. Generally, structures were densely filled with particles (Figure 2.2a) and background staining was limited to single particles within structures (Figure 2.2b). Dense gold particle labelling was only found in dendrites and somata.

VGlutT1- and VGluT2-immunolabelled structures were identified by the presence of electron-dense DAB reaction product adhering to membranes, including the internal plasma membrane and the external membranes of organelles, notably vesicles and mitochondria (Figure 2.3). DAB reaction product was only found in axons and boutons. Typically, the DAB reaction product filled the entire bouton and no background labelling was seen. Tissue from 5 rats was systematically scanned and every TH-positive dendrite was examined. Dendrites were examined in at least 5 serial sections and all synapses formed were recorded.

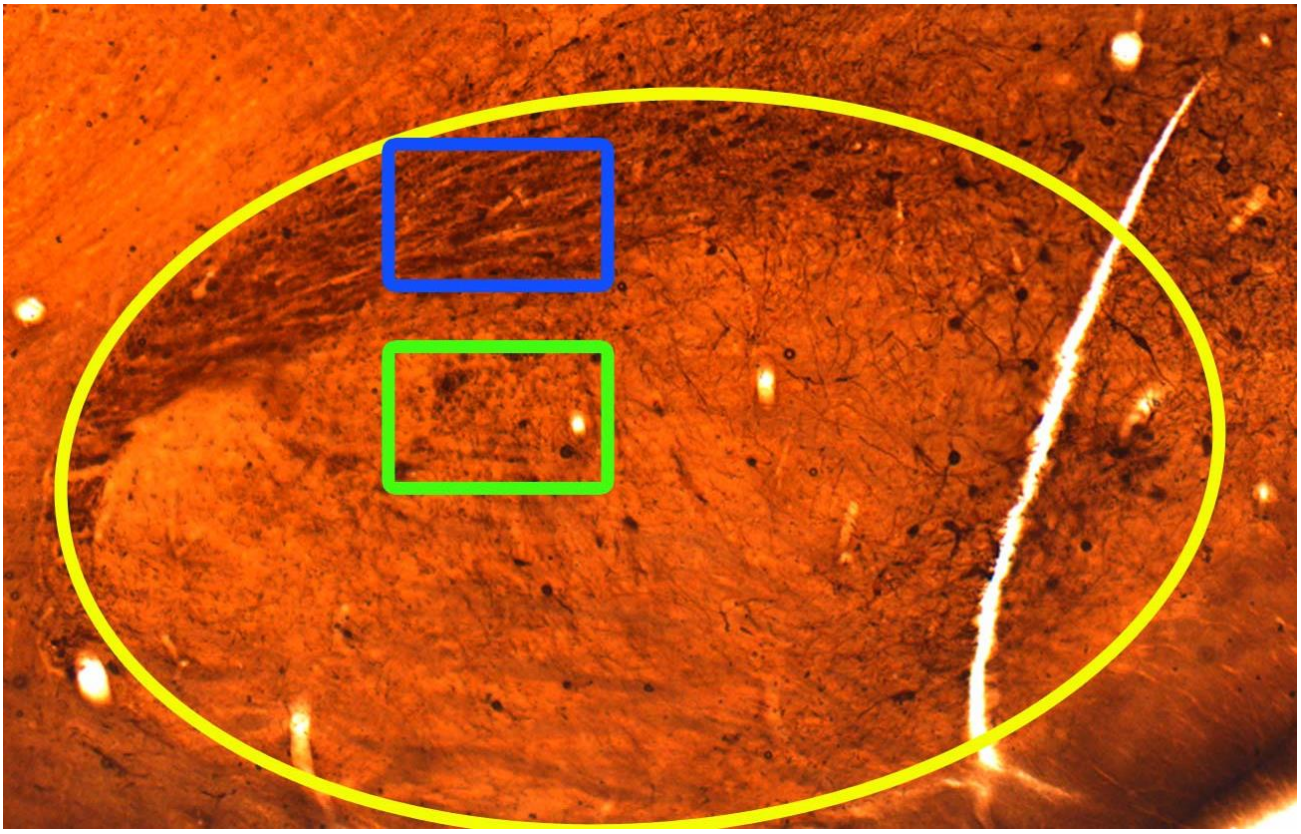


Figure 2.1: A light micrograph showing the area of substantia nigra used in analysis.

A sagittal section of rat brain immunolabelled for TH and VGluT1. Coloured boxes show the areas of brain sampled for analysis with SNc in blue and SNr in green. Note the intense band of labelling within the SNc showing the border between the two functional regions of SN (approximate border of SN based on atlas images shown in yellow).

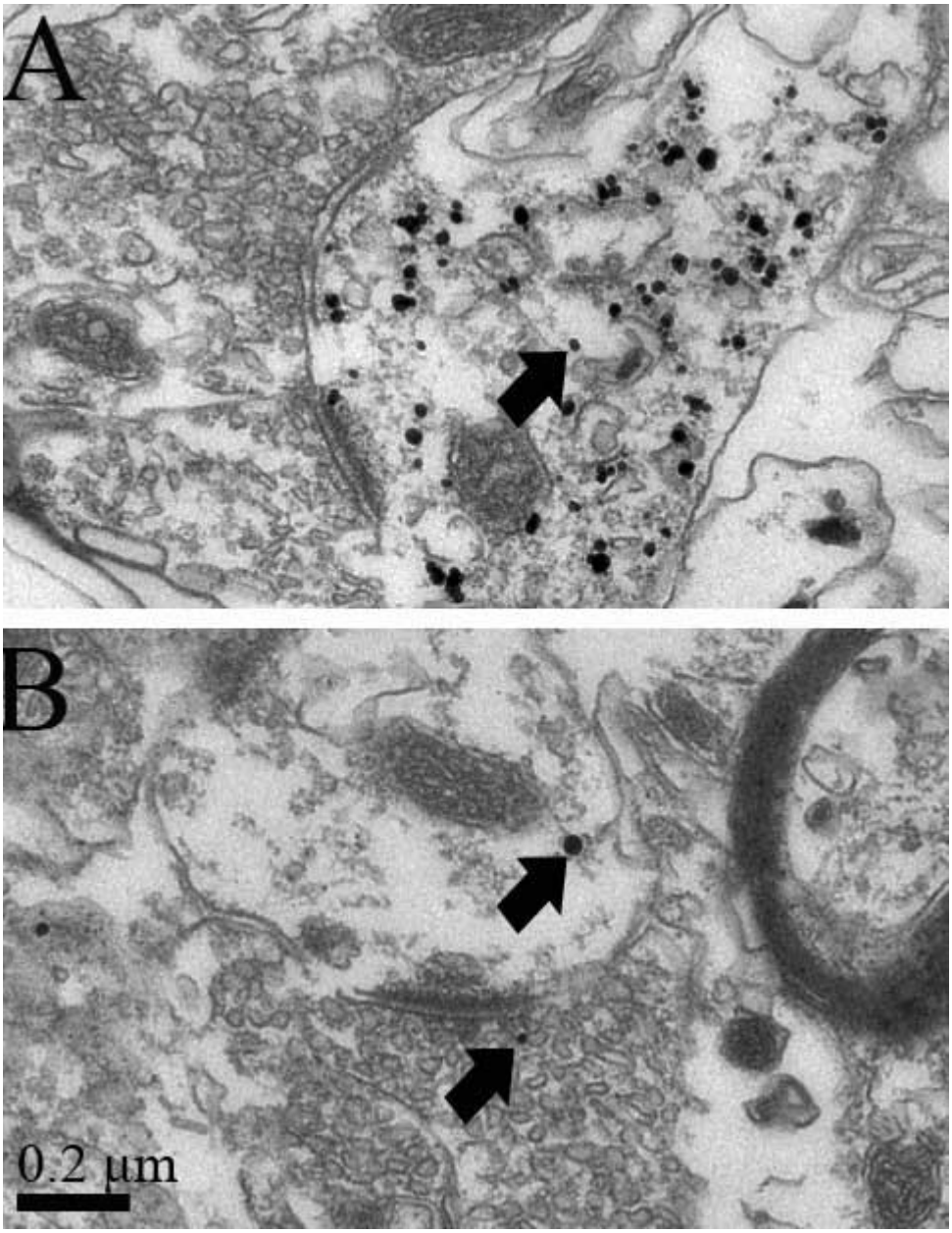


Figure 2.2: Examples of conjugated immunogold labelling.

A) An example of positive labelling for TH. B) An example of background labelling. Immunogold labelling was deemed positive by the presence of more than three gold particles within any given structure, although typically, labelling was much denser. Scale bar in B also applies to A. Examples of gold particles are shown with black arrows.

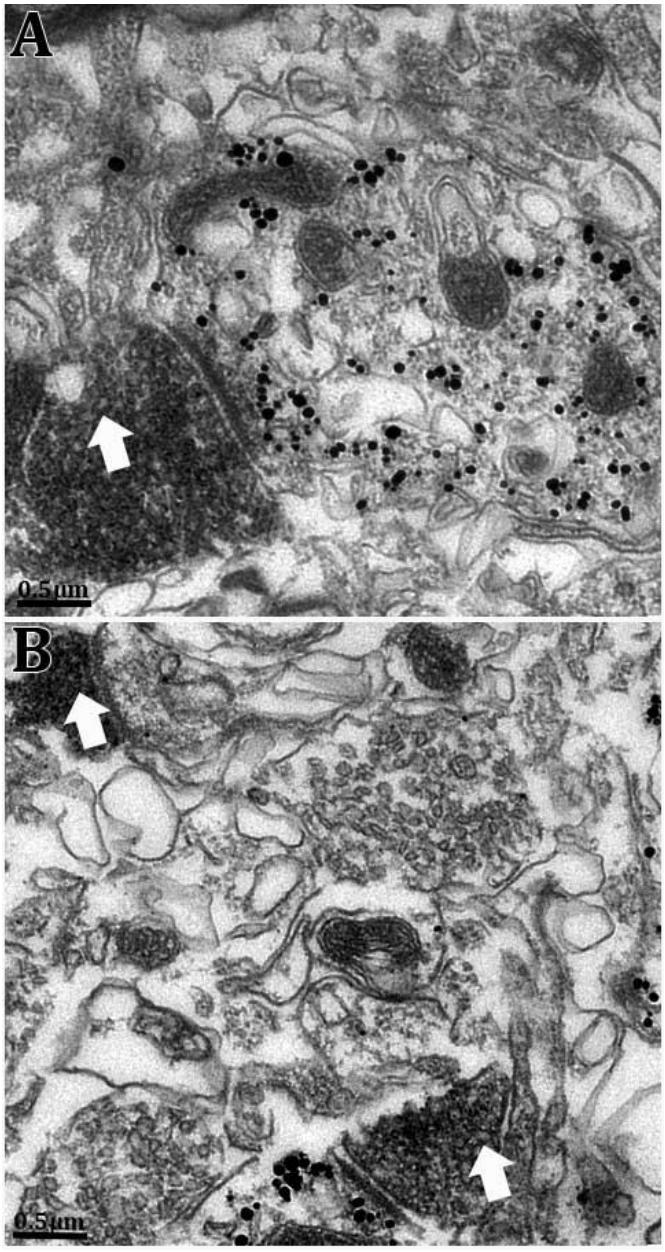


Figure 2.3: Micrographs showing DAB immunolabelling.

Examples of A) immunoperoxidase labelling for VGluT2 in a presynaptic bouton (tissue double labelled for VGluT2 and TH) and B) immunoperoxidase labelling for VGluT1 in presynaptic boutons (tissue double labelled for VGluT1 and TH). Notice how DAB reaction product adheres to membranes, particularly the vesicle membranes (white arrows).

Synapses were defined as regions where a bouton and its target are parallel and both a presynaptic and postsynaptic thickening of the plasma membranes is visible, the presynaptic bouton contains vesicles and electron dense material is present within the synaptic cleft. Synapses were categorised as either, type-1 or type-2 and either immunolabelled or unlabelled. Type-1 synapses (also referred to as asymmetric synapses) are defined as having a thick dense postsynaptic thickening of the plasma membrane (greater than ~20 nm), whereas type-2 synapses (also referred to as symmetric synapses) had relatively thinner postsynaptic thickening (less than 15 nm) examples of each are shown in Figure 2.4.

Type-2 synapses are deemed to be formed by putative inhibitory GABAergic boutons (Beaulieu & Somogyi, 1990). Dopaminergic boutons also produce type-2 synapses but these boutons are not generally found within the substantia nigra of rodents (Juraska *et al.*, 1977; Cragg *et al.*, 2004). Noradrenaline (NA) also produces type-2 synapses, again the production of NA also requires TH and boutons would therefore be immunopositive if present (Seguela *et al.*, 1990). Type-1 synapses are either excitatory synapses formed by glutamatergic boutons (Barbaresi *et al.*, 1997), or modulatory synapses formed with boutons utilising transmitters such as acetylcholine (Bevan & Bolam, 1995), or serotonin (Parent *et al.*, 2010).

2.3.3 TH-immunopositive structures within the SN

Pars Compacta

All TH-immunolabelled structures within the SNc were identified as dendrites or somata. Due to the large size of somata and the high magnification used (indicated magnification 25,000x) somata were not analysed during this study. Dendrites (Figures

2.2a and 2.5) ranged in cross sectional area from 0.25 μm^2 to 4.24 μm^2 (n = 198). The mean (± standard deviation) area of dendrites was 0.98 ± 0.20 μm^2 with 56% of dendrites within one standard deviation of the mean.

Pars Reticulata

Again all TH-immunolabelled structures were identified as dendrites or somata. However, the frequency of labelled structures was much lower, and as a result a larger amount of tissue was analysed to have a comparable number of dendrites. TH-immunopositive dendrites ranged in cross sectional area from 0.13 μm^2 to 2.57 μm^2 (n = 108). The mean (± standard deviation) area of dendrites was 0.84 ± 0.50 μm^2 with 68% of dendrites within one standard deviation of the mean.

2.3.4 Glutamatergic input to TH-immunopositive structures in the SNc

Proportion of synaptic boutons formed by VGluT1- and VGluT2-immunopositive boutons

In VGluT1-immunolabelled tissue a total of 253 TH-positive dendrites were examined. These formed synapses with a total of 241 axon boutons. Of the 241 boutons, 131 formed type-1 synapses, 15 of which were immunolabelled for VGluT1 (Figure 2.5a). The remaining 110 boutons formed type-2 synapses, none of which were immunolabelled.

In VGluT2-immunolabelled tissue 245 TH-positive dendrites were examined which formed synapses with a total of 246 boutons. Type-1 synapses were formed by 147 boutons, 43 of which were immunolabelled for VGluT2 (Figure 2.5b). Type-2 synapses were formed by 99 boutons, none of which were immunolabelled.

Each animal was considered separately and a mean calculated for each (n = 5). The mean and standard deviation of these means was then calculated and statistical analysis performed, data summarised in Figure 2.6a. Within the SNc 53.1 ± 7.9% (mean ± standard deviation) of synapses with TH-immunopositive dendrites were type-1; the remaining 46.9 ± 7.9% were type-2. VGluT1-labelled boutons formed 7.6 ± 6.0% of the total synapses (14% of all type-1 synapses) and VGluT2-labelled boutons formed 21.9 ± 6.3% of the total synapse (41% of all type-1 synapses). The remaining type-1 synapses (45%) were unlabelled; they were either false negatives for one of the glutamate markers, use a transporter that has yet to be defined, or were formed by cholinergic, serotonergic or noradrenergic boutons (Bolam *et al.*, 1991; Futami *et al.*, 1995; Parent *et al.*, 2010; Parent *et al.*, 2011; Watabe-Uchida *et al.*, 2012).

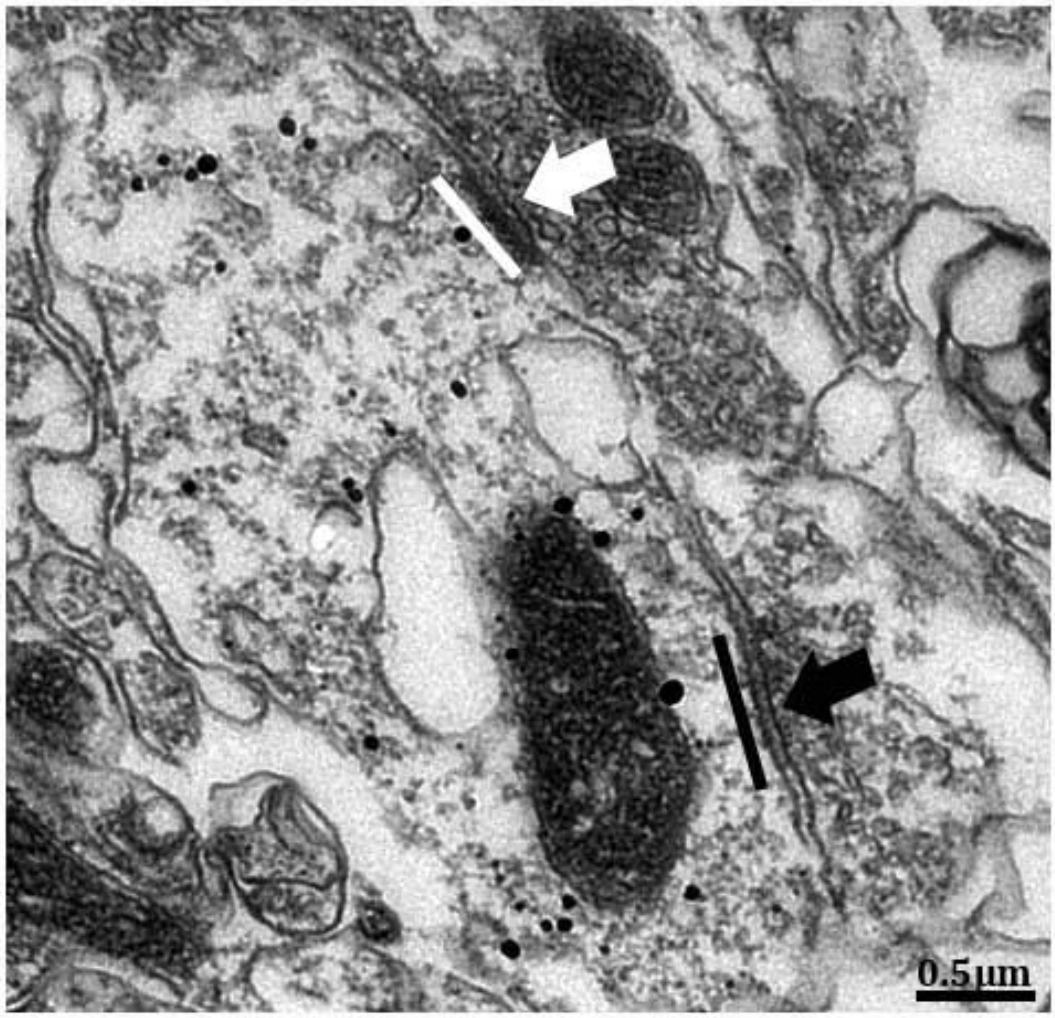


Figure 2.4: Examples of types of synapses formed with a TH-immunopositive dendrite.

Synapses were defined as regions where a bouton and its target are parallel and both a presynaptic and postsynaptic thickening is visible in the plasma membranes. The presynaptic bouton contains vesicles and electron dense material is present within the synaptic cleft. Synapses were categorised as either, type-1 or type-2 and either immunolabelled or unlabelled. Type-1 synapses (white arrow) are defined as having a thick postsynaptic density (greater than ~20 nm; parallel to white line), whereas type-2 synapses (black arrow) had relatively thinner postsynaptic thickening (less than 15 nm; parallel to black line).

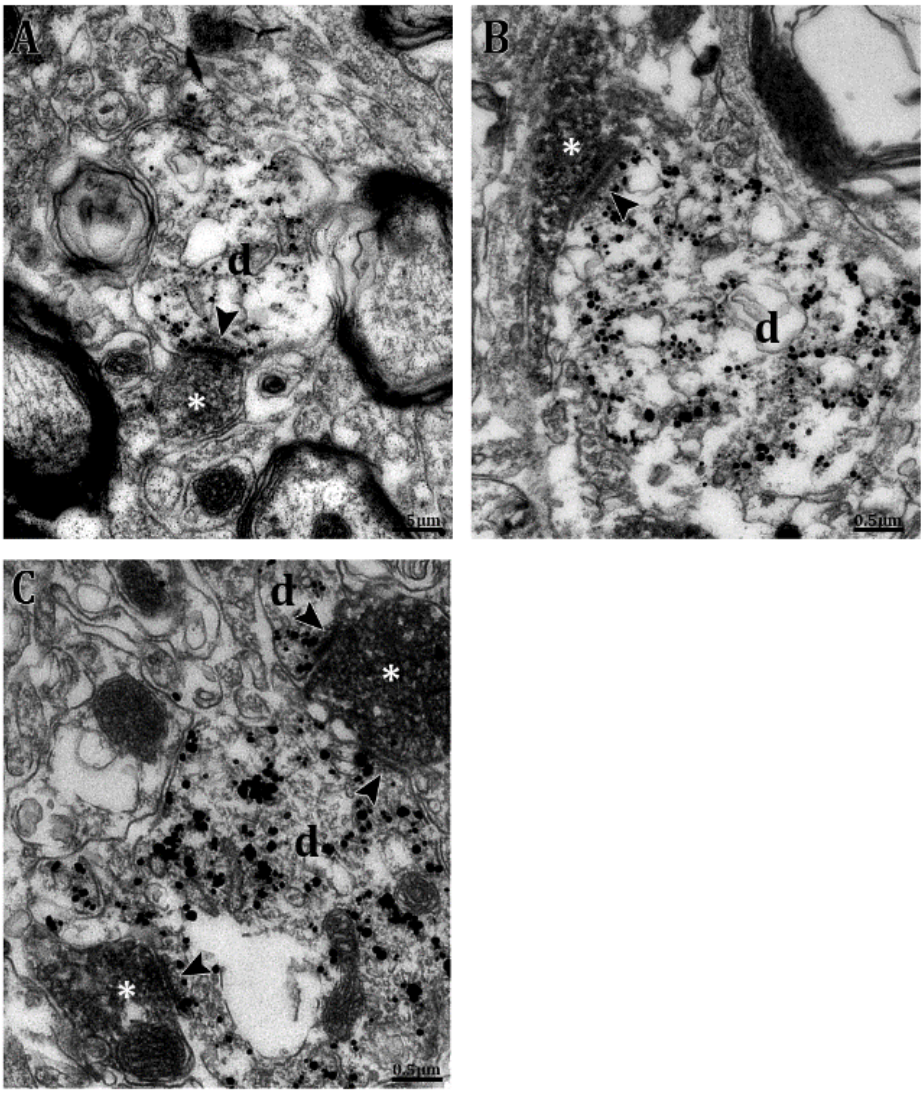


Figure 2.5: Glutamatergic synapses with TH-immunopositive dendrites.

A) A VGluT1-immunopositive bouton (*) forming a type-1 synapse (black arrowhead) with a TH-immunopositive dendrite (d) located within the SNc, B) A VGluT2-immunopositive bouton (*) forming a type-1 synapse (black arrowhead) with a TH-immunopositive dendrite (d) located within the SNc and C) A VGluT2-immunopositive bouton (*) forming a type-1 synapse (black arrowhead) with a TH-immunopositive dendrite (d) located within the SNr.

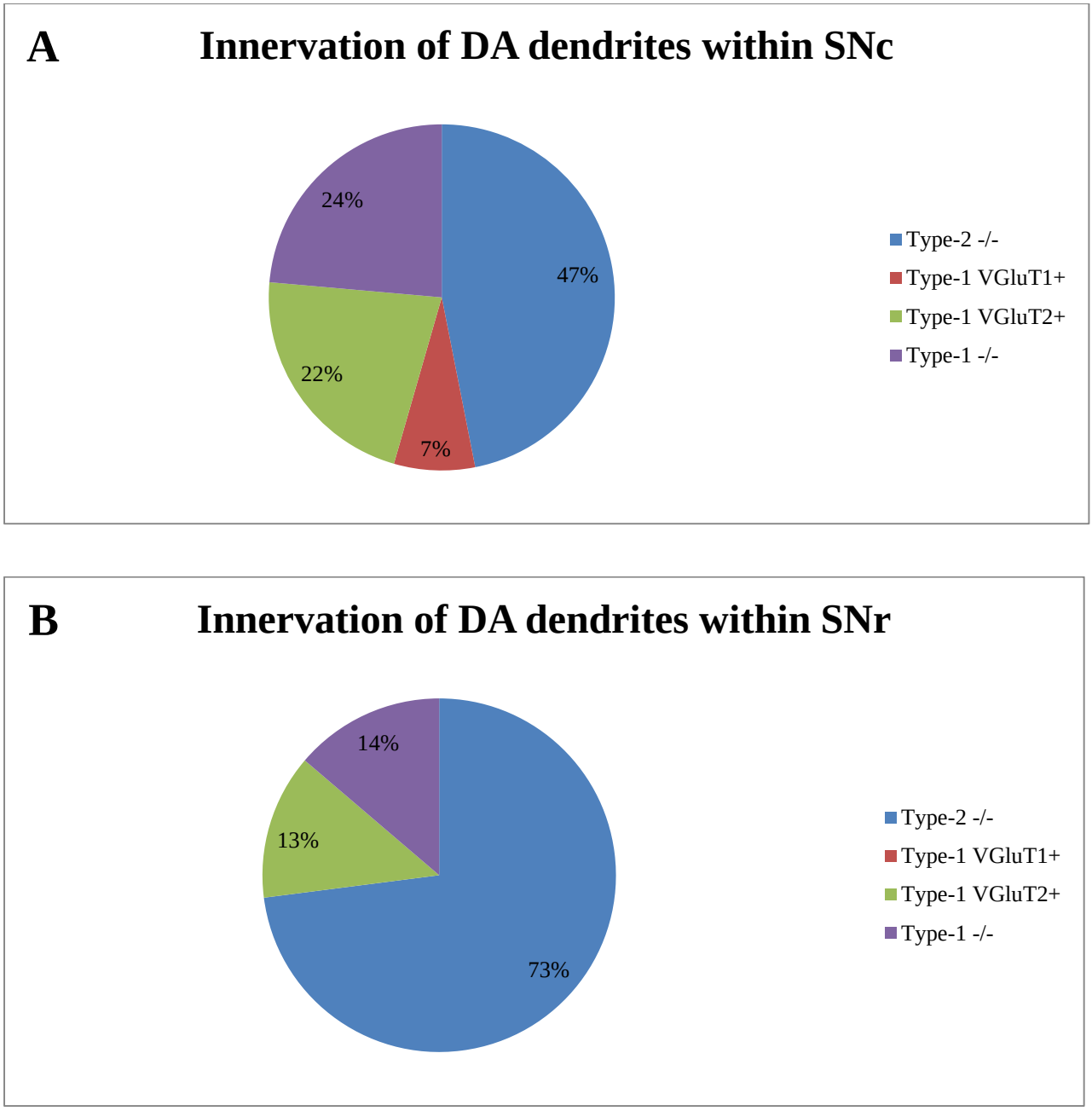


Figure 2.6: Summary of the proportion of immunolabelled synaptic boutons.

Summary pie-graphs showing the proportion of boutons forming synapses with TH-immunopositive dendrites in: A) SNc (487 synapses examined across 3 animals) and B) SNr (493 synapses examined across 3 animals). Data is separated by the type of synapse formed and the presence of immunolabelling within the bouton.

Characteristics of VGluT1-immunopositive boutons within SNc

Boutons forming synapses with TH-immunopositive structures were measured in each of the 5 sections to reveal the morphology of each subtype. In total, 104 boutons within the SNc were analysed in VGluT1-immunolabelled tissue (n = 3 animals). Of these, 10 were immunopositive for VGluT1. The mean cross-sectional area of VGluT1-immunopositive boutons was 0.23 ± 0.02 μm^2, with an active zone length of 0.24 ± 0.03 µm. The TH-immunopositive structures targeted by VGluT1-immunopositive boutons had a cross-sectional area of 0.84 ± 0.40 μm^2 and were all dendrites. Data summarised in Table 2.1.

Characteristics of VGluT2-immunopositive boutons within SNc

In VGlutT2-immunolabelled tissue, 94 boutons across 3 animals were analysed. Of these 24 were immunopositive for VGluT2. The mean cross-sectional area of VGluT2-immunopositive boutons was 0.39 ± 0.07 μm^2, with an active zone length of 0.29 ± 0.03 µm. The TH-immunopositive structures targeted by VGluT2-immunopositive boutons had a cross-sectional area of 0.94 ± 0.22 μm^2 and again were all dendrites. Data summarised in Table 2.1.

A

Labelling	Synapse Type	Terminal Size (μm^2)	Size of Target (μm^2)	Active Zone Size (μm)	Main Target Type	Secondary Target Type
VGluT1+ (n=10)	1	0.23 ± 0.02	0.84 ± 0.40	0.24 ± 0.03	Dendrites (89%)	Somata (11%)
VGluT1- (n=49)	1	0.28 ± 0.06	0.81 ± 0.37	0.28 ± 0.02	Dendrites (100%)	
VGluT1- (n=45)	2	0.28 ± 0.03 (a)	1.28 ± 0.22 (a)	0.27 ± 0.02 (a)	Dendrites (97%)	Somata (3%)

(a) Type-2 boutons have statistically larger area, active zone and target size in SNc than in SNr ($p<0.05$).

B

Labelling	Synapse Type	Terminal Size (μm^2)	Size of Target (μm^2)	Active Zone Size (μm)	Main Target Type	Secondary Target Type
VGluT2+ (n=24)	1	0.39 ± 0.07	0.94 ± 0.22	0.29 ± 0.03	Dendrites (100%)	
VGluT2- (n=27)	1	0.22 ± 0.03	0.63 ± 0.11	0.30 ± 0.02	Dendrites (100%)	
VGluT2- (n=43)	2	0.31 ± 0.04	0.82 ± 0.19	0.25 ± 0.04	Dendrites (100%)	

Table 2.1: Summary of the morphological characteristics of synaptic boutons and their targets.

A) VGluT-1 immunolabelled tissue from SNc, B) VGluT-2 immunolabelled tissue from SNc, C) VGluT-2 immunolabelled tissue from SNr. Sizes shown as mean ± standard deviation.

C

Labelling	Synapse Type	Terminal Size (μm^2)	Size of Target (μm^2)	Active Zone Size (μm)	Main Target Type	Secondary Target Type
VGluT2+ (n=19)	1	0.43 ± 0.06 (b)	1.21 ± 0.30	0.30 ± 0.06	Dendrites (100%)	
VGluT2- (n=14)	1	0.22 ± 0.01 (b)	0.74 ± 0.19	0.25 ± 0.03	Dendrites (100%)	
VGluT2- (n=75)	2	0.23 ± 0.02 (a)	0.76 ± 0.17 (a)	0.22 ± 0.05 (a)	Dendrites (100%)	

(a) Type-2 boutons have statistically larger area, active zone and target size in SNc than in SNr ($p<0.05$).

(b) VGluT2-immunopositive boutons forming type-1 synapses had a statistically larger area than VGluT2-immunonegative boutons forming type-1 synapses ($p<0.05$).

Table 2.1: Summary of the morphological characteristics of synaptic boutons and their targets.

A) VGluT-1 immunolabelled tissue from SNc, B) VGluT-2 immunolabelled tissue from SNc, C) VGluT-2 immunolabelled tissue from SNr. Sizes shown as mean ± standard deviation.

Characteristics of type-2 synapse forming boutons within SNc

In VGluT1-immunolabelled tissue, 45 of the 104 boutons formed type-2 synapses. As found previously all of these boutons were immunonegative. The mean cross-sectional area of boutons was 0.28 ± 0.03 μm^2, with an active zone length of 0.27 ± 0.02 µm. The dendrites targeted by these boutons had a cross-sectional area of 1.28 ± 0.22 μm^2 and unlike previously both TH-immunopositive dendrites and TH-immunopositive somata were targeted with a 95:5 ratio (somata not measured due to their large size). Data summarised in Table 2.1.

2.3.5 Glutamatergic input to TH-immunopositive structures in the SNr

Proportion of synaptic boutons formed by VGluT1- and VGluT2-immunopositive boutons

The analysis performed above was repeated on the grids containing SNr tissue. In VGluT1-immunolabelled tissue 188 TH-positive structures were examined, receiving a total of 298 synapses. All TH-positive structures examined within SNr were dendrites. In the VGluT2-labelled tissue 160 TH-positive structures were examined, which received a total of 195 synapses. Again synapses were examined in 5 serial sections to identify the type of synapse formed.

Within the SNr 27.0 ± 5.1% of synapses with TH-immunopositive dendrites were type-1; the remaining 73.0 ± 5.1% were type-2. No boutons were immunolabelled for VGluT1 and 13.3 ± 5.4% boutons were VGluT2-positive (Figure 2.5c; 49% of all type-1 synapses). The remaining type-1 synapses were unlabelled (51% of all type-1 synapses). This is summarised in Figure 2.6b.

Characteristics of VGluT2-immunopositive boutons

In the previous analysis no boutons forming synapses with TH-immunopositive structures in the SNr were immunopositive for VGluT1. In tissue immunolabelled for VGluT2, 108 boutons were analysed (forming 33 type-1 and 75 type-2 synapses). Of these, 19 synapses were formed with boutons immunopositive for VGluT2. The mean cross-sectional area of boutons was 0.43 ± 0.06 μm^2 with an active zone length of 0.30 ± 0.06 µm. The mean cross-sectional area of their TH-immunopositive targets was 1.21 ± 0.30 μm^2. Data are summarised in Table 2.1.

Characteristics of unlabelled boutons forming type-1 synapses

As no VGluT1-immunolabelled boutons forming synapses with TH-immunopositive structures within the SNr it can be presumed that all VGluT2-immunonegative type-1 boutons are also VGluT1-immunonegative. Of the 108 boutons analysed, 14 formed type-1 synapses and were immunonegative for VGluT2. The mean cross-sectional area of boutons was 0.22 ± 0.01μm^2 with an active zone length of 0.25 ± 0.03µm. The mean cross-sectional area of their TH-immunopositive targets was 0.74 ± 0.19μm^2. Data are summarised in Table 2.1.

Characteristics of boutons forming type-2 synapses

Unlabelled boutons forming type-2 synapses were also examined within the SNr. Of the 108 boutons analysed, 75 formed type-2 boutons. The mean cross-sectional area of boutons was 0.23 ± 0.02 μm^2 with an active zone length of 0.22 ± 0.05 µm. The mean cross-sectional area of their TH-immunopositive targets was 0.76 ± 0.17 μm^2. Data are summarised in Table 2.1.

2.3.6 Statistical analyses

Proportions of immunopositive boutons

Within the SNc there was no significant difference ($p > 0.05$) between the proportions of type-1 and type-2 synapses made with TH-immunopositive dendrites. In contrast, within SNr there were significantly more ($p = 0.001$) type-2 synapses formed with putative dopaminergic dendrites than type-1. VGluT2-immunopositive boutons accounted for a higher proportion of type-1 synapses formed than VGluT1-immunopositive boutons in both regions (SNc: $p = 0.010$, SNr: $p = <0.001$).

Morphology of boutons

Within the SNc VGluT1-immunopositive boutons were not statistically different in morphology from VGluT2-immunopositive boutons (all p values > 0.05). Additionally, VGluT2-immunopositive boutons in the SNc were not statistically different in morphology from those found within the SNr in any way (all p values > 0.05).

Type-2 synapse forming boutons within the SNc were found to have statistical differences in morphology from those found within the SNr. Boutons within the SNc had larger cross-sectional areas ($p = 0.010$), larger active zones ($p = 0.025$) and targeted significantly larger structures within the SNr ($p = 0.001$).

Finally, the unlabelled boutons forming type-1 synapses in the SNr were found to have a smaller cross-sectional area than those which were VGluT2-immunopositive ($p= 0.002$), although the active zones and target sizes were comparable ($p = 0.513$ and 0.159 respectively).

2.4 Discussion

2.4.1 Summary of results

The results of the present study demonstrate that afferent innervation of the SN, and in particular putatively dopaminergic neurons in the SN, differs between the functionally distinct territories of the SN i.e. the pars compacta and the pars reticulata. Putatively dopamine (TH-immunopositive) neurons of the SNc receive an equal innervation, in terms of the numbers of synapses, from putative inhibitory (i.e. type-2 synapses) and putative excitatory (i.e. type-1 synapses) terminals. Indeed this is confirmed by the analysis of the excitatory input from VGluT-positive terminals that are derived from both cortical and subcortical areas. In contrast, the dopamine neurons of the SNr, receive primarily inhibitory innervation (i.e. type-2 synapses) and only receive excitatory input originating in subcortical structures.

Boutons providing inhibitory input to the SNc putatively dopaminergic structures (i.e. type-2 synapses with TH-immunopositive structures) derived from the striatum and GPe (Smith *et al.*, 1990a; Smith & Bolam, 1991; Bolam *et al.*, 1993; Bevan *et al.*, 1996) are larger than the boutons innervating dopaminergic structures in the SNr. They target larger dendrites, and therefore presumably more proximal, and form larger active zones. This suggests that individual inhibitory synapses on a dopaminergic neuron in the SNc will have a greater effect because of its more proximal location. However it should be noted that the overall inhibitory innervation of dopaminergic structures in the SNr is greater than those in the SNc and indeed, the inhibitory response of an individual dopaminergic neuron to an aversive stimulus correlates with the length of its dendrites in the SNr and proportion of GABAergic afferent terminals (Henny *et al.*, 2012).

The cross-sectional area of boutons, and the morphology of their synapses, providing excitatory glutamatergic innervation of dopaminergic neurons were similar regardless of their location or VGluT subtype.

The putatively excitatory VGluT2-negative innervation of SNr (and potentially SNc, although this could not be separated from the VGluT1-negative boutons using the above protocol) is formed by smaller boutons than the VGluT-immunopositive boutons. This suggests that this population is unlikely to be false negatives for either of the VGluT antibodies or indeed glutamatergic, and instead is likely to comprise cholinergic (Clarke *et al.*, 1987; Beninato & Spencer, 1988), or serotonergic boutons (Hashemi *et al.*, 2011; Parent *et al.,* 2011). Noradrenergic boutons are unlikely to account for the VGluT-negative type-1 synapses as only a single case of a TH-immunopositive bouton (which is likely to be noradrenergic) was observed, and this did not make contact with another TH-immunopositive structure; it is thus likely that any noradrenergic innervation is either very sparse (as seen in SN of guinea pig (Cragg *et al.,* 1997)) or not present. Additionally, the locus coeruleus, the main source of noradrenaline in the CNS, was not found to have monosynaptic connections with dopamine neurons of the SNc in the whole brain mapping performed by Watabe-Uchida (Watabe-Uchida *et al.*, 2012; Ferrucci *et al.,* 2013). Figure 2.7 shows a circuit diagram of the basal ganglia updated to reflect the results of these experiments.

2.4.2 Comparisons to previous studies

The afferent input to TH-positive neurons in the SN has been previously examined using electron microscopy by Henny et al (2012). Henny examined the afferent input to single

identified DA neurons of the SN using antibodies against VGluT2 and VGAT (vesicular GABA transporter, a marker of inhibitory boutons), noting whether the synapse formed

on dendrites within the SNc or SNr. The results of the current study of synapses formed by VGluT2-positive boutons and type 2 synapses (analogous to synapses formed by VGAT-immunopositive boutons) were not significantly different (single sample t-test, $p > 0.05$) from those obtained previously (Henny *et al*, 2012; Figure 2.8). Henny et al focused on the GABAergic boutons forming synaptic contacts with physiologically characterised DA neuron dendrites, noting that as dendrites extended from the SNc into the SNr a greater density of GABAergic innervation was found. Furthermore, this greater density of GABAergic innervation in the SNr was correlated with the response to aversive stimuli. Thus the small population of SNc DA neurons that are inhibited by aversive stimuli (Brown *et al.*, 2009; Henny *et al.*, 2012), are more likely to have a high density of GABAergic innervation in the SNr and the degree of inhibition correlates with the degree of GABA innervation. It may be that SNc dopamine neurons can be separated into two populations, distinct by afferent innervation and the location of dendrites which then correlates with their differing responses to aversive stimuli, implying distinct functional roles.

The analysis performed in this study is less time consuming, less technically demanding and uses less animals than the analysis performed by Henny et al, and the comparable results provide evidence for the accuracy of this simpler methodology. It should be noted however, that the analysis of Henny and colleagues was performed on single, physiologically identified dopamine neurons, whereas the current analysis was carried out at the *population level*, the data would thus average out any differences in differing subpopulations of DA neurons.

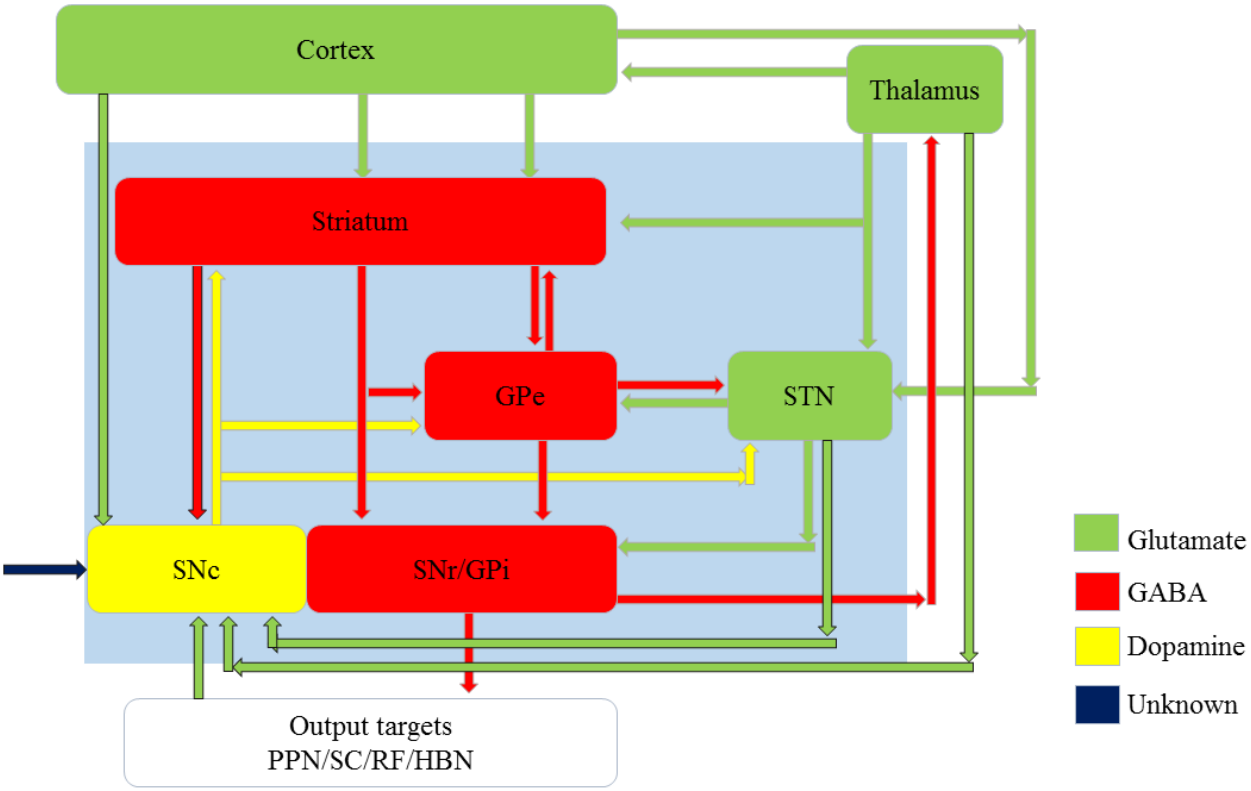
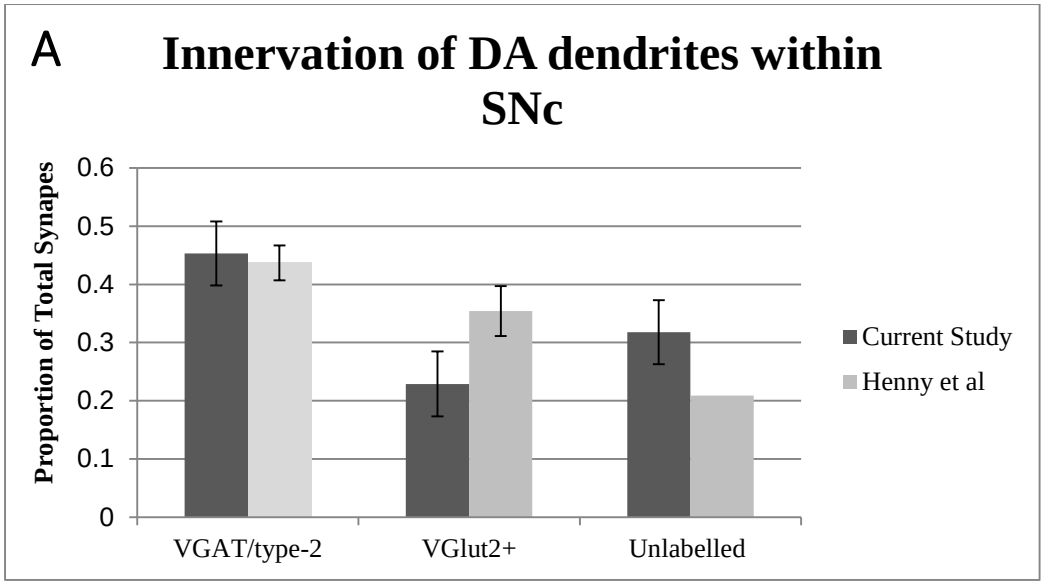


Figure 2.7: A more complete diagram of basal ganglia circuitry.

The standard model of basal ganglia circuitry updated to show the connectivity of dopaminergic neurons located within the SNc. Pathways studied in this thesis are highlighted.

GPe, globus pallidus external segment; GPi, globus pallidus internal segment; HBN, lateral habenula; PPN, pedunculopontine nucleus; RF, reticular formation; SC, superior colliculus; SNc, substantia nigra compacta; SNr, substantia nigra reticulate; STN, subthalamic nucleus.



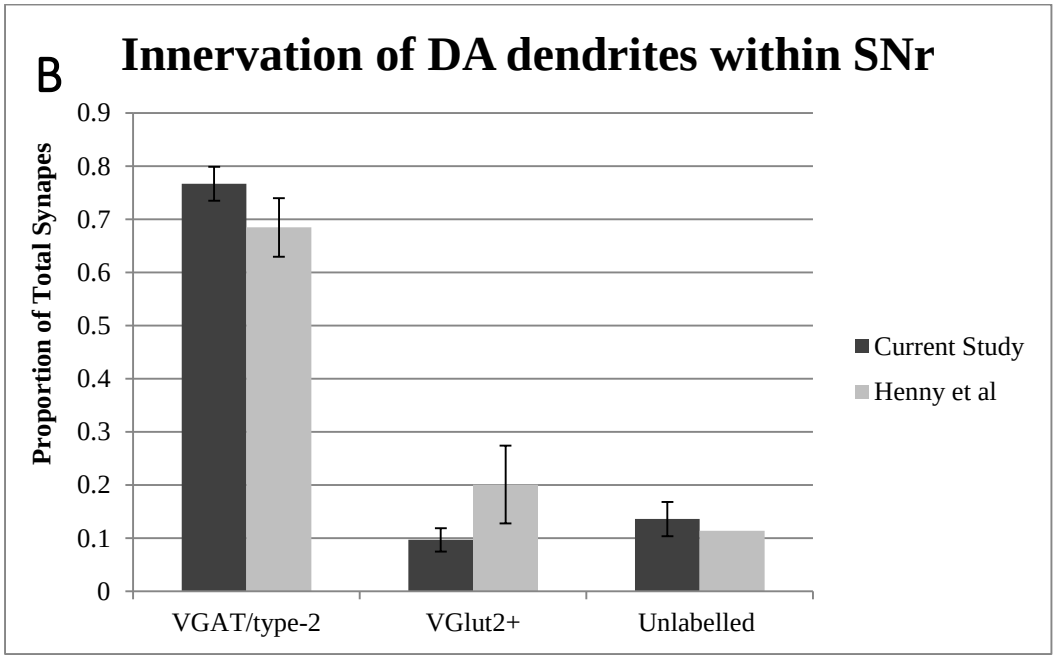


Figure 2.8: Comparison of current data to published work.

Data extracted from Henny et al (2012) was directly compared to the present study. In both SNc (A) and SNr (B) no statistical differences were found between the proportions of VGAT-immunopositive boutons and type-2 synaptic boutons or the proportions of unlabelled synaptic boutons.

2.4.3 Functional significance of glutamate in the SNc

Several early studies (Carter, 1982; Kornhuber *et al.*, 1984; Nitsch *et al.*, 1984; Sakai, 1988; Naito & Kita, 1994) reported a direct projection from the cortex to the substantia nigra, although the post-synaptic targets of the cortical afferents (i.e. dopaminergic or GABAergic) were not identified. However, this projection has been largely omitted from standard models of substantia nigra innervation. Typically, models show only GABAergic innervation from the striatum and globus pallidus with additional pathways from PPN, STN and dorsal raphe. A recent whole brain analysis of monosynaptic connections of dopaminergic neurons within the SNc, using a modified rabies virus, revealed a much broader picture (Watabe-Uchida *et al.*, 2012) with additional direct projections from prefrontal cortex, somatosensory cortex, M1 and M2 motor cortices, hypothalamus, amygdala and small projections from several thalamic nuclei including parafascicular nucleus. This study confirms the presence of direct monosynaptic connections between VGluT1-positive terminals (putatively cortical in origin) and DA neurons of the SNc. This means that cortical information can flow through the basal ganglia via four different pathways (Figure 2.9b), each with a differing number of synapses and a different conduction latency: through the indirect pathway, through the direct pathway, through the cortico-subthalamic pathway (sometimes referred to as the hyperdirect pathway) and directly to the neurons of the SNc. These parallel pathways may be transmitting similar information about a stimulus, priming the output nuclei with the early signals and rapidly reinforcing them with the later signals.

Dopamine neurons are known to rapidly increase firing, in the form of burst, in response to a rewarding stimuli (Schultz, 1998). The somatosensory system is in a strong position to supply information regarding rewarding stimuli, and thus the cortio-nigral projection

could assist in the rapid dopaminergic response to reward. The motor cortices are known to contribute to the cortico-subthalamic pathway and are believed to aid in the centre-surround theory of fine motor control (Nambu *et al.*, 2002), silencing unwanted motor programs prior to selecting the appropriate motor pattern. The cortico-nigral projection from M1 and M2 may be aiding in this centre-surround activity by increasing dopamine concentrations both in the subthalamic nucleus but also in the entire basal ganglia.

A large amount of the subcortical innervation of SNc, and to a lesser extent the SNr, is likely to be arising from PPN based on previous findings (Futami *et al.*, 1995). PPN is again implicated in the reward circuit (Inglis *et al.*, 2000), switching the brain from an inactive sleep state to an active alert state (Mena-Segovia *et al.*, 2008) and is also implicated in the planning of movement (Tattersall *et al.*, 2014). Indeed, lesions of the PPN prevent rats from forming reward-based conditional responses (Florio *et al.*, 1999). Pan and Hyland (Pan & Hyland, 2005) proposed that PPN neurons relay the timing of salient events to the dopaminergic reward system, inducing a burst of firing within DA neurons during a salient stimulus. PPN activity appears to selectively influence burst activity of DA neurons, without affecting overall firing rate. It is suggested that PPN responds to all salient activity, assigning timing, whilst additional inputs such as the somatosensory system may transmit information on the rewarding nature of the stimulus.

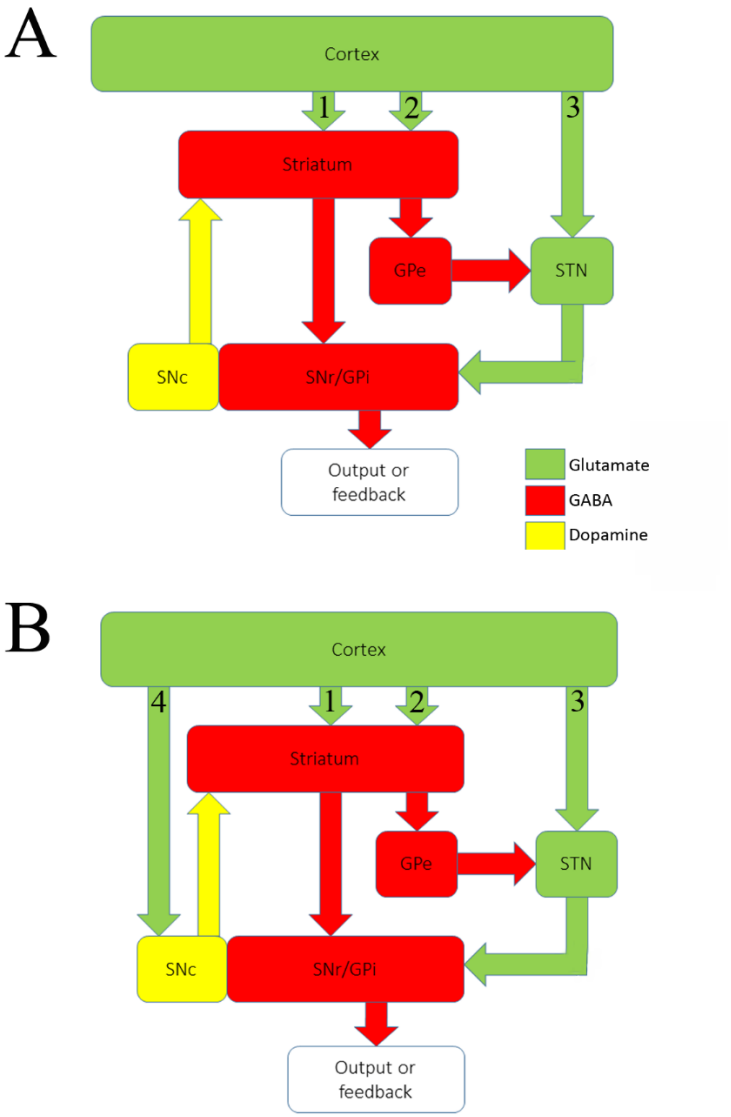


Figure 2.9: Cortical information flow though the basal ganglia.

A highly simplified diagram showing the various pathways of cortical innervation of the basal ganglia. A) The classical three pathways of cortical information flow. B) An updated model showing four parallel pathways of cortical information flow.

GPe, globus pallidus external segment; GPi, globus pallidus internal segment; SNc, substantia nigra compacta; SNr, substantia nigra reticulate; STN, subthalamic nucleus.

Indeed it has been shown that the superior colliculus can supply dopaminergic neurons with short-latency input related to visual information (Comoli *et al.*, 2003), the cortical innervation to dopaminergic neurons may transmit the related somatosensory information about the stimulus allowing DA neurons to link visual stimuli with rewarding stimuli. DA neurons summate information from various sources about the nature of stimuli, linking attention, sensation and timing, resulting in accurate reward-prediction – a well-documented function of the dopamine system (Schultz, 1998). Together this data suggests that the glutamatergic innervation of the substantia nigra warrants further investigation, both to the source of innervation but also the resulting effects on dopamine neuron firing and dopamine release within the basal ganglia.

Chapter Three

Innervation of the Subthalamic Nucleus

3.1 Introduction

The STN is the only nucleus within the basal ganglia which utilises the excitatory amino acid, glutamate, in its projections, which innervate a wide range of basal ganglia nuclei (Smith & Parent, 1988; Smith *et al.*, 1998). As such it is able to exert substantial influence over the activity of targeted brain regions. STN neurons receive innervation from a wide range of sources, but it is generally accepted that the main controllers of STN neuron firing are the cerebral cortex and globus pallidus external segment (GPe) (Joel & Weiner, 1997). Extrinsic synaptic excitation does not create the firing pattern of STN neurons, simply modifying the timing of autonomic pacemaker firing. This makes predicting the responses of STN neurons more complex than simply balancing excitatory and inhibitory inputs (Wilson & Bevan, 2011).

In some disease states, such as Parkinson's disease, beta oscillations are present in large areas of the basal ganglia and cortex (Brown, 2006; Little & Brown, 2014). It is currently not known where this oscillatory activity is generated but reciprocal connections between GPe and STN form a recurrent feedforward loop, which is capable of generating oscillations (van Schouwenburg *et al.*, 2013). Additionally, the wide-spread control which the STN and GPe exert over the basal ganglia and its output nuclei could allow the oscillation to entrain many brain regions (see Section 1.3.2).

Understanding the afferent input to STN neurons can help develop computational models of basal ganglia firing both in normal and disease states, potentially uncovering the likely role of the STN in the generation of oscillations. Furthering knowledge of the control of STN neuron firing can help to develop new treatment strategies for movement disorders. Both historically and currently the STN has been central to surgical treatments

of movement disorders, either by lesioning or deep brain stimulation (Chao *et al.*, 2007). The mechanism behind these treatments is still unknown, although multiple theories exist, and therefore it is essential to uncover more about this small, but critical nucleus.

The aim of this study was to quantify the main projections to the STN. A quantitative analysis of synapses formed with dendrites in the STN was conducted on tissue immunolabelled to reveal markers of cortical glutamatergic- (vesicular glutamate transporter 1; VGluT1), subcortical glutamatergic- (vesicular glutamate transporter 2; VGluT2), GABAergic- (vesicular GABA transporter; VGAT), catecholaminergic such as dopaminergic- (TH), or cholinergic- (vesicular acetylcholine transporter; VAChT) terminals.

3.2 Materials and Methods

3.2.1 Animals

All experiments were conducted in accordance with the Animals (Scientific Procedures) Act 1986 (UK). Procedures were performed on adult male Sprague Dawley rats (350-480g).

3.2.2 Tissue Preparation

Rats were anaesthetised with sodium pentobarbitone (200 mg/kg, Rhône Mérieux) then perfused through the heart with ~ 50 ml of phosphate buffered saline (PBS, 0.01 M phosphate buffer, pH 7.4, 0.876% NaCl, 0.02% KCl) followed by 300 ml of fixative (0.1 M phosphate buffer, pH 7.4, 3% paraformaldehyde, 0.1% glutaraldehyde) over ~20 min. Free fixative was removed by post-perfusion with PBS. The brain was removed and stored in PBS until cut into 60 µm parasagittal sections using a vibrating blade microtome (VT1000S; Leica).

3.2.3 Immunohistochemistry

All methods were conducted as previously published (Moss & Bolam, 2008; Henny *et al.*, 2012; Doig *et al.*, 2014).

All sections were washed three times in PBS and placed into a cryoprotectant (0.05 M PB, 25% sucrose, 10% glycerol) overnight (~15 h) before freeze-thawing. Each section was placed in separate wells of a 6-well plate and excess cryoprotectant removed. The plate was then placed into liquid nitrogen for approximately 30 s, removed and warmed cryoprotectant was immediately added to the well. Sections were then stored in

cryoprotectant for at least one hour before the freeze-thaw process was repeated, thawing with warmed PBS. Sections were then washed three times with PBS.

Sections were immunolabelled to reveal: VGluT1, VGluT2, TH, VGAT (vesicular GABA transporter; marker of GABAergic boutons) or VAChT (vesicular acetylcholine transporter; marker of cholinergic boutons)

NGS-PBS (10%, Vector Laboratories) was used to block sections before the addition of primary antibodies. Antibodies against TH (mouse monoclonal antibody, SigmaT2928, 1:1000 dilution), VGAT (rabbit, Synaptic Systems 131-003, 1:500 dilution), VGluT2 (rabbit, Synaptic Systems 135-403, 1:2000 dilution), VGluT1 (rabbit, MAb Tech VGlutT1-3, 1:2000) or VAChT (rabbit, Sigma V-5387, 1:500 dilution) and left overnight shaking at room temperature. Antibodies were diluted in PBS containing 2% NGS. Sections were washed three times in PBS and then incubated with a biotin-conjugated goat antibody against rabbit or mouse antibodies accordingly (rabbit: BA1000, Vector, diluted 1:200 in PBS; mouse: BA9200, Vector diluted 1:1000 in PBS) for 2 h at room temperature on a shaker. Sections were then washed three times in PBS and incubated in an avidin-biotin-peroxidase complex (ABC; Vector Laboratories, prepared according to the manufacturers' instructions) for 90 min with shaking at room temperature.

After the ABC incubation, sections were washed three times in PBS and twice in TRIS buffer (0.05 M, pH 7.4). Diaminobenzidine (DAB; 2 ml of 0.025% in TRIS buffer; Sigma) was added to sections and left for 20 min at room temperature with regular shaking. H_2O_2 (final concentration: 0.002%; BDH) was added and the reaction was allowed to continue for 5-6 min until staining was revealed. The reaction was stopped by removal of the DAB solution and addition of TRIS buffer; the sections were then

washed 3 times in TRIS buffer and three times with 0.1 M phosphate buffer (PB; pH 7.4).

The sections were then placed flat in glass Petri dishes and osmium tetroxide (1% in PB; Oxkem) was applied for ~20min. They were then washed three times with 0.1 M PB and dehydrated in a series of ethanol dilutions (twice for 10 min in 50% ethanol, 45 min in 70% ethanol that included 1% uranyl acetate (TAAB), 15 min in 95% ethanol, and twice for 10 min in dry absolute ethanol). Sections were then washed twice in propylene oxide (Sigma) for 10 min, placed into resin (Durcupan ACM; Fluka) using modified forceps and left overnight at room temperature. The resin was then warmed to reduce its viscosity, sections were placed on greased microscope slides, a greased coverslip was applied, and the resin was cured at 65°C for 48 h.

3.2.4 Controls for the immunolabelling

Control experiments were run to ensure the specificity of the antibodies used. Double labelling was carried out as described previously using immunogold and DAB (Section 2.2.3) using the following combinations: 1) VGluT1 & VGluT2, 2) VGluT1 & TH, 3) VGluT2 & TH, 4) VGAT & TH. Attempts were made to double label VAChT & VGluT2, VAChT & VGluT1 and VAChT & VGAT but were repeatedly unsuccessful. To test antibody specificity all single immunolabelling experiments were carried out with either the primary or secondary antibody omitted, and resulted in no noticeable immunolabelling when tissue was examined under the light or electron microscope. Additionally, cross-reactivity was not seen when a single secondary antibody was omitted from double immunolabelled tissue.

3.2.5 Electron microscopic analysis

All sections were examined in the light microscope for quality and distribution of immunolabelling and regions of STN were identified for electron microscopic analysis. The coverslips were removed, and areas from the STN were cut from the slide, glued to the top of a resin block and trimmed with razor blades. Serial sections, ~50 nm thick (silver/grey), were then cut using an ultramicrotome (EM UC6; Leica Microsystems), and collected on pioloform-coated, single-slot copper grids (Agar Scientific). The sections were then lead stained to improve contrast for electron microscopic examination. A Philips CM10 electron microscope was used to examine sections of tissue. All analyses were performed at a minimum of ~5 μm from the tissue–resin border (i.e., the surface of the section). The maximum distance from the tissue–resin border examined was determined by the penetration of the antibody/reagents together with the angle at which the tissue–resin was sectioned and was therefore variable.

Single section analysis

Tissue was systematically scanned (indicated magnification: 25,000x) in straight lines, parallel to the tissue-resin border and all synapses within frame were counted until a total of 150 synapses had been recorded. Synapses were categorised as either, type-1 or type-2 and either immunolabelled or unlabelled. Type-1 synapses are defined as having a thick postsynaptic density (greater than ~20 nm), whereas type-2 synapses had relatively thinner postsynaptic thickening (less than 15 nm). This was repeated in three animals to give the proportion of synapses characterised as type-1 or type-2 and the proportion of synapses formed by immunopositive boutons. Data are displayed as mean and standard deviation of the mean.

Serial section analysis

Low magnification micrographs were recorded (indicated magnification: 5,800x) and all immunopositive boutons in frame were recorded. Each bouton was then examined in 5 serial sections at higher magnification (indicated magnification: 25,000x), using the low magnification micrograph as a map of the grid. In VGluT1, VGluT2, VGAT and VAChT immunolabelled tissue, ~15 boutons were analysed per grid. In TH immunolabelled tissue ~7 boutons were analysed per grid. Micrographs were taken of each bouton in each of the 5 serial sections. Micrographs were then analysed in Fiji (Fiji: an open-source platform for biological-image analysis) to record the area of the bouton, length of the active zone of the synapse, area of the target structure, the type of structure targeted (e.g. spine or dendrite) and a rough estimate of the area of single vesicles was made.

3.2.6 Statistical analysis

All statistical calculations were performed using the programme SigmaPlot (Version Systat Software, San Jose, CA). All data was tested for normality and Student's t-test was used if data passed. If data were not normal then the Wilcoxon Mann-Whitney test was used. All p-values are two tailed. Differences were considered significant when $p < 0.05$.

3.3 Results

3.3.1 Light microscopic observations

The patterns of immunolabelling for each antibody were as previously described (Omelchenko & Sesack, 2006; Doig *et al.*, 2010; Henny *et al.*, 2012) and were consistent with prior observations within the basal ganglia laboratories in the MRC unit.

VGluT1 and VGluT2 immunoreactivity was observed within bouton-like structures and no co-localisation was observed in double-labelled control tissue, this was also the case on examination of control experiments at electron microscopic level. TH labelling showed no co-localisation with VGluT1, VGluT2 or VGAT, again this was confirmed at the electron microscope level. VAChT was not successfully double labelled using DAB and immunogold techniques, but would be expected to co-localise with VGluT2 and VGAT based on previous studies performed using an antibody against choline acetyltransferase, the synthetic enzyme of acetylcholine and thus a marker of cholinergic boutons (Bevan *et al.*, 1997; Clarke *et al.*, 1997).

Small bouton-like structures were observed within the STN in VGluT1, VGluT2, and VGAT labelled tissue. These are presumed to indicate the presence synaptic boutons. Boutons were not clearly visible in TH and VAChT labelled tissue. Although this does not rule out the presence of synaptic boutons that may only be detectable at the electron microscope level.

In light of the well-established topographic organisation of the STN it was important to ensure all samples were from the same region (Joel & Weiner, 1997; Marani *et al.*, 2008). The STN was localised and scored with a scalpel to ensure all blocks prepared

for electron microscopy were taken from comparable areas. Figure 3.1 shows the region removed from slides for analysis at the electron microscope level.

3.3.2 Synapses formed by VGluT1-, VGluT2- and VGAT-positive boutons in the STN

Electron microscopic analysis was carried out on tissue from three animals single immuno-labelled for: VGluT1, VGluT2 or VGAT. Labelled structures were identified by the presence of electron-dense DAB reaction product adhering to membranes including the internal plasma membrane and the external membranes of organelles, notably vesicles and mitochondria. DAB reaction product was only found in axons. Typically, the DAB reaction product filled the entire bouton, although some boutons displayed a patchy labelling surrounding the vesicles only (Figure 3.2).

Tissue was systematically scanned and all synapses within frame were counted until a total of 150 synapses had been recorded in each grid. Synapses were defined as regions where a bouton and its target are parallel and both a presynaptic and postsynaptic thickening of the plasma membranes is visible, the presynaptic bouton contains vesicles and electron dense material is present within the synaptic cleft. Synapses were categorised as either, type-1 or type-2 and either immunolabelled or unlabelled. Type-1 synapses (also referred to as asymmetric synapses) are defined as having a thick postsynaptic density, whereas type-2 synapses (also referred to as symmetric synapses) had relatively thinner postsynaptic densities (see Figure 3.3).

VGluT1-immunopositive boutons

In accordance with previous studies, all synapses formed by VGluT-immunopositive boutons were type-1 (Figure 3.4). This is typical of glutamatergic synapses from the

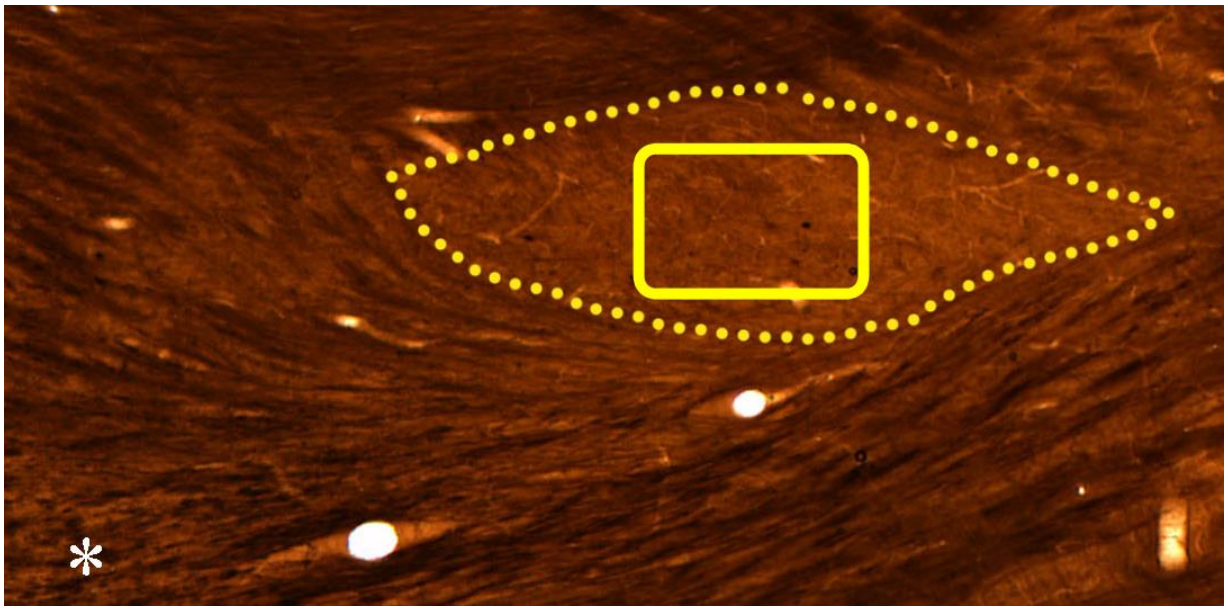


Figure 3.1: The location of the sub-region of subthalamic nucleus used in this experiment.

The figure shows a section immunolabelled for TH. The yellow dotted line indicates a rough border of the STN with the yellow box showing the approximate location sampled for electron microscopy. The white * shows the beginnings of the dopaminergic band of neurons comprising the substantia nigra pas compacta.

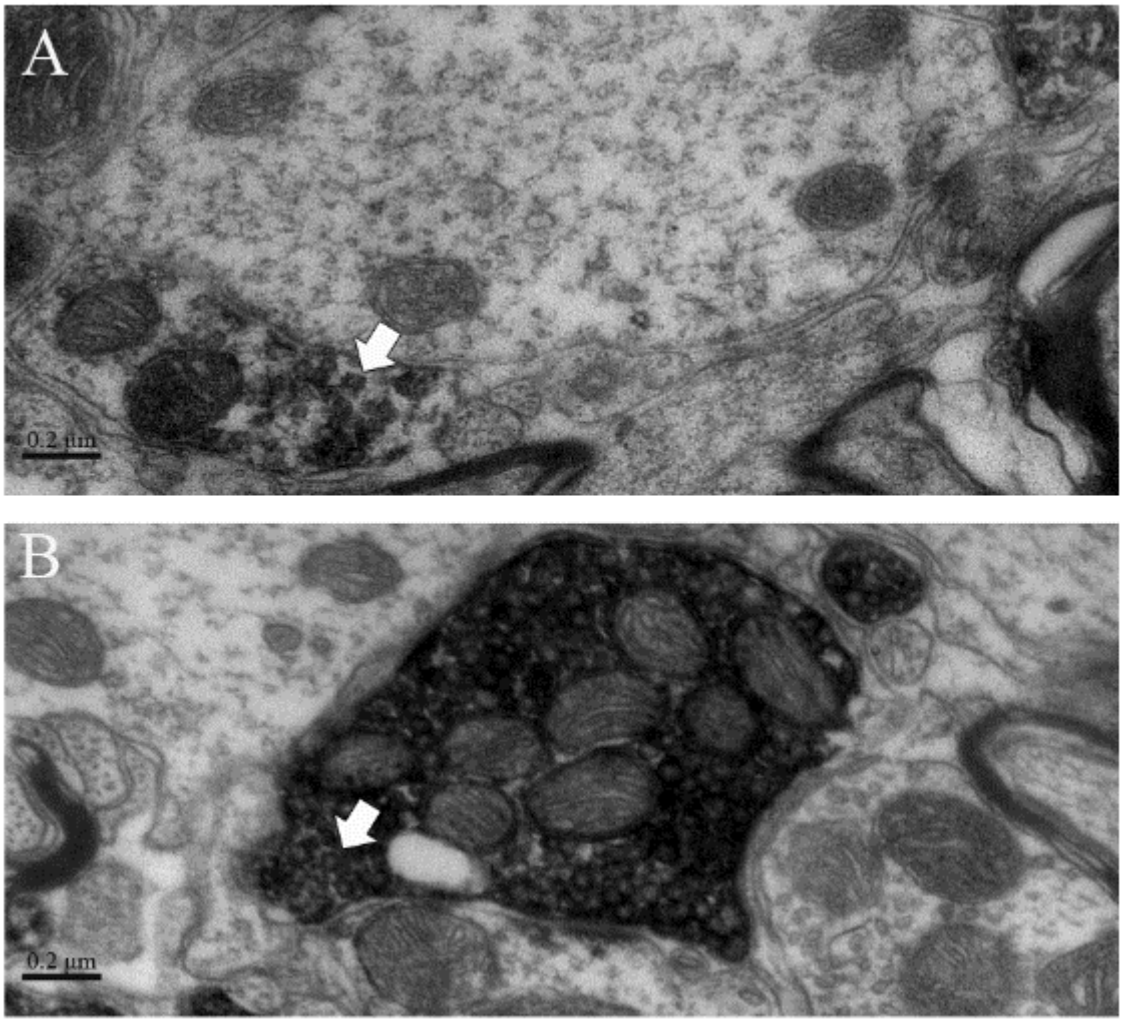


Figure 3.2: Examples of DAB immunolabelling.

A) Patchy immunoperoxidase labelling and B) Dense immunoperoxidase labelling. Both synaptic boutons are immunolabelled for VGluT2 and form type-1 synapses. Notice how DAB reaction product adheres to membranes, particularly the vesicle membranes (white arrows).

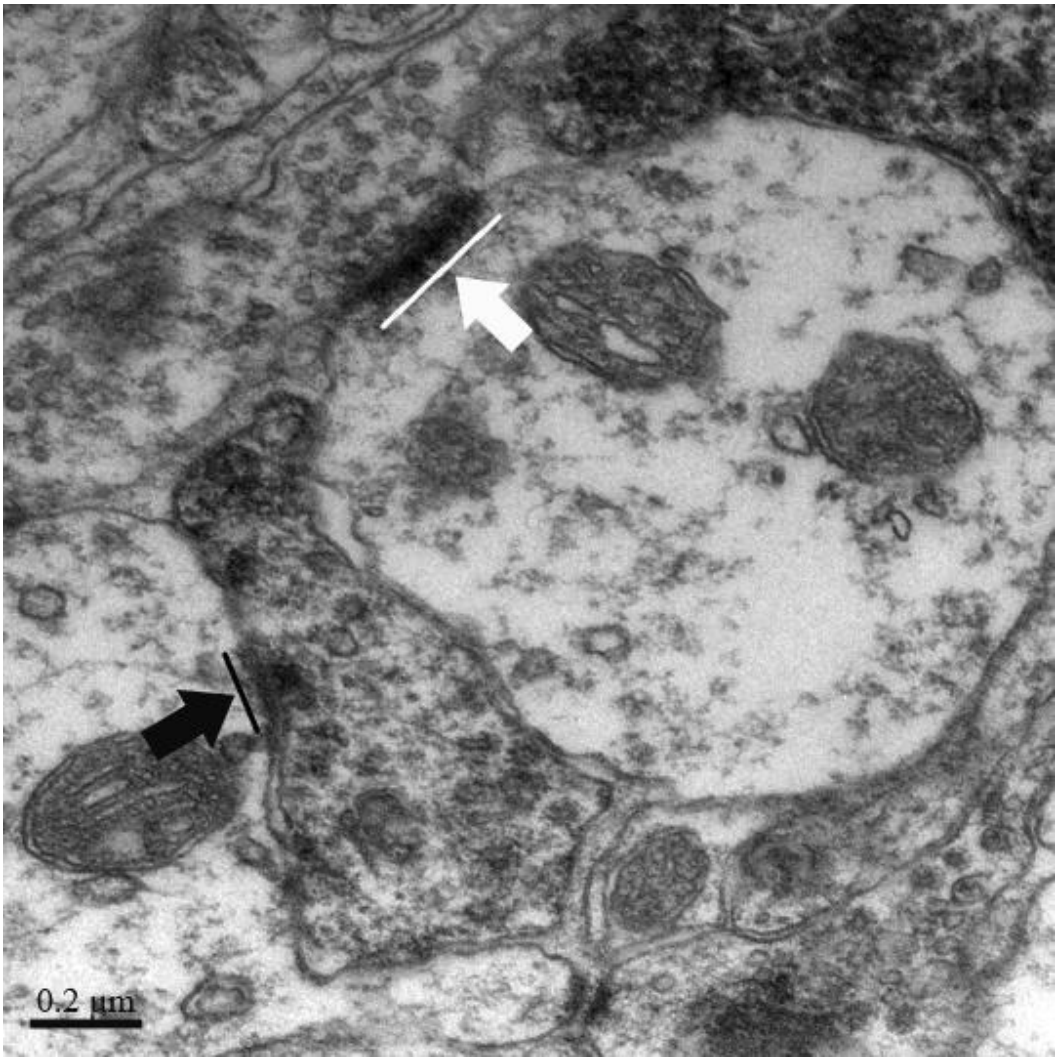


Figure 3.3: Examples of types of identified synapses.

Synapses were defined as regions where a bouton and its target are parallel and both a presynaptic and postsynaptic thickening is visible in the plasma membranes. The presynaptic bouton contains vesicles and electron dense material is present within the synaptic cleft. Synapses were categorised as either, type-1 or type-2 and either immunolabelled or unlabelled. Type-1 synapses (asymmetric synapses; white arrow) are defined as having a thick postsynaptic density (greater than ~20 nm; parallel to white line), whereas type-2 synapses (symmetric synapses; black arrow) had relatively thinner postsynaptic thickening (less than 15 nm; parallel to black line).

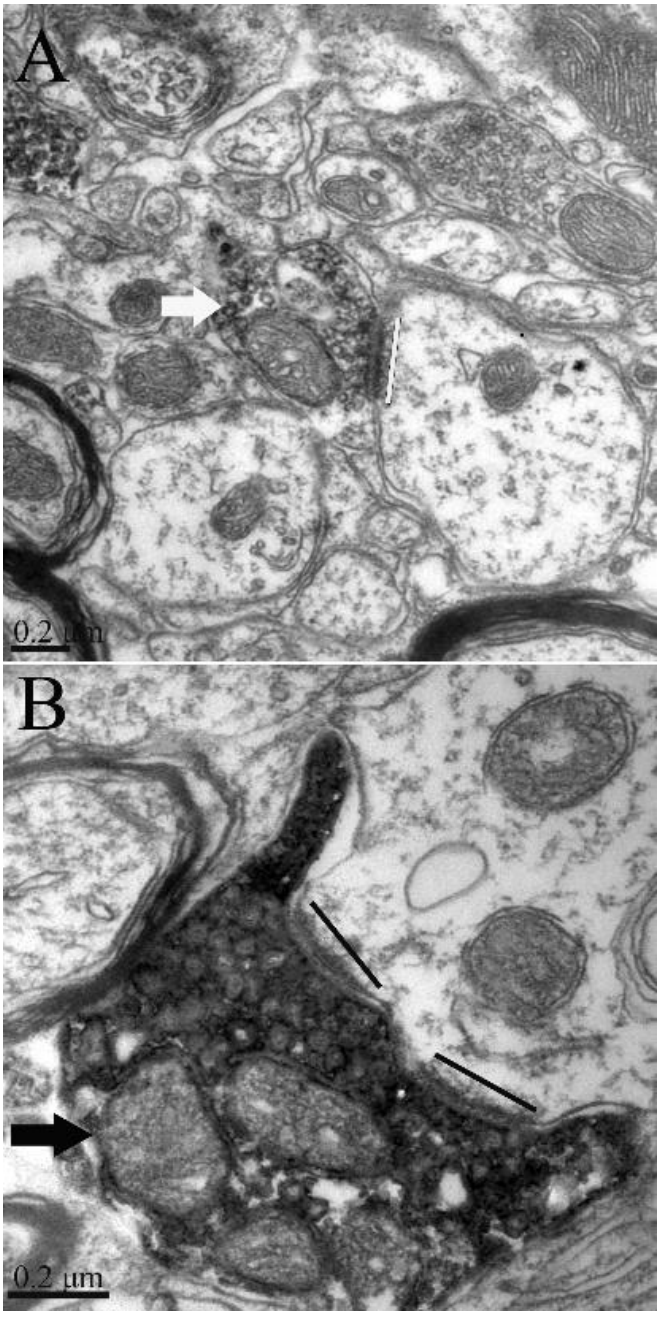


Figure 3.4: Micrographs showing synaptic boutons providing cortical and subcortical glutamatergic innervation of the STN.

A) VGluT-1 immunopositive bouton (white arrow) forming a type-1 synapse (parallel with white line) with a dendrite. B) A VGluT-2 immunopositive bouton (black arrow) forming a synapse (parallel with black lines) with a dendrite.

cortex, thalamus and other subcortical regions (Bevan & Bolam, 1995; Bevan *et al.*, 1995). In VGluT1-labelled tissue, 51.1% ± 3.4% (mean ± S.D. of 3 animals) synapses were categorised as type-1 and 48.9% ± 3.4% synapses were categorised as type-2. VGluT1-immunopositive boutons formed 18.0% ± 2.7% synapses, all of which were classified as type-1 (Figure 3.5). None of the boutons forming type-2 synapses were immunopositive.

VGluT2-immunopositive boutons

In VGluT2-labelled tissue, 54.4% ± 2.5% synapses were categorised as type-1 and 45.6% ± 2.5% as type-2. VGluT2-immunopositive boutons also formed exclusively type-1 synapses, and accounted for 31.1% ± 2.4% of all synaptic boutons recorded. As with the VGluT1-labelled tissue, none of the boutons forming type-2 synapses were immunopositive (Figure 3.5).

VGAT-immunopositive boutons

All synapses formed by VGAT-immunopositive boutons were type-2, i.e. the type of synapse typically associated with inhibitory GABAergic boutons (Smith *et al.*, 1990a; Bevan & Bolam, 1995). Boutons were generally large and abundant mitochondria, features typical of GABAergic boutons derived from the globus pallidus (external segment; Figure 3.6) (Bevan *et al.*, 1997; Smith *et al.*, 1998). In tissue immunolabelled for VGAT, 46.0% ± 1.7% of all synaptic terminals were categorised as type-1 and 54.0% ± 1.8% were type-2. VGAT-immunopositive synaptic boutons formed 44.7% ± 1.3% of all synaptic terminals seen (Figure 3.5).

Summary of distributions

Taken together the data suggest that innervation of the STN consists of ~50% type-1 synapses and ~50% type-2 synapses. These appear to be separate populations with no overlap in the subtypes examined here. Glutamatergic input (VGluT1- and VGluT2-immunopositive boutons) exclusively form type-1 synapses. When only type-1 synapses forming boutons are considered, VGluT1- and VGluT2-immunopositive synaptic boutons account for approximately 98%; with 36% and 62% VGluT1- and VGluT2-immunopositive respectively.

Inhibitory GABAergic input exclusively forms type-2 synapses, with VGAT-immunopositive boutons accounting for approximately 89% of the type-2 synapses forming synaptic boutons.

This leaves approximately 2% of type-1 synapses and 11% of type-2 synapses unaccounted for; i.e. ~7% of the total innervation of the STN.

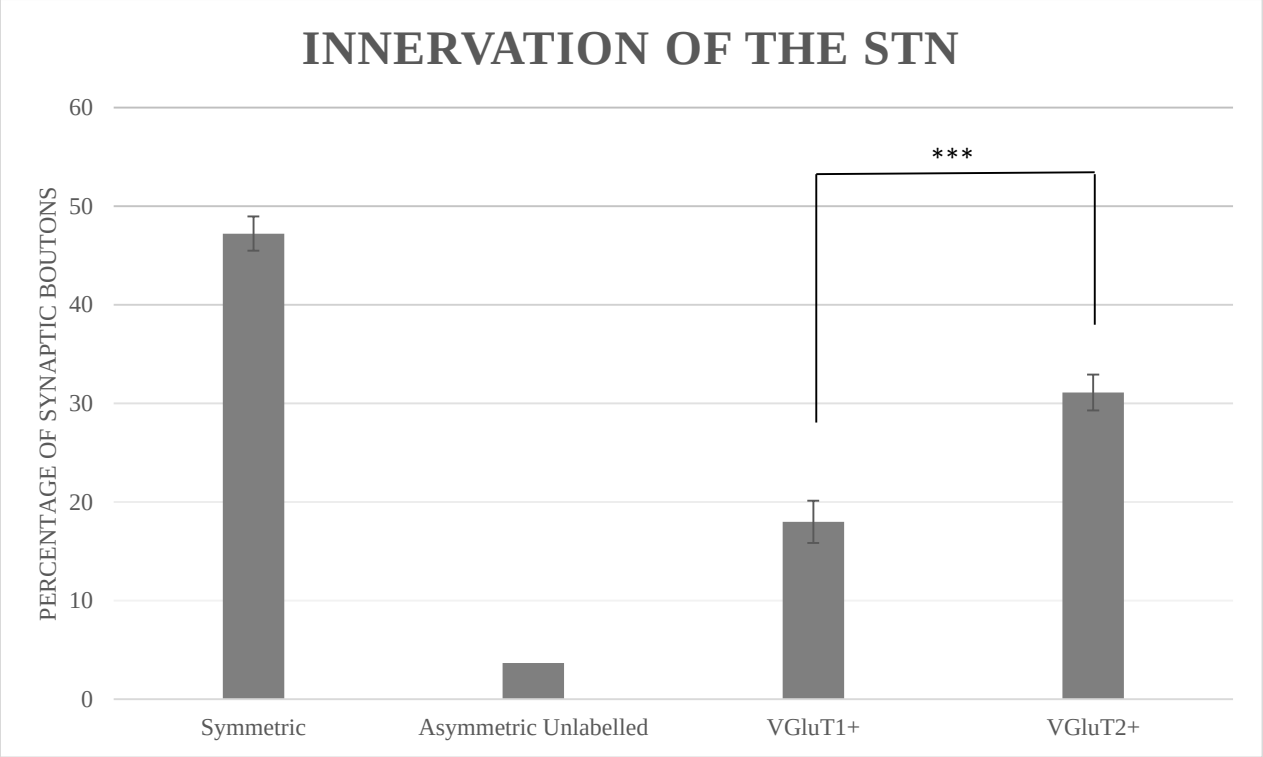


Figure 3.5: Plot of the percentage of synaptic boutons labelled by each antibody.

Significantly more VGluT2-immunopositive synaptic boutons were present than VGluT1-immunopositive synaptic boutons (labelled ***, $p<0.001$).

Mean ± standard deviation. n= 3 animals, 150 synapses examined per animal.

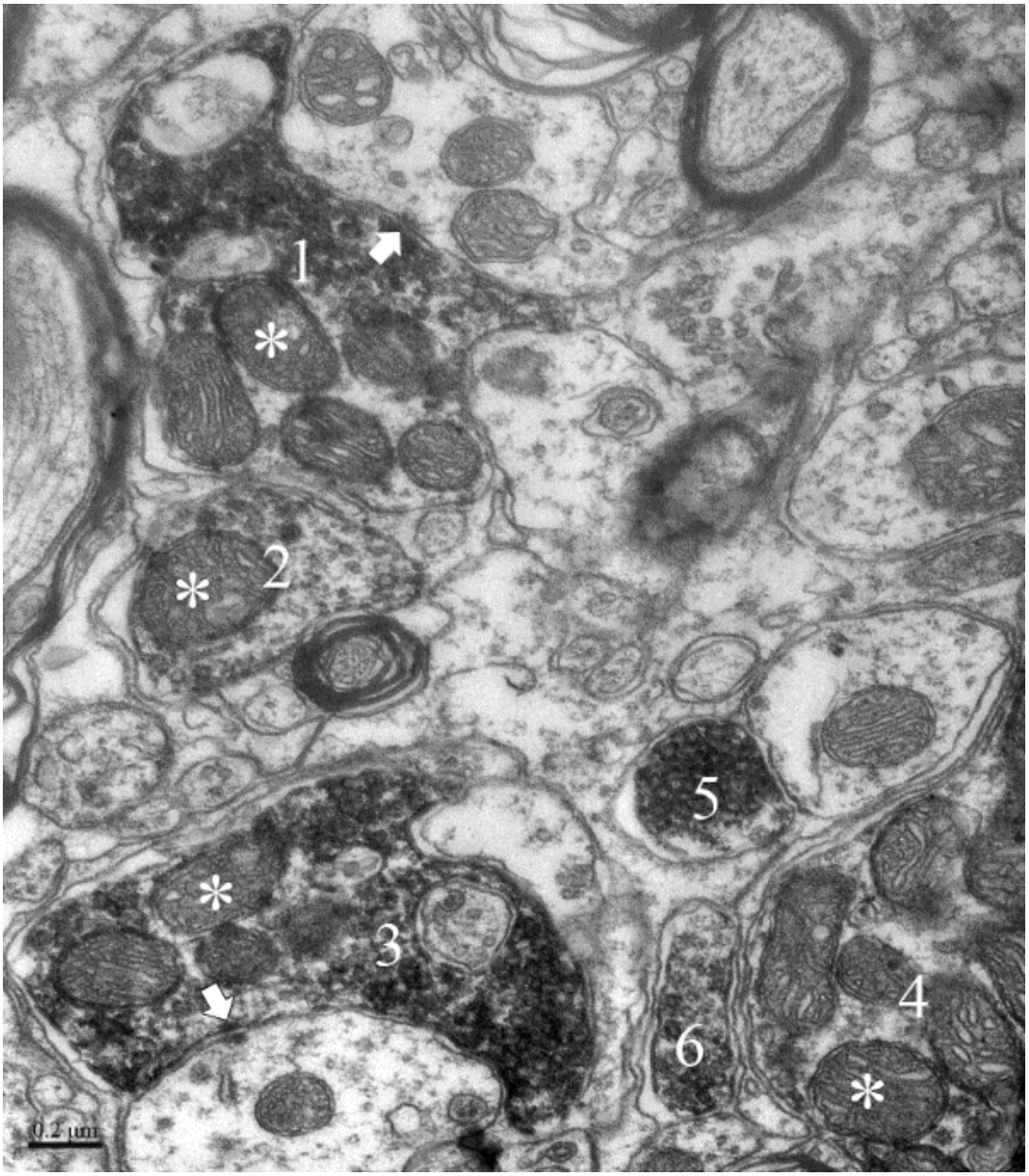


Figure 3.6: Micrograph showing inhibitory input to STN dendrites.

Six boutons labelled for VGAT are shown above. Of the six boutons shown, four (1-4) display the classic large size, with large numbers of mitochondria (examples labelled with white *) that is characteristic of efferents from the globus pallidus. Two of these boutons form type-2 synapses (white arrows). Two examples of smaller boutons (5 & 6) without mitochondria are also immunopositive for VGAT.

3.3.3 Synapses formed by VAChT and TH-positive boutons in the STN

To determine the nature of the immunonegative boutons in the STN, immunolabelling was performed to identify boutons utilizing two key groups of neurotransmitters in the STN, acetylcholine and catecholamines such as dopamine and noradrenaline. Sections were thus immunolabelled for VAChT, the vesicular transporter for acetylcholine, and TH, the rate-limiting enzyme involved in catecholamine synthesis. Dense DAB reaction product was seen within boutons in both experiments, although TH labelling was lighter and more localised to the cytoplasm (Figure 3.7, B). VAChT labelling was generally localised around vesicles and membranes in a similar manner to the other vesicular transport proteins (Figure 3.7, A).

The tissue was systematically scanned in the same manner as described above. Synapses were categorised in the same way as previously, although it should be noted that the distinction between type-1 and type-2 synapses was not as clear with TH-labelled boutons (Figure 3.8).

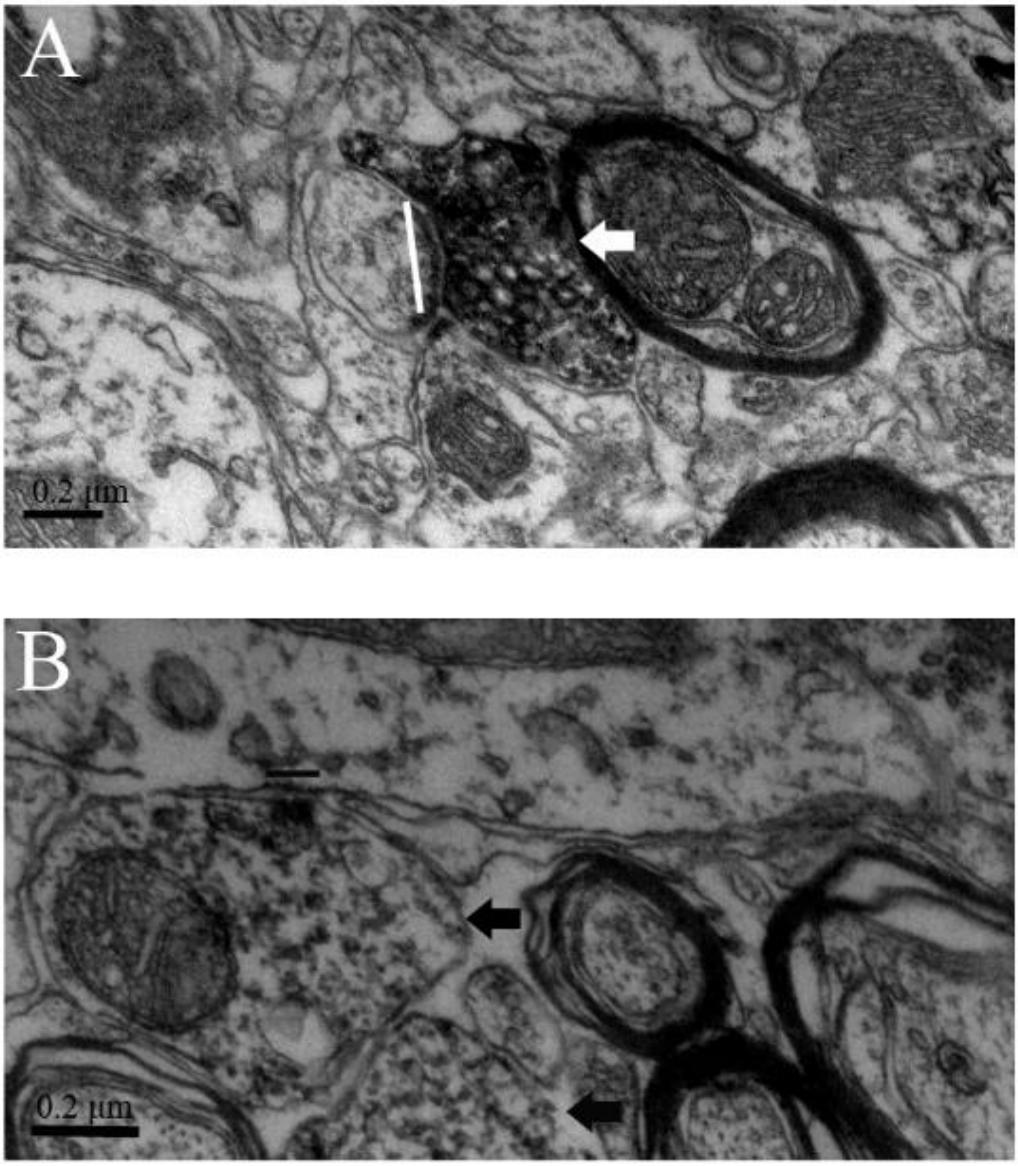


Figure 3.7: Micrographs showing TH- and VAChT- immunopositive terminals in the STN.

A) VAChT-immunolabelled bouton (white arrow) forming a type-1 synapse with an unlabelled spine (parallel to white line) and B) TH-labelled boutons (black arrows), one forming a type-2 synapse with an unlabelled dendrite (parallel to black line). Notice that DAB reaction product in the TH-labelled structures is less dense than that formed at VAChT-immunoreactive sites.

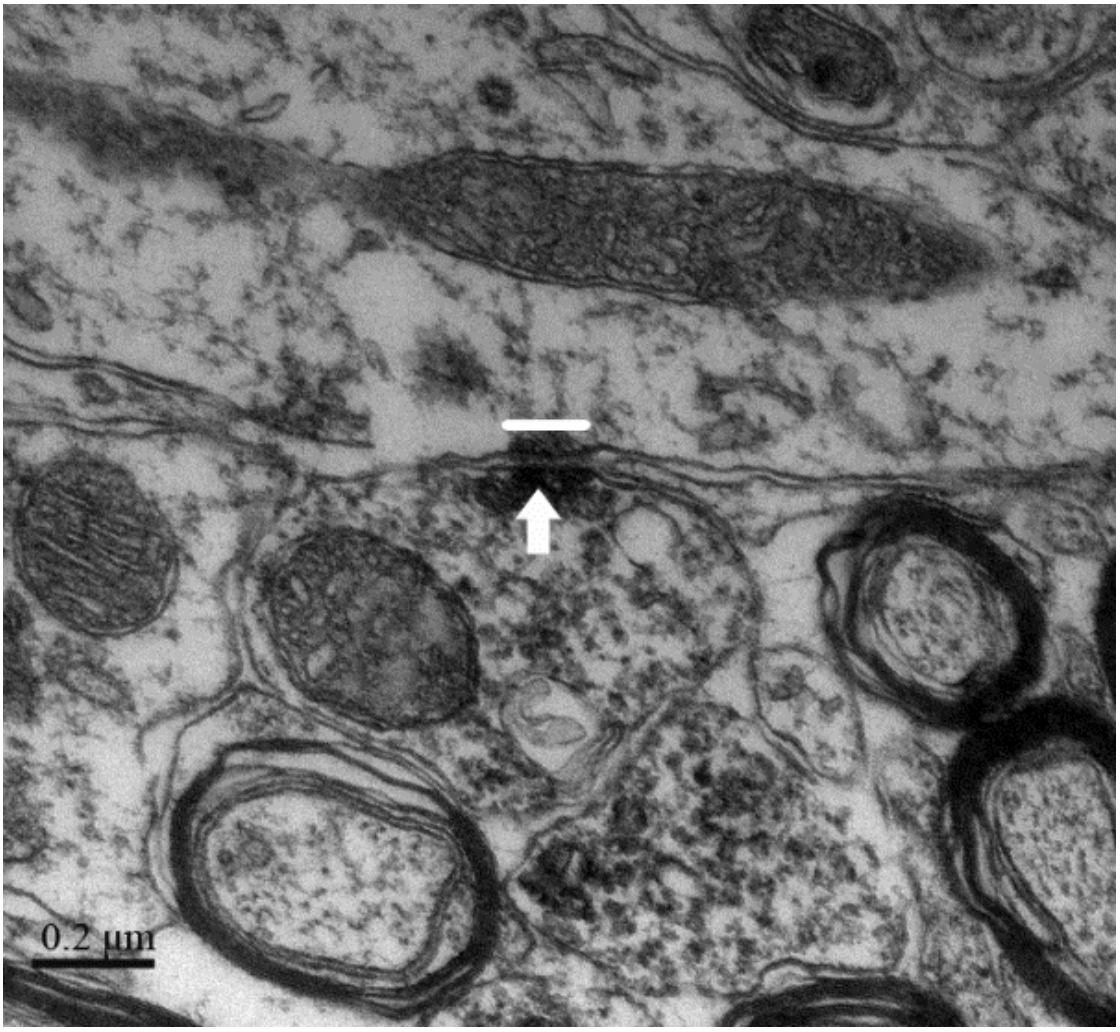


Figure 3.8: Micrograph showing the difficulty of classifying synapses formed by TH-positive boutons in single sections.

Single section micrograph of synapse formed by a TH-immunopositive bouton (white arrow). The post-synaptic thickening (parallel with white line) is as large as a type-1 synapse but is much less electron dense. Figure 3.7b shows another section of this synapse which was classified as type-2 when serial sections were taken into account. It is thus likely to be over simplifying the situation to divide synapses simply into just type-1 or type-2.

VAChT-immunopositive boutons

Synapses formed by VAChT-immunolabelled boutons were either type-1 or type-2, and this was confirmed when boutons were examined in serial sections (Section 3.3.5). Previously, cholinergic terminals have been described to form only type-1 synapses (Bevan & Bolam, 1995; Clarke *et al.*, 1997), although examination of the figures in those papers reveals what appear to be much smaller post-synaptic densities than those typically associated with type-1 synapses, such as those seen in the VGluT-positive boutons.

In VAChT-labelled tissue, 49.3% ± 0.9% boutons gave rise to type-1 synapses and 50.7% ± 0.9% giving rise to type-2 were recorded. Type-1 synapses formed by VAChT-immunopositive synaptic boutons accounted for 4.4% ± 1.2% of all synapses, type-2 synapses formed by VAChT-immunopositive boutons accounted for 6.0% ± 2.2% of the total synapses seen (Figure 3.9). It should be noted that the distinction between type 1 and type 2 synapses is not as clear-cut as for those boutons using amino acid transmitters (Figure 3.8); for this reason VAChT-positive boutons were further analysed (Section 3.3.6) to further elucidate the exact proportion of boutons giving rise to each subtype, as they are likely to be performing a different role physiologically.

TH-immunopositive boutons

Synapses formed by TH-positive boutons were also of both type-1 and type-2, as shown previously (Cragg *et al.*, 2004). The difference between the two synapse types was less clear-cut (Figure 3.8) and the proportion of boutons was small, so for this stage of the analysis they were not sub-divided. Of the 450 synapses visualised across three animals, only 19 were formed by TH-labelled boutons (mean proportion of synapses: 4.2% ± 1.2%). The mean proportion of the synapses was 48.0% ± 1.8% type-1 and 52.0% ±

1.8% type-2, which is consistent with the ~50:50 ratio seen in the VGluT1, VGluT2 and VGAT tissue (Figure 3.9).

3.3.4 Morphological characteristics of VGluT1- and VGluT2-positive synaptic boutons.

In order to further understand the role played by various neurotransmitter types, the morphological characteristics of each type of synaptic bouton were examined. Boutons were visualised in 5 consecutive sections to provide insight into the 3D structure of the synapse/bouton (Figure 3.10). The size of the bouton forming the synapse was measured at its largest point, along with the length of the active zone at its longest point. The size and type of target were also recorded. Spines were identified by their size and shape, the presence of spiny apparatus and absence of mitochondria. Dendrites were typically larger, and often contained mitochondria and endoplasmic reticulum (Figure 3.11). Additionally, the cross-sectional area of several vesicles within the bouton was measured to roughly compare sizes between the various immunopositive boutons.

VGluT1-immunopositive boutons had cross-sectional areas of 0.29 μm^2 ± 0.01 μm^2 (all values are mean and standard deviation of mean, n= 46) and ranged from 0.47 μm^2 to 0.08 μm^2, although the vast majority were within 1 standard deviation of the mean (70%). Their postsynaptic targets were mostly spines (65%) and dendrites (35%). A single exception was seen, forming a synapse with a soma (Figure 3.12; bouton size 0.36 μm^2). The mean size of boutons was not different between those forming synapses with spines vs. dendrites (0.29 ± 0.1μm^2 and 0.27 ± 0.06μm^2 respectively; p value= 0.767).

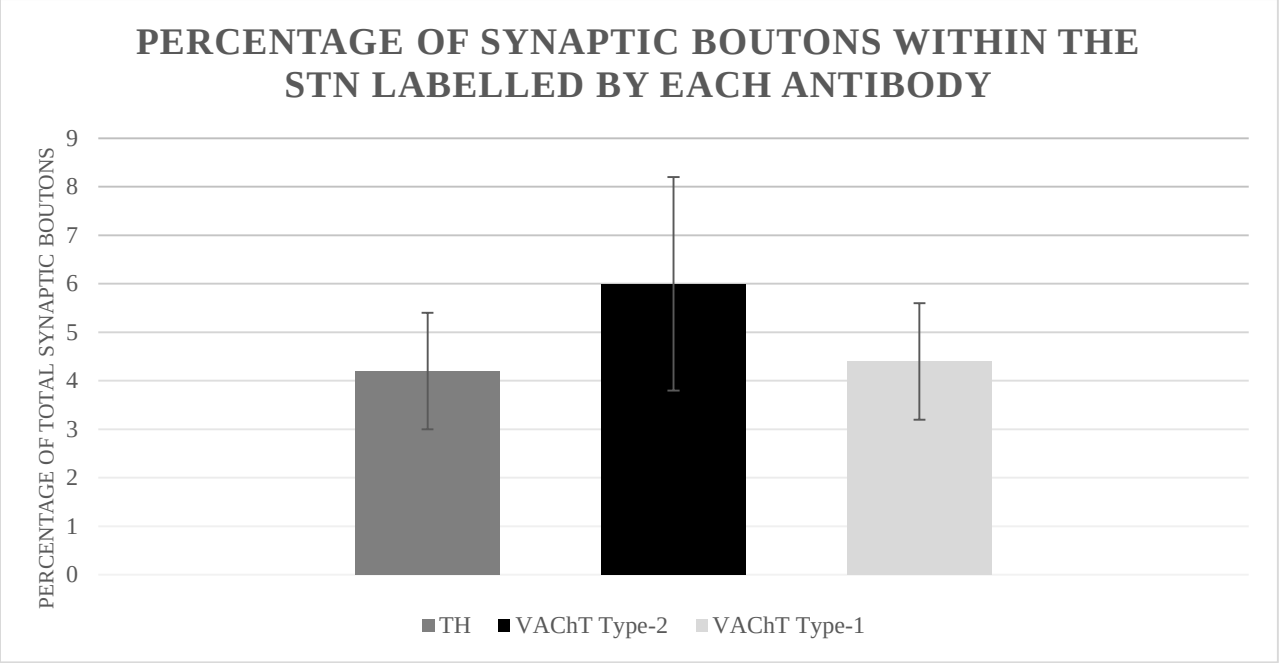


Figure 3.9: Percentage of all synaptic boutons within the STN labelled by either VAChT or TH antibodies.

Together the number of TH- and VAChT-immunopositive synaptic boutons comprised approximately 15% of the total of all synaptic boutons within the STN.

Mean ± standard deviation, n = 3 animals, 150 synaptic boutons per animal.

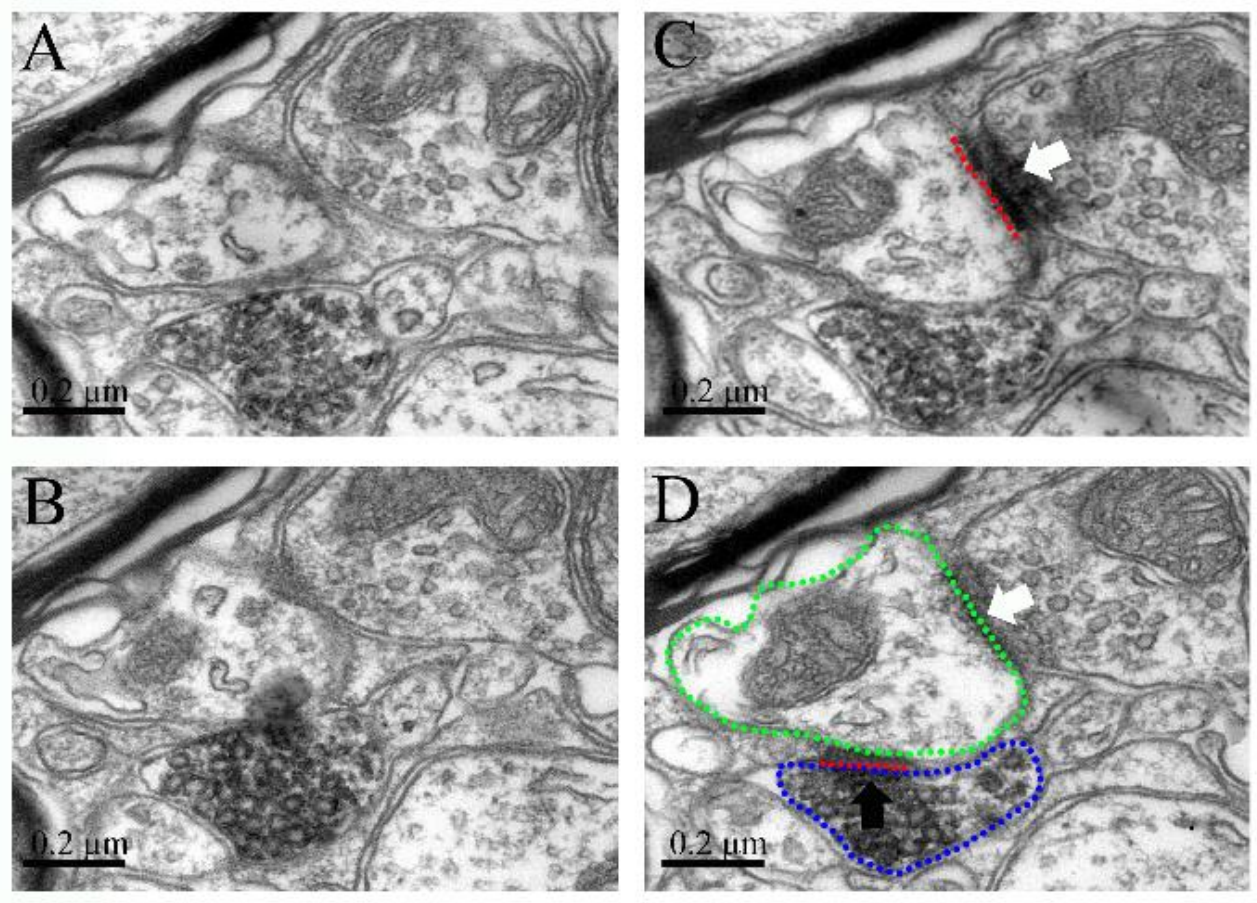


Figure 3.10: Micrographs showing serial section analysis.

Four consecutive serial sections of the same boutons (A-D; each ~50 nm thick), one of which is immunopositive for VAChT, were examined. Each bouton was examined in five sections. When a synapse was observed (arrows) the following measurements were made in each section and the largest recorded: length of active zone (red dotted line length), bouton size (blue dotted line area) and target size (green dotted line area). The type of synapse formed was also noted (white arrow: type-1, black arrow: type-2).

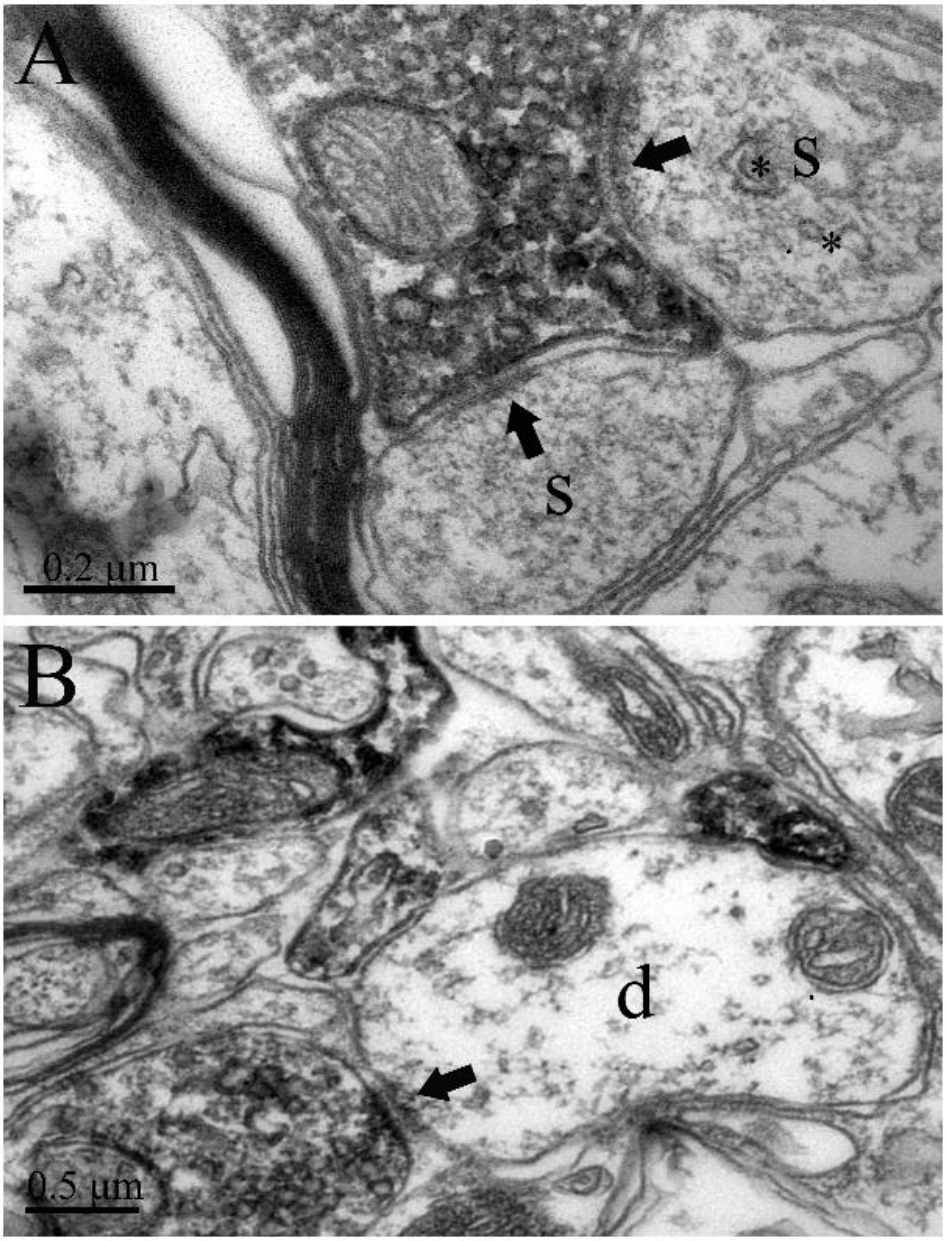


Figure 3.11: Micrographs showing the differences between spines and dendrites.

VGluT-1-immunopositive boutons forming type-1 synapses (black arrows) with two spines (s) in A) and a dendrite (d) in B). Spines are characterised by a small size with a regular shape, a lack of mitochondria and sometimes the presence of specialised reticular membranes referred to as spine apparatus (*). Dendrites are larger in size, often with a less uniform shape and can contain of mitochondria.

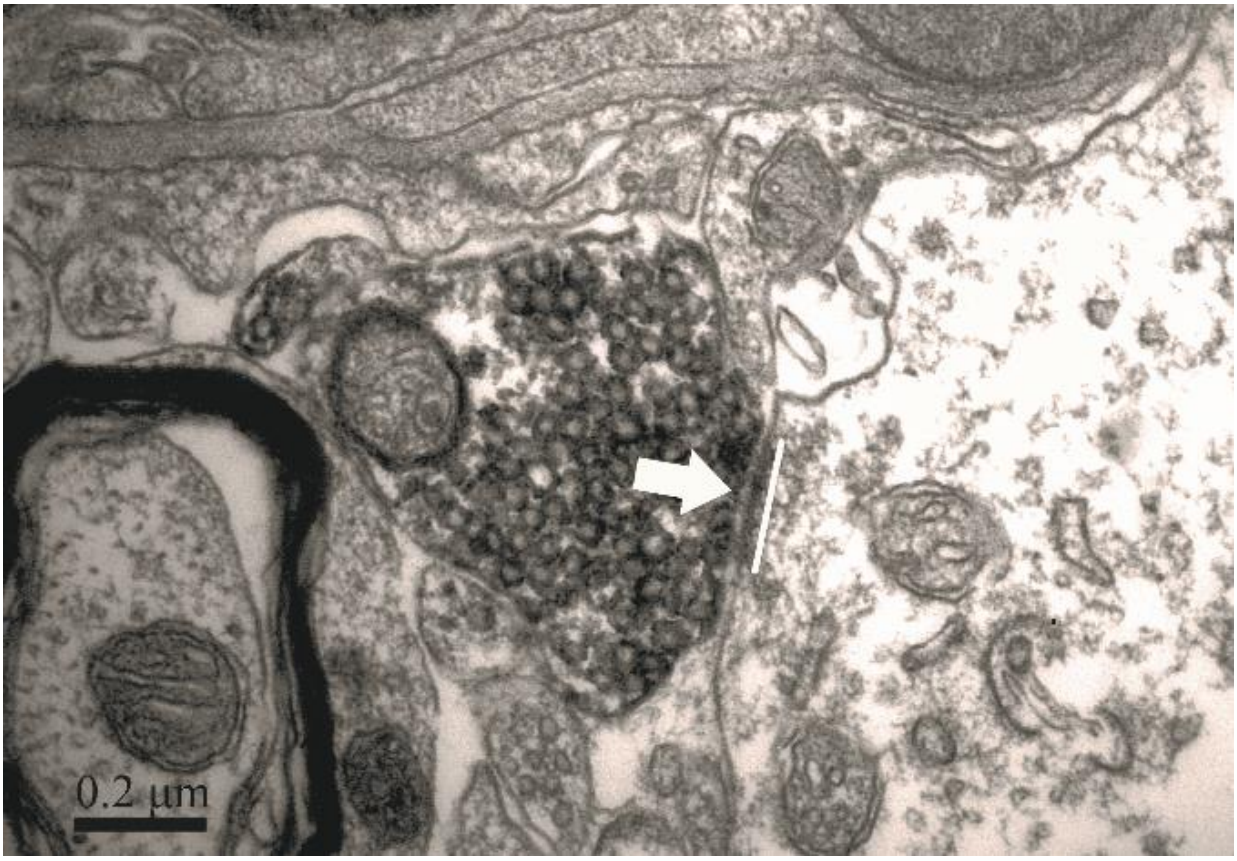


Figure 3.12: Micrograph showing cortical input to an STN neuron somata.

A rare example ofVGluT1-positive bouton forming a type-1 synapse (white arrow and line) with a cell body; only one such synapse was seen during the analysis.

The mean size of the active zone of synapses formed by VGluT1-immunopositive boutons was 0.22 ± 0.07 µm. Synapses formed with spines had smaller active zones than those with dendrites (0.19 ± 0.06 µm vs. 0.30 ± 0.08 µm respectively; p value = 0.010).

The mean size of all structures targeted by VGluT1-immunopositive boutons was 0.24 ± 0.17 μm^2. Spines had a mean size of 0.12 ± 0.05 μm^2 (range: 0.04 to 0.26 μm^2). Dendrites were larger with a mean size of 0.51 ± 0.21 μm^2 (range: 0.21 to 0.80 μm^2; p value = 0.005). Typically, vesicles were roughly half the size of VGluT2, VGAT and VAChT vesicles.

VGluT2-immunopositive boutons (n = 44) were larger than VGluT1 with a mean cross-sectional area of 0.45 ± 0.19 μm^2 (range: 0.21 to 0.85μm^2; p value = 0.010) there was however more variation in size with only 61% of boutons within 1 S.D. of the mean. In contrast to VGluT1-positve boutons; VGluT2-positive boutons formed synapses principally with dendrites (75%), the remainder formed synapses with somata and a single example formed a synapse with a spine. The mean size of boutons differed slightly between those forming synapses with dendrites and somata (0.46 ± 0.17 μm^2 and 0.35 ± 0.13 μm^2 respectively) although this was not statistically significant (p value = 0.238).

The mean size of active zone of synapses formed by VGluT2-immunopositive boutons was 0.27 ± 0.09 µm. Synapses formed with somata had smaller active zones than those formed with dendrites (0.19 ± 0.05 µm vs. 0.28 ± 0.10 µm) although this was not statistically significant (p value = 0.321).

The mean size of all structures (excluding somata) targeted by VGluT2-immunopositive boutons was 1.01 ± 0.31 μm^2. This is significantly larger than structures targeted by VGluT1-immunopostive boutons (p value <0.001). Dendrites had a mean size of 1.08 ±

0.26μm^2, (range: 0.12 μm^2 to 1.40 μm^2). Somata were too large to measure the magnification used. Data is summarised in Table 1. Vesicles were approximately the same size as vesicles within VGAT- and VAChT-immunopositive boutons (see below).

3.3.5 Morphological characteristics of VGAT-positive synaptic boutons.

VGAT-positive synaptic boutons (n = 46) were generally much larger than the VGluT-immunopositive boutons (VGluT1 p value = 0.001, VGluT2 p value = 0.003), with abundant mitochondria and a large quantity of vesicles (Figure 3.6). The mean bouton cross-sectional area was 0.96 ± 0.49 μm^2 with a range from 0.27 to 2.59μm^2 with 68% of boutons within 1S.D. of the mean. VGAT-positive synaptic boutons primarily targeted dendrites (82%) with the remaining 18% targeting somata. No boutons were seen forming synapses with spines. The mean cross-sectional area of dendrites targeted by VGAT-positive boutons was 1.12 ± 0.75μm^2, and ranged from 0.20 to 2.92 μm^2. The active zones of synapses formed by VGAT-positive boutons was also larger than the VGluT-positive boutons, at 0.40 ± 0.21μm (p value = 0.004). The mean length of active zones of synapses formed with dendrites and somata differed slightly but not significantly (0.43 ± 0.23μm and 0.27 ± 0.06μm respectively; p value = 0.401). These results are summarised in Table 1. Vesicles were approximately the same size as vesicles within VGluT2- and VAChT-immunopositive boutons.

3.3.6 Morphological characteristics of TH- and VAChT-positive synaptic boutons.

TH-immunopositive boutons

Boutons immunolabelled for TH (n = 18) have previously been shown to form both type-1 and type-2 synapses in the STN (Cragg *et al.*, 2004). Figure 3.8 shows the

difficulty defining type-1 and type-2 synapses in a single section, however when examined in serial sections the differences became clearer. In serial sections 28% of boutons formed type-1 synapses and 72% type-2 synapses. It should be noted that only a small number of boutons were analysed due to weak immunolabelling and a low number of boutons found forming synapses in the STN, meaning the ratios shown here may change with a larger study.

The mean cross-sectional area of TH-positive boutons was 0.36 ± 0.09 μm^2, (range: 0.21 to 0.51μm^2) with 83% of boutons within one S.D. of the mean. TH-positive boutons primarily targeted dendrites (58%) with the remaining 42% targeting spines. No boutons were seen forming synapses with somata. The mean size of dendrites targeted by TH boutons was 0.33 ± 0.23 μm^2, (range: 0.13 to 2.04μm^2). The mean length of active zones of synapses formed by TH-positive boutons were smaller than the VGluT-immunopositive boutons, at 0.13 ± 0.02 µm ($p < 0.001$), with the active zones of synapses formed with dendrites and spines similar in size (0.12 ± 0.03 µm and 0.13 ± 0.07 µm respectively). Subdivision of the data into type-1 and type-2 synapses revealed no significant differences between any data points (mean bouton size; 0.36 ± 0.09 vs 0.35 ± 0.08, mean active zone size; 0.12 ± 0.03 vs 0.13 ± 0.01, or mean target size; 0.32 ± 0.23 vs 0.36 ± 0.28; p values all >0.05). Vesicles were approximately the same size as vesicles within VGluT1 immunopositive boutons, and roughly half the size of vesicles found within VGluT2, VGAT, and VAChT immunopositive boutons. These results are summarised in Table 3.2.

VAChT-immunopositive boutons

VAChT-positive boutons also showed a variety in synapse type, which was not previously shown (Bevan & Bolam, 1995). Again the differences between type-1 and 2

for this transmitter type were difficult to distinguish in single sections, although clearer than the TH-immunolabelled boutons, the synapses were therefore examined in serial sections.

Table 3.1: Summary of the terminal size, target size and type and active zone size of VGluT1-, VGluT2- and VGAT-immunopositive synaptic boutons in the STN.

Sizes shown as mean ± standard deviation.

Labelling	Synapse Type	Terminal Size (μm^2)	Size of Target (μm^2)	Active Zone Size (μm)	Main Target Type	Secondary Target Type	Remaining Targets
VGluT1 (n=46)	1	0.29 ± 0.10 (a)(b)	0.24 ± 0.17 (c)(d)	0.22 ± 0.07	Spines (65%)	Dendrites (30%)	Somata (5%)
VGluT2 (n=44)	1	0.45 ± 0.19 (a)(b)	1.01 ± 0.31 (c)	0.27 ± 0.09	Dendrites (75%)	Somata (19%)	Spines (6%)
VGAT (n=46)	2	0.91 ± 0.44 (b)	0.93 ± 0.61 (d)	0.30 ± 0.15	Dendrites (82%)	Somata (18%)	N/A

(a) VGluT2-immunopositive boutons are significantly larger than VGluT1-immunopositive boutons (p=0.01)

(b) VGAT-immunopositive boutons are significantly larger than VGluT1- (p=0.001) and VGluT2-immmunopositive boutons (p=0.003)

(c) VGluT2-immunopositive boutons target significantly larger structures than VGluT1-immunopositive boutons (p<0.001)

(d) VGAT-immunopositive boutons target significantly larger structures than VGluT1-immunopositive boutons (p=0.001)

Table 3.2: Summary of the terminal size, target size and type and active zone size of VAChT and TH boutons.

Sizes shown as mean ± standard deviation.

Labelling	Synapse Type	Terminal Size (μm^2)	Size of Target (μm^2)	Active Zone Size (μm)	Main Target Type	Secondary Target Type	Remaining Targets
VAChT (n=23)	1	0.28 ± 0.13	0.29 ± 0.24	0.25 ± 0.08	Spines (75%)	Dendrites (25%)	N/A
VAChT (n=17)	2	0.18 ± 0.09	0.51 ± 0.36	0.22 ± 0.11	Dendrites (44%)	Spines (30%)	Somata (13%) Axons (13%)
VAChT Combined	both	0.22 ± 0.11 (a)	0.40 ± 0.30	0.23 ± 0.10 (b)			
TH (n=5)	1	0.36 ± 0.09	0.32 ± 0.23	0.12 ± 0.03	Dendrites (60%)	Spines (40%)	N/A
TH (n=13)	2	0.35 ± 0.08	0.36 ± 0.28	0.13 ± 0.01	Dendrites (57%)	Spines (43%)	N/A
TH Combined	both	0.36 ± 0.09 (a)	0.33 ± 0.23	0.13 ± 0.02 (b)			

(a) TH-immunopositive boutons are significantly larger than VAChT-immunopositive boutons ($p = 0.002$)

(b) The active zones of synapses formed by VAChT-immunopositive boutons are significantly larger than TH-immunopositive synaptic boutons ($p= 0.005$)

In serial sections, 42% of synapses were classified as type-1 and 58% type-2 (n = 40). Each subtype of synapse had a very different innervation pattern, with the type-1 synapses targeting only spines (75%) and dendrites (25%). The type-2 synapses included more varied targets: dendrites (44%), spines (30%), somas (13%) and axons (13%). Due to the rarity of synapses formed with axons, these have been removed from the group analysis.

The mean bouton size forming type-1 synapses was 0.28 ± 0.13 μm^2 (range: 0.14 to 0.52 μm^2) with 50% of boutons within one S.D. of the mean. The mean size of targets was 0.29 ± 0.24 μm^2, and ranged from 0.13 to 1.34μm^2. The active zones of synapses formed by VAChT-positive boutons were not statistically different from the VGluT-positive boutons, at 0.25 ± 0.08 µm (p value = 0.992), with the active zones of synapses formed with dendrites and spines of similar size (0.24 ± 0.11 µm and 0.26 ± 0.13 µm respectively; p-value = 0.631).

Boutons forming type-2 synapses were not significantly different in morphology from boutons forming type-1 synapses in any of the measurements taken. The mean cross-sectional area was 0.18 ± 0.09 μm^2 (range: 0.13 to 0.58μm^2) with 81% of boutons within one S.D. of the mean. The mean cross-sectional area of targets was 0.51 ± 0.36 μm^2 (range: 0.13 to 1.39 μm^2). Active zones were 0.22 ± 0.11 µm in length, with the active zones of synapses formed with dendrites and spines similar in length (0.24 ± 0.04 µm and 0.23 ± 0.09 µm respectively). Vesicles were approximately the same size regardless of whether a bouton formed type-1 or type-2 synapses, and were similar in size to vesicles found within VGAT and VGluT immunopositive boutons. Data is summarised in Table 3.2.

During both the single section analysis and the serial section analysis, rare examples (n = 5) of axo-axonic synapses were seen formed by VAChT-labelled boutons (Figure 3.13), two of these boutons formed synapses with VAChT labelled axons, with the remaining three forming synapses with unlabelled axons. Two examples were examined in the serial section analysis. In both cases the VAChT-labelled bouton formed a type-2 synapse with an unlabelled axon, which went on to give rise to a type-1 synapse onto an unlabelled structure. The bouton areas (0.15 & 0.13 μm^2), active zones (0.39 & 0.26 μm) and target areas (0.41 & 0.34 μm^2) were not statistically different from the type-2 synapse forming VAChT-immunopositive boutons reported above.

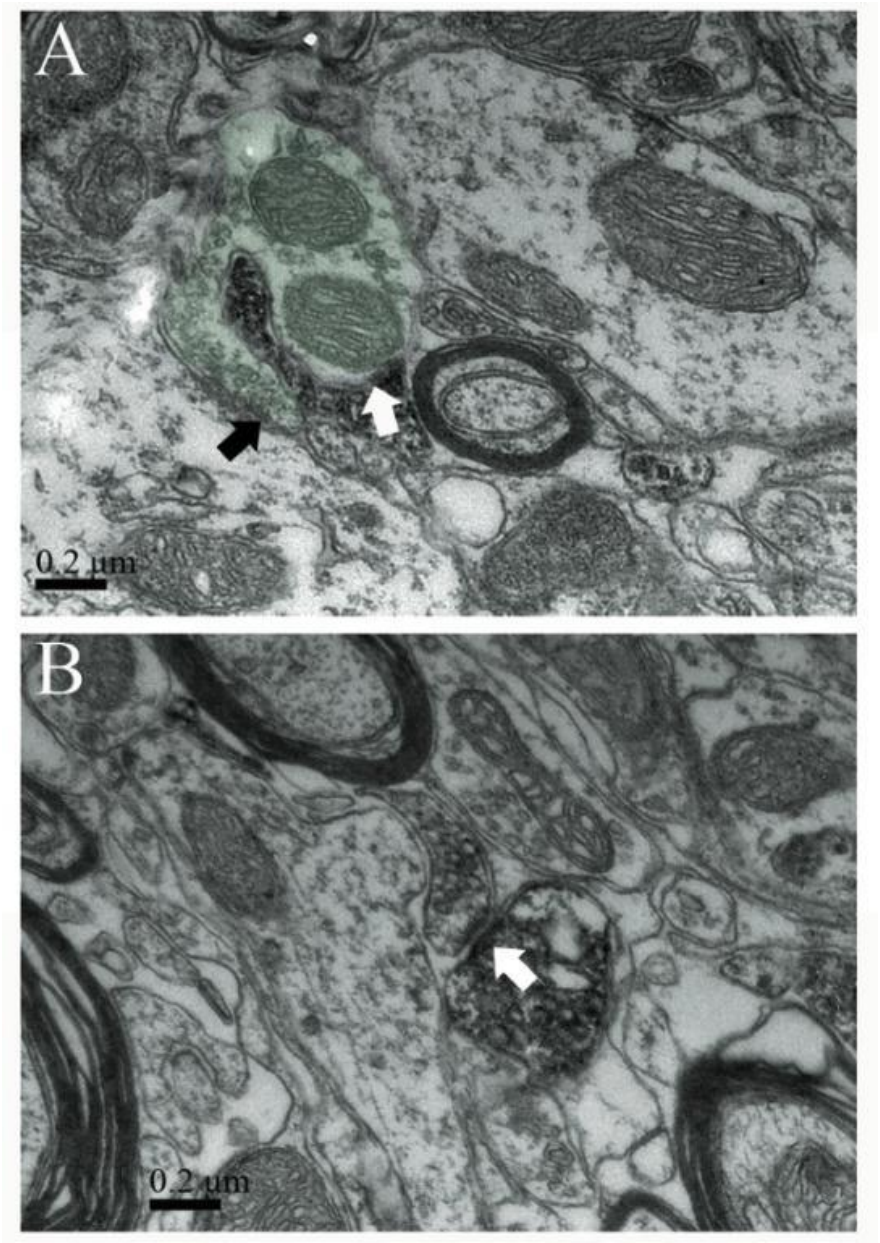


Figure 3.13: Example micrographs showing axo-axonic synapses.

A) A VAChT- immunopositive bouton forms a type-2 synapse (white arrow) with the axon of an unlabelled bouton (shaded green), which then goes on to form a type-1 synapse (black arrow) with an unlabelled dendrite. B) A VAChT-immunopositive bouton forms a type-2 synapse with another VAChT immunopositive bouton (white arrow). Examples of VAChT-immunopositive boutons forming synapses with other VAChT-immunopositive boutons were seen twice during the single section analysis.

3.4 Discussion

3.4.1 Summary of results

The main findings of the present study are first, that type-1 (excitatory) and type-2 (inhibitory) inputs provide equal innervation of the STN. Secondly, subcortical glutamatergic (VGluT2-immunopostive) inputs give rise to a significantly larger number of synapses than cortical glutamatergic (VGluT1-immunopositve) inputs. Thirdly, that VGluT1, VGluT2 and VGAT immunopositive boutons accounted for approximately 93% of boutons providing synaptic contact within the STN. Fourthly, that terminals containing catecholamines account for relatively few of the synaptic boutons within the STN and finally, that cholinergic synaptic boutons form both type-1 and type-2 synapses and may potentially contain a second neurotransmitter. Catecholamine-containing terminals may utilise either dopamine or noradrenaline (NA), I propose at this time that these terminals are most likely to be dopaminergic in nature as dopaminergic terminals have been directly visualised in rodent tissue (Cragg *et al.*, 2004) and noradrenergic terminals have only been visualised in monkey tissue (Carpenter *et al.*, 1981) or indirectly suggested in rodents (Arcos *et al.*, 2003; Belujon *et al.*, 2007). Indeed it was found by one study that tracer injections into the locus coeruleus (the main source of NA) did not result in labelling within the STN in rodents (Canteras *et al.*, 1990). Also, it should be noted that dopaminergic neurons have been proposed to release dopamine extra-synaptically meaning that the numbers of TH-immunopositive synaptic terminals may not equate the true magnitude of dopaminergic innervation.

As covered previously (Section 1.3.1) glutamatergic boutons arise from both cortical and subcortical sources, with subcortical sources including mesopontine tegmentum (specifically PPN), and CM/Pf thalamic nuclei. Cortical regions include the frontal

cortex, motor cortex and primary somatosensory cortex (Jackson & Crossman, 1983; Canteras *et al.*, 1990). GABAergic boutons are likely to arise from GPe and mesopontine tegmentum (Canteras *et al.*, 1990).

3.4.2 Dopamine and acetylcholine release in the STN

The PPN is known to give rise to glutamatergic, GABAergic and cholinergic projections to the STN (Bevan & Bolam, 1995), and the midbrain is known to give rise to a dopaminergic projection to the STN (Cragg *et al.*, 2004). Therefore, the relative proportions of VAChT and TH –immunopositive bouton were also studied.

TH-immunopositive boutons accounted for a very small population of boutons (~4%). VAChT-labelled boutons accounted for 11% of boutons producing synapses within the STN. When combined with the VGluT1, VGluT2 and VGAT data this amounts to 109%, not taking into account false-negatives and innervation from other sources that give rise to less dense projections such as serotonergic boutons from the raphe (Parent *et al.*, 2010). This suggests that two or more of the targeted proteins may be co-localised within a single population of neurons. During control experiments VGluT1, VGluT2 and VGAT did not show co-localisation and the TH-expressing population of boutons is too small to account for discrepancy in percentages. ChAT has been shown to localise in PPN neurons immunopositive for glutamate, therefore, the most likely candidate is VAChT (Clarke *et al.*, 1997). It would be interesting to investigate the two different types of innervation the VAChT-immunopositive boutons represent; the boutons forming type-1 synapses primarily with spines and the boutons forming type-2 synapses with a wide variety of targets. As only type-1 synapses were formed by VGluT2-immunopositive boutons it can be assumed that only type-1 synapse forming VAChT-immunopositive bouton can co-localise VGluT2 and VAChT. There may also be co-

localisation of ACh and GABA in the boutons forming type-2 synapses neurons (Clarke *et al.*, 1997), it has been shown in the basal forebrain (Leisman *et al.*, 2014) . These may represent separate sources of ACh innervation of the STN, and potentially functionally separate pathways of information flow.

Unfortunately, during the control experiments double-labelling for VAChT with VGluT2 or VGAT were unsuccessful, possibly due to interactions between the antibodies used in these experiments. It would be useful to repeat the double labelling experiments with a different combination of antibodies, although there is currently a shortage of good VAChT antibodies for electron microscopy.

Additionally, the presence of axo-axonic synapses formed by VAChT-immunopositive boutons is an interesting area for further research to verify if these synapses are a general feature within the STN. Axo-axonic synapses are proposed to change synaptic plasticity presynaptically, by changing release probability within post-synaptic axons (Fink *et al.*, 2014). Axo-axonic synapses formed by VAChT-immunopositive boutons were all found making contact with an axon in close proximity to the post-synaptic structure forming a type-1 putatively excitatory synapse. Therefore, the dynamics of these excitatory synapses may change in the presence or absence of acetylcholine, increasing the importance of acetylcholine release when determining STN firing.

3.4.3 Glutamatergic control of STN firing

Traditionally, the cortico-subthalamic pathway (sometimes referred to as the 'hyper-direct pathway') has been shown to be the primary source of excitatory post-synaptic potentials to STN neurons in electrophysiological studies (Nambu *et al.*, 2000), although

it should be noted that the thalamo-subthalamic pathway has not been extensively studied. Whilst there may be physically more VGluT2-immunopostive boutons producing synapses within the STN compared to VGluT1-immunopositive boutons, many factors can determine the strength of synaptic innervation, including the levels of receptors present within the synapse, synaptic plasticity and the location of synapses within the dendritic tree, and so the proportion of innervation is only part of the story when discussing glutamatergic control of the STN.

The STN has also been proposed to have glutamatergic intranuclear axon collaterals which would be immunopositive against VGluT2 (Kita *et al.*, 1983), although the presence of these collaterals is controversial (Wilson *et al.*, 2004). This means that the VGluT2-immunopositive boutons giving rise to synapses may consist of both extrinsic projections to the STN from the PPN and/or the thalamus (Smith *et al.*, 2004) and synapses formed by STN neurons. To fully understand external control of the STN the quantity of innervation from thalamus (Sugimoto *et al.*, 1983; Smith *et al.*, 1998), and the PPN (Hammond *et al.*, 1983) needs to be elucidated, separating the proportion of VGluT2-immunopostive boutons forming synapses that originate from external projections from those formed by intranuclear collaterals.

Subcortical excitatory (VGluT2) boutons account for 57% of type-1 synapses. When putative PPN (VAChT) boutons are removed from this (a maximum of 12% of type-1 synapses assuming that all boutons had co-localisation), the subcortical innervation is still larger than the cortical innervation (45% verses 35%) suggesting that the thalamus may have a larger role than previously expected. Additionally, VGluT2-immunopositive boutons had a significantly larger cross-sectional area and targeted larger post-synaptic structures – a sign of more proximal innervation, and thus in a position to have more

influence over STN neuron firing activity. Together these results suggest that the thalamo-subthalamic pathway may be a prominent source of glutamate in the STN. Indeed when examined electrophysiologically, it has been found that stimulation of the parafascicular nucleus (Pf) of the thalamus provides a strong excitatory drive to both ipsilateral and contralateral STN (Mouroux *et al.*, 1995).

Thalamic Pf neurons have been implicated in the sensory-motor pathways linking spinal pathways regarding visual, audio and somatosensory systems to target cortical structures (Nakamura *et al.*, 2006). This thalamo-subthalamic pathway may well carry sensory information directly related to motor actions, which combined with the PPN inputs – a nucleus implicated in sensory-motor and reward processing (Inglis *et al.*, 2000), allowing the STN to integrate sensation with movement before targeting areas such as the dopaminergic neurons of the SNc as part of the reward pathway. This theory is supported by Bevan et al (1997) who showed synaptic integration of motor and sensory inputs to single neurons within the STN (Bevan *et al.*, 1997).

3.4.4 Deep-brain stimulation of the STN

The STN has long been targeted as a therapeutic site for deep-brain stimulation (DBS) protocols in the treatment of Parkinson's disease. Electrodes are chronically implanted in the STN and stimulated at high frequencies, typically 130-190Hz (Byrd *et al.*, 2000). This has resulted in dramatic motor symptom relief and it has become established as a leading treatment for drug-resistant Parkinson's disease. However, the exact mechanism by which DBS relieves symptoms is unknown. Several theories have been developed to explain the effect, ranging from inactivation of the STN via depolarisation block and inactivation of voltage-gated channels – indeed this was the initial logic underlying the

development of DBS as a treatment for Parkinson's disease, to antidromic activation of afferent inputs to the STN, to direct activation of STN neurons (Chiken & Nambu, 2014). Clearly, all of these theories cannot be correct and understanding the connectivity of the STN including its afferents can help develop better computational models to stimulate DBS in normal and Parkinsonian conditions. The current results show that the thalamic and PPN afferents to STN need to be examined in more detail when discussing control of STN firing in healthy, Parkinsonian conditions and during DBS treatment.

Another theory regarding DBS mechanism is that high frequency stimulation disrupts a pathogenic oscillation which has been found in the STN, basal ganglia and indeed the cortex (Brown, 2006). Both the thalamus and PPN have been found to display the classic beta frequency of oscillations seen in both affected patients and experimental Parkinsonian animals, and the origin of this putatively pathogenic oscillation is still not known. It may be that thalamic oscillations entrain the STN into the beta rhythm, where it is then propagated to the entire basal ganglia via the extensive efferent connections of the STN, including reciprocal connections with the GPe (Mallet *et al.*, 2008). A computational study performed by Nevado-Holgado et al found that rhythmic inputs from the thalamus, striatum and cortex are sufficient to generate Parkinsonian oscillations (Nevado-Holgado *et al.*, 2014). Disruptions in this rhythm within the STN, and potentially antidromically to afferent nuclei, may allow information to flow through the basal ganglia resulting in movement, without becoming 'trapped' by the pathogenic oscillations. However, it may be that disrupting any one part of the oscillating network is sufficient to prevent basal ganglia and cortical entrainment and so further work is required to determine if thalamic nuclei drive the beta rhythm throughout the basal ganglia via its connections to STN and striatum.

3.4.5 Conclusion

Whilst our knowledge of afferent and efferent connections of STN neurons is growing, it is clear that there is much more work to be done. Many issues are yet to be resolved, such as the mechanism underlying DBS, the presence, or not, of intranuclear connections, and perhaps most importantly, the main driver of STN activity in normal and pathologic conditions. This study has highlighted the importance of thalamic and other subcortical excitatory inputs in the control of STN firing, and the potential of acetylcholine to hold a much larger role than currently understood. Figure 3.14 is an expanded circuit diagram of the basal ganglia, updated to include the data from this thesis. Clearly the connectivity is not as simplistic as early models have shown and a wide range of sources influence basal ganglia information flow at locations other than the traditional input structure of the striatum. Until a full profile of innervation to the STN, and the electrophysiological response of STN neurons to these inputs, is understood, the models of Parkinson's disease and the action of DBS in the STN will not be accurate enough to finally understand the mechanism behind its dramatic effects.

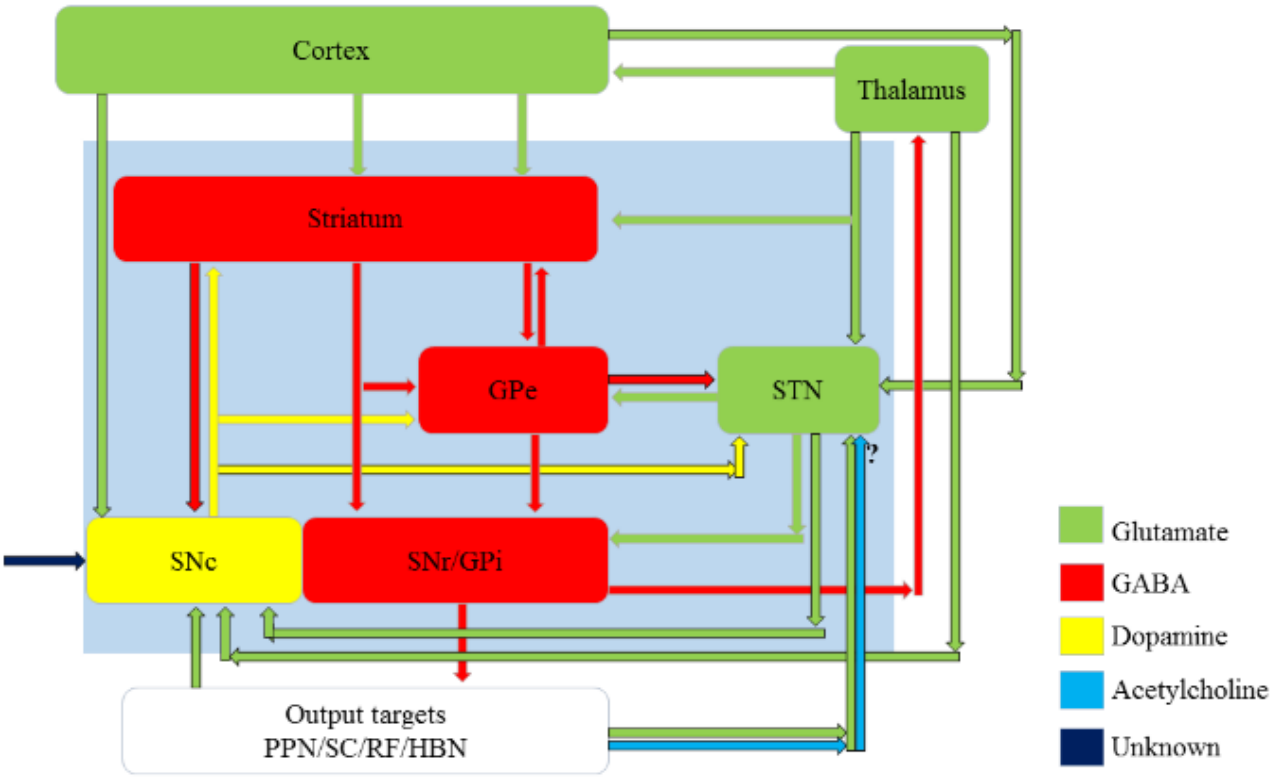


Figure 3.14: An updated diagram showing the connectivity of the basal ganglia circuit.

Pathways of interest during this thesis are highlighted, ? indicates the potential co-release of two transmitters.

GPe, globus pallidus external segment; GPi, globus pallidus internal segment; HBN, lateral habenula; PPN, pedunculopontine nucleus; RF, reticular formation; SC, superior colliculus; SNc, substantia nigra compacta; SNr, substantia nigra reticulate; STN, subthalamic nucleus.

Chapter Four

General Discussion

4.1 Summary and Conclusions

Understanding the connectivity between cortical and subcortical areas with the basal ganglia can aid the development of accurate models of information processing and neuronal firing, and reveal the potential functional roles of each nucleus. The investigations in the thesis have explored the afferent connectivity of two key areas in the basal ganglia: the dopaminergic neurons of the substantia nigra and the neurons of the subthalamic nucleus.

The proportions of glutamatergic innervation arising from cortical or subcortical sources was explored using antibodies against vesicular glutamate transports specific to either cortical (VGluT1) or subcortical (VGluT2) terminals. In addition to glutamate innervation, the inhibitory innervation was examined, as were the cholinergic inputs (using antibodies against the vesicular transporter for acetylcholine; VAChT) and dopaminergic inputs (using antibodies against the rate limiting enzyme in dopamine synthesis; tyrosine hydroxylase [TH]).

4.1.1 Synaptic weight

This study examined synaptic input in two different ways, firstly the proportion of innervation originating from each brain region and secondly, examining the morphological characteristics of each projection. Whilst it is clear that more innervation from a particular region will allow a larger effect on the target neurons, not all synapses are created equal. The location of synapses, along with the physical characteristics of each synapse, determine the relative strength of the synapse. This is referred to as the weight of the synapse and is important when developing computational models of neuron firing. Due to the importance of synaptic weighting in model development

several key characteristics were measured: the target dendrite area, the synaptic terminal area and the length of the active zone.

The pre-synaptic active zone of a synapse appears as an electron-dense thickening under the electron microscope, allowing its length to be measured. This electron-dense thickening consists of a range of specialised proteins, including ion channels, scaffolding proteins and proteins involved in the exocytosis of vesicles into the synaptic cleft (Sudhof, 2012). It has previously been shown that the number of docked vesicles (i.e. vesicles which are primed, ready to be released in response to stimulation) is linked to the size of the active (Schikorski & Stevens, 1997), suggesting that a larger active zone has a higher probability of releasing vesicles in response to a set stimulus. Indeed, this has been tested in the hippocampus and a linear relationship was found between release probability and active zone size (Holderith *et al.*, 2012). Therefore, we can predict that synaptic terminals with larger active zones are likely to hold a larger synaptic weighting than those with small active zones.

Another measure which allows an estimation of synaptic weighting is the physical size of structures comprising the synapse, both pre- and post-synaptic. It has been repeatedly shown that increasing the strength of a synapse increases the area of both the pre-synaptic terminal and the post-synaptic spine (Schikorski & Stevens, 1999; Murthy *et al.*, 2001; Meyer *et al.*, 2014). In the case of axo-dendritic synapses, where terminals form synapses directly with the dendrite of a neuron, again increased dendrite area will correlate with an increased synaptic weight of the connection. This is due to the simple fact that dendritic area generally increases when more proximal to the somata. Therefore, the post-synaptic response has less distance to propagate and thus will have a larger effect on the post-synaptic somata (Magee, 2000).

Whilst these measures suggest a possible weight of synapses, it should be noted that short-term plasticity events, such as those induced by NMDA receptors, will also strongly affect the weight of a synapse. Therefore, these measures are only a snapshot of the potential synaptic weight for each connection.

4.1.2 Chapter two: innervation of dopamine neurons within the substantia nigra

The main findings of this study were that, firstly, in addition to subcortical sources, glutamatergic projections to the dopamine neurons of the SN include a direct cortical projection, specifically to dendrites located within the SNc compartment. This is the first time synapses from cortical sources have been shown making contact to SNc dopamine neurons and backs up recent suggestions of a monosynaptic pathway from cortex to SNc shown using a viral vector (Watabe-Uchida *et al.*, 2012).

Secondly, the innervation of dopaminergic dendrites differs depending on the compartment of SN that they are located in, with dendrites in the SNr receiving mainly inhibitory inputs (~70%) and dendrites in the SNc receiving equal innervation from excitatory and inhibitory synaptic boutons. Thirdly, a large proportion of the putatively excitatory synaptic boutons to both compartments (type-1 synapses) was not labelled using either VGluT1 or VGluT2, suggesting that there is either another unknown glutamatergic vesicular transporter, or that the projection utilises another transmitter such as acetylcholine. These results are in agreement with those shown for individual dopamine neurons (Henny *et al.*, 2012) suggesting that the innervation of dopamine neurons depends only on the location of their dendrites.

Finally, the morphological characteristics of each projection type were examined. Glutamatergic boutons from both cortical and subcortical sources were similar both in cross-sectional area and the size of their targeted structures. Unlabelled, putative excitatory (type-1 synaptic boutons) terminals had a significantly smaller cross-sectional area than glutamatergic boutons, again suggesting that these belong to a separate projection and are not due to technical error. Boutons providing putatively inhibitory input to dopamine neurons of the SN are larger within the SNc compartment than the SNr compartment. This suggests that the inhibitory input to SNc dendrites may be capable of greater inhibition of dopamine neurons, due to larger boutons and a more proximal location of synapse (as dopamine neuron cell bodies are located within the SNc).

4.1.3 Chapter three: innervation of the subthalamic nucleus

The innervation of neurons within the STN was also examined to further explore the afferent control of the STN. The main findings of this study are that excitatory and inhibitory innervation of STN neurons are approximately equal in terms of number of synapses, with only a very small number of synaptic contacts from TH-positive axons. A significantly larger proportion of glutamatergic boutons arise from subcortical sources compared to cortical regions. This suggests that the subcortical areas innervating STN neurons, PPN and CM/Pf thalamic nuclei, may have a greater role in control of STN firing than previously considered. Prior studies have focused on the cortico-subthalamic pathway as the main source of glutamate to the STN and this perhaps needs to be re-examined. The morphology of the synaptic terminals examined here provides further evidence for VGluT2-expressing terminals creating stronger synapses than putative

cortical terminals. VGluT-2-expressing terminals were both larger and contacted larger structures than VGluT1-expressing terminals. The active zones of VGluT1-expressing terminals were also the smallest, with the exception of TH-expressing boutons.

Boutons containing acetylcholine appear to arise from at least two separate populations of neurons, one producing type-1 synaptic boutons and another producing type-2 synaptic boutons. Additionally, at least part of this projection may comprise boutons which co-localise ACh and either glutamate or GABA.

TH-expressing terminals were sparse, with the smallest active zones recorded in this study. However, the boutons of TH-expressing terminals were significantly larger than VAChT-expressing terminals, and comparable to the VGluTs. It is therefore likely that many synapses may have been missed in the analysis due to the small size of dopamine active zones (the most identifiable part of a synapse), or that dopamine release may be extrasynaptic. Both of these scenarios would explain why such a small projection was uncovered by this study, despite the documented effects of dopamine within the STN and a high density of dopamine receptors (Dupuis *et al.*, 2013; Galvan *et al.*, 2014).

4.1.4. Conclusions of the thesis

Overall, the studies in this thesis have shown that subcortical regions give rise to large numbers of glutamatergic synapses in the BG, not just the main input structure the striatum, but the STN and the dopamine neurons of the SN. This is in agreement with recent studies implicating the STN as a joint input structure of the BG with the GPe as a central processor (Figure 1.4; Section 1.1.3). The striatum is known to receive glutamatergic innervation from both cortical and subcortical regions (Doig *et al.*, 2010),

and this is mirrored in the STN. The STN appears to receive inputs from both motor regions (motor cortex) and sensory regions (sensory cortex, Pf nucleus and PPN), suggesting an integrative role in BG processing.

Additionally, the dopaminergic neurons of the SN receive a direct innervation from cortical regions and a large proportion of input which is putatively excitatory in nature but does not appear to use glutamate. Understanding the sources of input and the relative proportion from each, can help us to create models of dopamine firing which may help to explain the many roles of dopamine and the various deficits which may cause dopaminergic disorders.

Taken together the data within this thesis help to expand our knowledge of the connectivity of the BG. An updated model of BG activity should include a much larger range of inputs to SN, and potentially assign an input role to the STN (Figure 4.1). Further research is needed to expand the sources of input to both these regions, specifically separating the relative importance of each subcortical region.

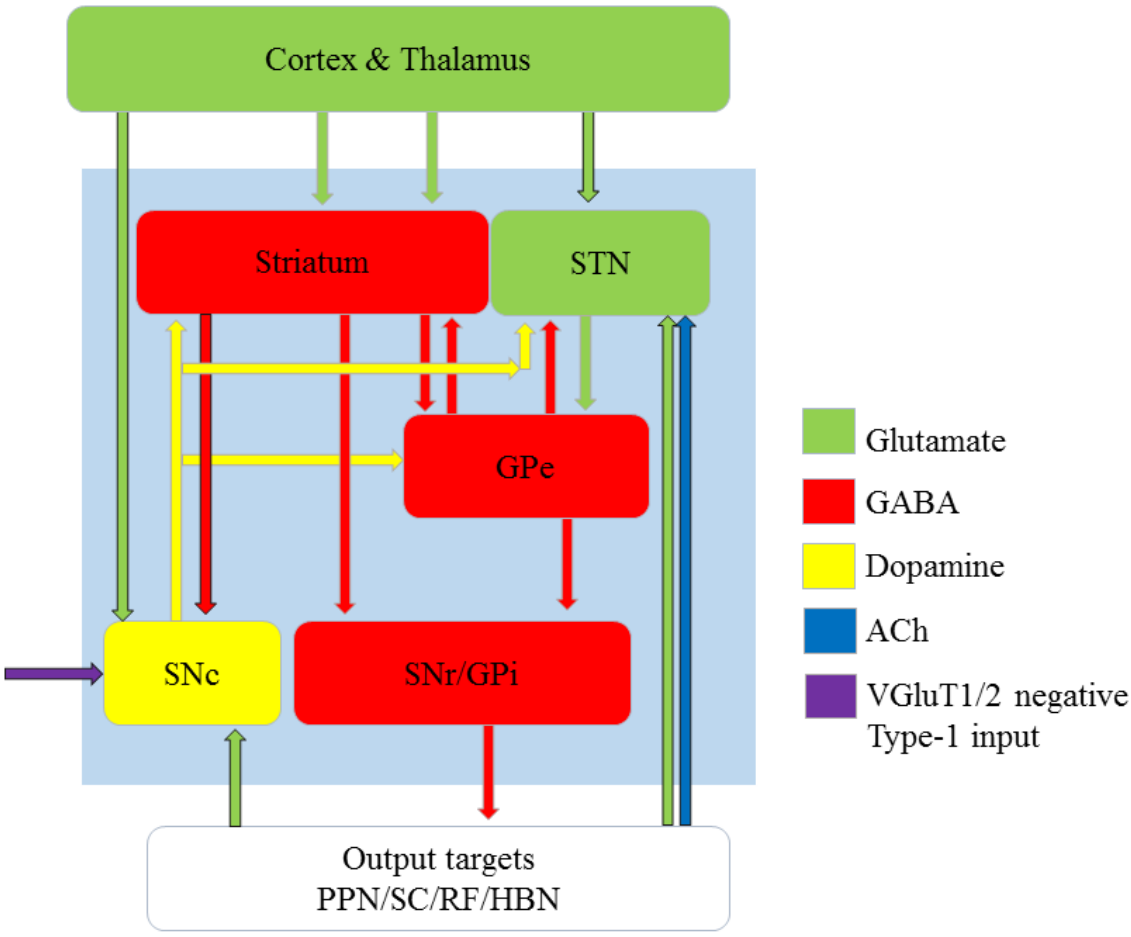


Figure 4.1: A revised circuit diagram showing the connectivity of the basal ganglia.

In this model the STN and striatum act as the main input structures and then sending reciprocal projections to the GPe. The GPe then collates the information sending to all aspects of the basal ganglia. The SNc receives input from a wide range of sources and sends projections to the entire basal ganglia.

GPe, globus pallidus external segment; GPi, globus pallidus internal segment; HBN, habenula; SC, superior colliculus; SNc, substantia nigra pars compacta; SNr, substantia nigra pars reticulata; *STN, subthalamic nucleus; PPN, pendunculopontine nucleus; RF, reticular formation.*

4.2 Technical Considerations

The studies performed in this thesis have all been conducted using electron microscopy and immunohistochemistry. Each technique comes with benefits and potential drawbacks. Electron microscopy is the most accurate tool to identify synapses and when combined with immunohistochemistry can show the presence of synaptic boutons from identified brain regions. However, electron microscopy is a difficult and time-consuming method which limits the amount of tissue which can be examined in a set time period. Additionally, only two different immunolabels can be used in any given section when prepared for electron microscopy. This seriously limits the ability to identify structures which require more than one biomarker to identify them, for example separating the ventral and dorsal tier dopaminergic neurons would require immunolabels for TH, calbindin, and a third antibody to identify the source of synaptic boutons.

Immunohistochemistry also has limitations, namely specificity of antibodies. In order to be suitable for electron microscopy antibodies must be highly specific for the target protein, as excessive background staining will appear immunopositive at the electron microscopic level. There are also limitations as to the identification of the source of synaptic boutons using immunohistochemistry. Not all projections have specific protein biomarkers, for example glutamatergic projections from the thalamus and the PPN both use VGluT2. In an attempt to separate these populations a protein which is highly expressed in the thalamic nucleus pf, the main source of thalamic input to the STN, was targeted using antibodies previously used to label Pf neuron somata, cerebellin-1 (Wei *et al.*, 2007), and the striatum and STN examined. This is because both these areas receive a strong projection from the pf. However, the protein is either not present in the axon terminals of Pf neurons or was at a level too low to detect using florescence microscopy.

At this time, no further antibodies or markers are commercially available/known to separate these populations.

Finally, immunohistochemistry has physical limitations. Antibodies can only penetrate a short distance through tissue. In light microscopy tissue is often treated with detergents to allow antibodies to penetrate deeper. However, detergents damage the integrity of neuronal ultrastructure resulting in unusable electron micrographs. To overcome this, freeze-thawing the tissue can help increase the penetration of antibodies but direct comparisons between freeze-thawing and the use of detergents have not yet been made.

However, at present the only method available that can confirm the presence of synapses with certainty is electron microscopy. Combining the data obtained from electron microscopy with newer techniques can help overcome some of these issues, demonstrating the importance of multidisciplinary research.

4.3.Future Directions

The data produced in this thesis has opened up several interesting areas of potential research in future, some of which shall be covered in detail below with suggested experimental protocols to answer each question.

4.3.1. Elucidating the source of type-1 synaptic boutons in the SNc

Whilst this study was able to show the relative proportions of cortical and subcortical glutamatergic boutons forming synapses with dopaminergic neurons of the SNc, there are several potential regions which may be supplying each subtype. For example subcortical inputs are made up of projections from thalamus, the STN and the PPN. To fully understand the afferent control of dopamine neurons the proportions of each source providing the input needs to be further analysed.

At present there are no antibodies which can separate these terminals from these regions biochemically, as they all use VGluT2. Tracer studies have been generally unsuccessful for quantification methods due to the inability to inject a nucleus fully, without overlap in neighbouring brain regions. A potential solution to this could be surgical ablation of the nucleus in question, for example the PPN, and studying the number of degenerating terminals making contacts with dopaminergic neurons. The PPN could then be analysed to determine the exact region supplying degenerated terminals to the SNc.

Additionally, a large proportion of the type-2 input to dopaminergic neurons of the SNc were not labelled with VGluT1 or VGluT2, and so repeating the above experiments using antibodies against markers for cholinergic and serotoninergic terminals would help to fill this knowledge gap.

4.3.2. Differences in afferent input between dopamine neurons

This study sought to determine the afferent input to dopamine neurons, but did not take into account any potential variation between subtypes. Whilst it has been suggested that inputs to calbindin- (CB-) positive dopaminergic neurons and CB-negative dopaminergic neurons are likely to be similar (Henny *et al.*, 2012), it has not been directly studied. CB-positive dopamine neurons fire at a slower rate compared to CB-negative (Neuhoff *et al.*, 2002) and whilst it may be due to differences in membrane properties it may also be due to differential inputs. Studying this using the methods in this thesis however, would prove challenging due to the limitation of using only two antibodies at a time. In order to overcome this, a fluorescent immunolabel could be used to determine the CB-positive region of the SNc. Once determined, careful sectioning could enable a specific selection of dopamine neurons, labelled with both fluorescent and DAB antibodies, to be processed for electron microscopy.

4.3.3. Studying the input/output profile of non-dopaminergic SNc neurons

Dopaminergic neurons are not the only neurons within the SNc. GABAergic neurons are also present within the SNc, and little is known regarding the innervation of these neurons or their efferent targets. This could studied in two ways, firstly in a manner similar to above, using antibodies against GABAergic neurons develop a profile of afferent inputs. Uncovering the efferent profiles of these cells could prove more challenging, a viral vector method such as those used to uncover single dopamine neurons (Matsuda *et al.*, 2009) could be used, with immunohistochemistry to ensure cell bodies are located in the correct location.

4.3.4. Defining the anatomical nature of STN neurons

Whilst it is accepted that approximately ~94% of STN neuron are glutamatergic projection neurons, this still leaves ~6% of neurons unaccounted for. Whilst this may seem insubstantial it should be considered that the striatum is also approximately ~95% projection neurons, yet it is widely accepted that the ~5% of interneurons hold varied and critical roles in information processing. Therefore, it would be unwise to assume that the STN is a homogeneous structure without further analysis. In light of the similar afferent innervation pattern of STN neurons compared to striatum, and its potential role as an input nucleus, the presence or not of interneurons should be investigated. Stereological counting of neurons which are immunopositive for a range of biomarkers (such as PV, CR, CB, NOS or GABAergic biomarkers) could help to fully characterise any potential subpopulations within the STN, and then the innervation patterns of each population could be determined using the methods such as those used in this thesis.

4.3.5. Determining the source of ACh in STN and any co-localisation of transmitters

Another experiment which would be useful to fully characterise the afferent input to STN neurons would be to determine if ACh is co-localised within synaptic boutons along with another neurotransmitter, and to determine if the source of cholinergic synaptic boutons is from more than one nucleus. To fully elucidate the sources of monosynaptic input to STN neurons a genetic technique such as that used by Watabe-Uchida *et al* (2012) could provide information regarding all possible sources of innervation. Once all the potential sources of input have been identified, immunohistochemistry could be performed using a range of fluorescent antibodies,

combined with tracer studies, to determine the exact source and nature of projections to the STN.

4.3.6. The electrophysiological response to individual afferent stimulation

Whilst it is useful to determine the proportions of afferent inputs to selected neurons in the basal ganglia, there is more involved in afferent control of neuronal firing than the presence of synaptic boutons. The types of receptors within the synapse, combined with the location of the synapse on the post-synaptic neuron, release probability of transmitters from the bouton and other translational changes within the dendrite and bouton can affect synaptic strength (Wilson, 1988). Therefore, the only way to truly determine the exact role each projection plays in each nucleus is to record electrophysiologically from the post-synaptic neuron whilst stimulating the pre-synaptic bouton. With the advances in electrophysiology and optogenetics, this can be achieved by using juxtacellular recording and optogenetics to stimulate the targeted projection neurons (Kanbar *et al.*, 2011). Alternately, useful information can be gained about each projections effect on post-synaptic targets using *in vitro* electrophysiology recording techniques [see (Ellender *et al.*, 2013) for an example].

4.4. Final statement

It is clear that despite many decades of study, that a full profile of the basal ganglia connectivity has not been completed. This thesis has added and confirmed several pathways of afferent input to SN and STN, but there are many questions left to answer, and a long way to go until our understanding of basal ganglia information processing is at a sufficient level to understand the many disorders associated with basal ganglia

dysfunction. Ultimately, the more we can ascertain about basal ganglia connectivity, the more we can predict about its role in information processing and behavioural control.

Bibliography

Afsharpour, S. (1985) Light microscopic analysis of Golgi-impregnated rat subthalamic neurons. *J Comp Neurol*, **236**, 1-13.

Albin, R.L., Young, A.B. & Penney, J.B. (1989) The functional anatomy of basal ganglia disorders. *Trends Neurosci*, **12**, 366-375.

Albin, R.L., Young, A.B. & Penney, J.B. (1995) The functional anatomy of disorders of the basal ganglia. *Trends Neurosci*, **18**, 63-64.

Alegre, M., Lopez-Azcarate, J., Obeso, I., Wilkinson, L., Rodriguez-Oroz, M.C., Valencia, M., Garcia-Garcia, D., Guridi, J., Artieda, J., Jahanshahi, M. & Obeso, J.A. (2013) The subthalamic nucleus is involved in successful inhibition in the stop-signal task: a local field potential study in Parkinson's disease. *Exp Neurol*, **239**, 1-12.

Alexander, G.E. & Crutcher, M.D. (1990) Functional architecture of basal ganglia circuits: neural substrates of parallel processing. *Trends Neurosci*, **13**, 266-271.

Ambrosi, G., Cerri, S. & Blandini, F. (2014) A further update on the role of excitotoxicity in the pathogenesis of Parkinson's disease. *J Neural Transm* **121**, 849-859.

Apicella, P., Deffains, M., Ravel, S. & Legallet, E. (2009) Tonically active neurons in the striatum differentiate between delivery and omission of expected reward in a probabilistic task context. *Eur J Neurosci*, **30**, 515-526.

Aquino, C.C. & Lang, A.E. (2014) Tardive dyskinesia syndromes: current concepts. *Parkinsonism Relat Disord*, **20 Suppl 1**, S113-117.

Arcos, D., Sierra, A., Nunez, A., Flores, G., Aceves, J. & Arias-Montano, J.A. (2003) Noradrenaline increases the firing rate of a subpopulation of rat subthalamic neurones through the activation of alpha 1-adrenoceptors. *Neuropharmacology*, **45**, 1070-1079.

Aron, A.R. & Poldrack, R.A. (2006) Cortical and subcortical contributions to Stop signal response inhibition: role of the subthalamic nucleus. *J Neurosci*, **26**, 2424-2433.

Barbaresi, P., Gazzanelli, G. & Malatesta, M. (1997) Glutamate-positive neurons and terminals in the cat periaqueductal gray matter (PAG): a light and electron microscopic immunocytochemical study. *J Comp Neurol*, **383**, 381-396.

Barroso-Chinea, P., Castle, M., Aymerich, M.S., Perez-Manso, M., Erro, E., Tunon, T. & Lanciego, J.L. (2007) Expression of the mRNAs encoding for the vesicular glutamate transporters 1 and 2 in the rat thalamus. *J Comp Neurol*, **501**, 703-715.

Bear, M.F., Connors, B.W. & Paradiso, M.A. (2007) *Neuroscience : exploring the brain*. Lippincott Williams & Wilkins, Philadelphia, PA.

Beaulieu, C. & Somogyi, P. (1990) Targets and quantitative distribution of GABAergic synapses in the visual cortex of the cat. *Eur J Neurosci*, **2**, 896.

Beaulieu, J.M. & Gainetdinov, R.R. (2011) The physiology, signaling, and pharmacology of dopamine receptors. *Pharmacol Rev*, **63**, 182-217.

Belujon, P., Bezard, E., Taupignon, A., Bioulac, B. & Benazzouz, A. (2007) Noradrenergic modulation of subthalamic nucleus activity: behavioral and electrophysiological evidence in intact and 6-hydroxydopamine-lesioned rats. *J Neurosci*, **27**, 9595-9606.

Benhamou, L., Kehat, O. & Cohen, D. (2014) Firing pattern characteristics of tonically active neurons in rat striatum: context dependent or species divergent? *J Neurosci*, **34**, 2299-2304.

Beninato, M. & Spencer, R.F. (1988) The cholinergic innervation of the rat substantia nigra: a light and electron microscopic immunohistochemical study. *Exp Brain Res*, **72**, 178-184.

Bennett, B.D. & Bolam, J.P. (1993) Characterization of calretinin-immunoreactive structures in the striatum of the rat. *Brain Res*, **609**, 137-148.

Bennett, B.D. & Bolam, J.P. (1994a) Localisation of parvalbumin-immunoreactive structures in primate caudate-putamen. *J Comp Neurol*, **347**, 340-356.

Bennett, B.D. & Bolam, J.P. (1994b) Synaptic input and output of parvalbumin-immunoreactive neurons in the neostriatum of the rat. *Neuroscience*, **62**, 707-719.

Bentivoglio, M., van der Kooy, D. & Kuypers, H.G. (1979) The organization of the efferent projections of the substantia nigra in the rat. A retrograde fluorescent double labeling study. *Brain Res*, **174**, 1-17.

Berlanga, M.L., Simpson, T.K. & Alcantara, A.A. (2005) Dopamine D5 receptor localization on cholinergic neurons of the rat forebrain and diencephalon: a potential neuroanatomical substrate involved in mediating dopaminergic influences on acetylcholine release. *J Comp Neurol*, **492**, 34-49.

Bevan, M.D. & Bolam, J.P. (1995) Cholinergic, GABAergic, and glutamate-enriched inputs from the mesopontine tegmentum to the subthalamic nucleus in the rat. *J Neurosci*, **15**, 7105-7120.

Bevan, M.D., Booth, P.A., Eaton, S.A. & Bolam, J.P. (1998) Selective innervation of neostriatal interneurons by a subclass of neuron in the globus pallidus of the rat. *J Neurosci*, **18**, 9438-9452.

Bevan, M.D., Clarke, N.P. & Bolam, J.P. (1997) Synaptic integration of functionally diverse pallidal information in the entopeduncular nucleus and subthalamic nucleus in the rat. *J Neurosci*, **17**, 308-324.

Bevan, M.D., Francis, C.M. & Bolam, J.P. (1995) The glutamate-enriched cortical and thalamic input to neurons in the subthalamic nucleus of the rat: convergence with GABA-positive terminals. *J Comp Neurol*, **361**, 491-511.

Bevan, M.D., Smith, A.D. & Bolam, J.P. (1996) The substantia nigra as a site of synaptic integration of functionally diverse information arising from the ventral pallidum and the globus pallidus in the rat. *Neuroscience*, **75**, 5-12.

Bolam, J.P., Francis, C.M. & Henderson, Z. (1991) Cholinergic input to dopaminergic neurons in the substantia nigra: a double immunocytochemical study. *Neuroscience*, **41**, 483-494.

Bolam, J.P., Hanley, J.J., Booth, P.A. & Bevan, M.D. (2000) Synaptic organisation of the basal ganglia. *J Anat*, **196 (Pt 4)**, 527-542.

Bolam, J.P. & Pissadaki, E.K. (2012) Living on the edge with too many mouths to feed: why dopamine neurons die. *Mov Disord*, **27**, 1478-1483.

Bolam, J.P., Smith, Y., Ingham, C.A., von Krosigk, M. & Smith, A.D. (1993) Convergence of synaptic terminals from the striatum and the globus pallidus onto single neurones in the substantia nigra and the entopeduncular nucleus. *Prog Brain Res*, **99**, 73-88.

Brown, M.T., Henny, P., Bolam, J.P. & Magill, P.J. (2009) Activity of neurochemically heterogeneous dopaminergic neurons in the substantia nigra during spontaneous and driven changes in brain state. *J Neurosci*, **29**, 2915-2925.

Brown, P. (2006) Bad oscillations in Parkinson's disease. *J Neural Transm Suppl*, 27-30.

Brunelin, J., Fecteau, S. & Suaud-Chagny, M.F. (2013) Abnormal striatal dopamine transmission in schizophrenia. *Curr Med Chem*, **20**, 397-404.

Byrd, D.L., Marks, W.J., Jr. & Starr, P.A. (2000) Deep brain stimulation for advanced Parkinson's disease. *AORN J*, **72**, 387-390, 393-408; quiz 409-314, 416-388.

Cachope, R. & Cheer, J.F. (2014) Local control of striatal dopamine release. *Front Behav Neurosci*, **8**, 188.

Canteras, N.S., Shammah-Lagnado, S.J., Silva, B.A. & Ricardo, J.A. (1990) Afferent connections of the subthalamic nucleus: a combined retrograde and anterograde horseradish peroxidase study in the rat. *Brain Res*, **513**, 43-59.

Carpenter, M.B., Carleton, S.C., Keller, J.T. & Conte, P. (1981) Connections of the subthalamic nucleus in the monkey. *Brain Res*, **224**, 1-29.

Carter, C.J. (1982) Topographical distribution of possible glutamatergic pathways from the frontal cortex to the striatum and substantia nigra in rats. *Neuropharmacology*, **21**, 379-383.

Cebrian, C., Parent, A. & Prensa, L. (2005) Patterns of axonal branching of neurons of the substantia nigra pars reticulata and pars lateralis in the rat. *J Comp Neurol*, **492**, 349-369.

Cerasa, A., Fasano, A., Morgante, F., Koch, G. & Quattrone, A. (2014) Maladaptive plasticity in levodopa-induced dyskinesias and tardive dyskinesias: old and new insights on the effects of dopamine receptor pharmacology. *Front Neurol*, **5**, 49.

Chao, Y., Gang, L., Na, Z.L., Ming, W.Y., Zhong, W.S. & Mian, W.S. (2007) Surgical management of Parkinson's disease: update and review. *Interv Neuroradiol*, **13**, 359-368.

Chesselet, M.F. & Delfs, J.M. (1996) Basal ganglia and movement disorders: an update. *Trends Neurosci*, **19**, 417-422.

Chiken, S. & Nambu, A. (2014) Disrupting neuronal transmission: mechanism of DBS? *Front Syst Neurosci*, **8**, 33.

Clarke, N.P., Bevan, M.D., Cozzari, C., Hartman, B.K. & Bolam, J.P. (1997) Glutamate-enriched cholinergic synaptic terminals in the entopeduncular nucleus and subthalamic nucleus of the rat. *Neuroscience*, **81**, 371-385.

Clarke, P.B., Hommer, D.W., Pert, A. & Skirboll, L.R. (1987) Innervation of substantia nigra neurons by cholinergic afferents from pedunculopontine nucleus in the rat: neuroanatomical and electrophysiological evidence. *Neuroscience*, **23**, 1011-1019.

Comoli, E., Coizet, V., Boyes, J., Bolam, J.P., Canteras, N.S., Quirk, R.H., Overton, P.G. & Redgrave, P. (2003) A direct projection from superior colliculus to substantia nigra for detecting salient visual events. *Nat Neurosci*, **6**, 974-980.

Connolly, B.S. & Lang, A.E. (2014) Pharmacological treatment of Parkinson disease: a review. *JAMA*, **311**, 1670-1683.

Coxon, J.P., Van Impe, A., Wenderoth, N. & Swinnen, S.P. (2012) Aging and inhibitory control of action: cortico-subthalamic connection strength predicts stopping performance. *J Neurosci*, **32**, 8401-8412.

Cragg, S., Rice, M.E. & Greenfield, S.A. (1997) Heterogeneity of electrically evoked dopamine release and reuptake in substantia nigra, ventral tegmental area, and striatum. *J Neurophysiol*, **77**, 863-873.

Cragg, S.J. (2006) Meaningful silences: how dopamine listens to the ACh pause. *Trends Neurosci*, **29**, 125-131.

Cragg, S.J., Baufreton, J., Xue, Y., Bolam, J.P. & Bevan, M.D. (2004) Synaptic release of dopamine in the subthalamic nucleus. *Eur J Neurosci*, **20**, 1788-1802.

Dautan, D., Huerta-Ocampo, I., Witten, I.B., Deisseroth, K., Bolam, J.P., Gerdjikov, T. & Mena-Segovia, J. (2014) A major external source of cholinergic innervation of the striatum and nucleus accumbens originates in the brainstem. *J Neurosci*, **34**, 4509-4518.

Del Campo, N., Chamberlain, S.R., Sahakian, B.J. & Robbins, T.W. (2011) The roles of dopamine and noradrenaline in the pathophysiology and treatment of attention-deficit/hyperactivity disorder. *Biol Psychiatry*, **69**, e145-157.

DeLong, M.R. (1990) Primate models of movement disorders of basal ganglia origin. *Trends Neurosci*, **13**, 281-285.

Deniau, J.M., Hammond, C., Riszk, A. & Feger, J. (1978) Electrophysiological properties of identified output neurons of the rat substantia nigra (pars compacta and pars reticulata): evidences for the existence of branched neurons. *Exp Brain Res*, **32**, 409-422.

Deniau, J.M., Menetrey, A. & Charpier, S. (1996) The lamellar organization of the rat substantia nigra pars reticulata: segregated patterns of striatal afferents and relationship to the topography of corticostriatal projections. *Neuroscience*, **73**, 761-781.

Denys, D., Zohar, J. & Westenberg, H.G. (2004) The role of dopamine in obsessive-compulsive disorder: preclinical and clinical evidence. *J Clin Psychiatry*, **65 Suppl 14**, 11-17.

DiFiglia, M. & Rafols, J.A. (1988) Synaptic organization of the globus pallidus. *J Electron Microsc Tech*, **10**, 247-263.

Dimova, R., Vuillet, J., Nieoullon, A. & Kerkerian-Le Goff, L. (1993) Ultrastructural features of the choline acetyltransferase-containing neurons and relationships with nigral dopaminergic and cortical afferent pathways in the rat striatum. *Neuroscience*, **53**, 1059-1071.

Ding, J., Peterson, J.D. & Surmeier, D.J. (2008) Corticostriatal and thalamostriatal synapses have distinctive properties. *J Neurosci*, **28**, 6483-6492.

Doig, N.M., Magill, P.J., Apicella, P., Bolam, J.P. & Sharott, A. (2014) Cortical and thalamic excitation mediate the multiphasic responses of striatal cholinergic interneurons to motivationally salient stimuli. *J Neurosci*, **34**, 3101-3117.

Doig, N.M., Moss, J. & Bolam, J.P. (2010) Cortical and thalamic innervation of direct and indirect pathway medium-sized spiny neurons in mouse striatum. *J Neurosci*, **30**, 14610-14618.

Dupuis, J.P., Feyder, M., Miguelez, C., Garcia, L., Morin, S., Choquet, D., Hosy, E., Bezard, E., Fisone, G., Bioulac, B.H. & Baufreton, J. (2013) Dopamine-dependent long-term depression at subthalamo-nigral synapses is lost in experimental parkinsonism. *J Neurosci*, **33**, 14331-14341.

Eagle, D.M. & Baunez, C. (2010) Is there an inhibitory-response-control system in the rat? Evidence from anatomical and pharmacological studies of behavioral inhibition. *Neurosci Biobehav Rev*, **34**, 50-72.

Ellender, T.J., Harwood, J., Kosillo, P., Capogna, M. & Bolam, J.P. (2013) Heterogeneous properties of central lateral and parafascicular thalamic synapses in the striatum. *J Physiol*, **591**, 257-272.

Ellender, T.J., Huerta-Ocampo, I., Deisseroth, K., Capogna, M. & Bolam, J.P. (2011) Differential modulation of excitatory and inhibitory striatal synaptic transmission by histamine. *J Neurosci*, **31**, 15340-15351.

Espinosa-Parrilla, J.F., Baunez, C. & Apicella, P. (2013) Linking reward processing to behavioral output: motor and motivational integration in the primate subthalamic nucleus. *Front Comput Neurosci*, **7**, 175.

Fearnley, J.M. & Lees, A.J. (1991) Ageing and Parkinson's disease: substantia nigra regional selectivity. *Brain*, **114 (Pt 5)**, 2283-2301.

Feger, J., Bevan, M. & Crossman, A.R. (1994) The projections from the parafascicular thalamic nucleus to the subthalamic nucleus and the striatum arise from separate neuronal populations: a comparison with the corticostriatal and corticosubthalamic efferents in a retrograde fluorescent double-labelling study. *Neuroscience*, **60**, 125-132.

Ferrucci, M., Giorgi, F.S., Bartalucci, A., Busceti, C.L. & Fornai, F. (2013) The effects of locus coeruleus and norepinephrine in methamphetamine toxicity. *Curr Neuropharmacol*, **11**, 80-94.

Fink, A.J., Croce, K.R., Huang, Z.J., Abbott, L.F., Jessell, T.M. & Azim, E. (2014) Presynaptic inhibition of spinal sensory feedback ensures smooth movement. *Nature*, **509**, 43-48.

Florio, T., Capozzo, A., Puglielli, E., Pupillo, R., Pizzuti, G. & Scarnati, E. (1999) The function of the pedunculopontine nucleus in the preparation and execution of an externally-cued bar pressing task in the rat. *Behav Brain Res*, **104**, 95-104.

Freeze, B.S., Kravitz, A.V., Hammack, N., Berke, J.D. & Kreitzer, A.C. (2013) Control of basal ganglia output by direct and indirect pathway projection neurons. *J Neurosci*, **33**, 18531-18539.

Fremeau, R.T., Jr., Troyer, M.D., Pahner, I., Nygaard, G.O., Tran, C.H., Reimer, R.J., Bellocchio, E.E., Fortin, D., Storm-Mathisen, J. & Edwards, R.H. (2001) The expression of vesicular glutamate transporters defines two classes of excitatory synapse. *Neuron*, **31**, 247-260.

Fremeau, R.T., Jr., Voglmaier, S., Seal, R.P. & Edwards, R.H. (2004) VGLUTs define subsets of excitatory neurons and suggest novel roles for glutamate. *Trends Neurosci*, **27**, 98-103.

Futami, T., Takakusaki, K. & Kitai, S.T. (1995) Glutamatergic and cholinergic inputs from the pedunculopontine tegmental nucleus to dopamine neurons in the substantia nigra pars compacta. *Neurosci Res*, **21**, 331-342.

Galvan, A., Hu, X., Rommelfanger, K.S., Pare, J.F., Khan, Z.U., Smith, Y. & Wichmann, T. (2014) Localization and function of dopamine receptors in the subthalamic nucleus of normal and parkinsonian monkeys. *J Neurophysiol*, **112**, 467-479.

Gauthier, J., Parent, M., Levesque, M. & Parent, A. (1999) The axonal arborization of single nigrostriatal neurons in rats. *Brain Res*, **834**, 228-232.

Gerfen, C.R. (1992) The neostriatal mosaic: multiple levels of compartmental organization. *Trends Neurosci*, **15**, 133-139.

Gerfen, C.R., Herkenham, M. & Thibault, J. (1987) The neostriatal mosaic: II. Patch- and matrix-directed mesostriatal dopaminergic and non-dopaminergic systems. *J Neurosci*, **7**, 3915-3934.

Goldberg, J.A. & Reynolds, J.N. (2011) Spontaneous firing and evoked pauses in the tonically active cholinergic interneurons of the striatum. *Neuroscience*, **198**, 27-43.

Gonzales, K.K., Pare, J.F., Wichmann, T. & Smith, Y. (2013) GABAergic inputs from direct and indirect striatal projection neurons onto cholinergic interneurons in the primate putamen. *J Comp Neurol*, **521**, 2502-2522.

Gonzalez-Hernandez, T., Barroso-Chinea, P., Acevedo, A., Salido, E. & Rodriguez, M. (2001) Colocalization of tyrosine hydroxylase and GAD65 mRNA in mesostriatal neurons. *Eur J Neurosci*, **13**, 57-67.

Goodchild, R.E., Grundmann, K. & Pisani, A. (2013) New genetic insights highlight 'old' ideas on motor dysfunction in dystonia. *Trends Neurosci*, **36**, 717-725.

Grace, A.A. & Bunney, B.S. (1984a) The control of firing pattern in nigral dopamine neurons: burst firing. *J Neurosci*, **4**, 2877-2890.

Grace, A.A. & Bunney, B.S. (1984b) The control of firing pattern in nigral dopamine neurons: single spike firing. *J Neurosci*, **4**, 2866-2876.

Gras, C., Herzog, E., Bellenchi, G.C., Bernard, V., Ravassard, P., Pohl, M., Gasnier, B., Giros, B. & El Mestikawy, S. (2002) A third vesicular glutamate transporter expressed by cholinergic and serotoninergic neurons. *J Neurosci*, **22**, 5442-5451.

Graybiel, A.M. (1995) Building action repertoires: memory and learning functions of the basal ganglia. *Curr Opin Neurobiol*, **5**, 733-741.

Groenewegen, H.J. (2003) The basal ganglia and motor control. *Neural Plast*, **10**, 107-120.

Hagiwara, A., Fukazawa, Y., Deguchi-Tawarada, M., Ohtsuka, T. & Shigemoto, R. (2005) Differential distribution of release-related proteins in the hippocampal CA3 area as revealed by freeze-fracture replica labeling. *J Comp Neurol*, **489**, 195-216.

Hammond, C., Rouzaire-Dubois, B., Feger, J., Jackson, A. & Crossman, A.R. (1983) Anatomical and electrophysiological studies on the reciprocal projections between the subthalamic nucleus and nucleus tegmenti pedunculopontinus in the rat. *Neuroscience*, **9**, 41-52.

Hashemi, P., Dankoski, E.C., Wood, K.M., Ambrose, R.E. & Wightman, R.M. (2011) In vivo electrochemical evidence for simultaneous 5-HT and histamine release in the rat substantia nigra pars reticulata following medial forebrain bundle stimulation. *J Neurochem*, **118**, 749-759.

Hattori, T., Fibiger, H.C. & McGeer, P.L. (1975) Demonstration of a pallido-nigral projection innervating dopaminergic neurons. *J Comp Neurol*, **162**, 487-504.

Henny, P., Brown, M.T., Northrop, A., Faunes, M., Ungless, M.A., Magill, P.J. & Bolam, J.P. (2012) Structural correlates of heterogeneous in vivo activity of midbrain dopaminergic neurons. *Nat Neurosci*, **15**, 613-619.

Herzog, E., Bellenchi, G.C., Gras, C., Bernard, V., Ravassard, P., Bedet, C., Gasnier, B., Giros, B. & El Mestikawy, S. (2001) The existence of a second vesicular glutamate transporter specifies subpopulations of glutamatergic neurons. *J Neurosci*, **21**, RC181.

Herzog, E., Gilchrist, J., Gras, C., Muzerelle, A., Ravassard, P., Giros, B., Gaspar, P. & El Mestikawy, S. (2004) Localization of VGLUT3, the vesicular glutamate transporter type 3, in the rat brain. *Neuroscience*, **123**, 983-1002.

Hikosaka, O., Kim, H.F., Yasuda, M. & Yamamoto, S. (2014) Basal ganglia circuits for reward value-guided behavior. *Annu Rev Neurosci*, **37**, 289-306.

Hirsch, E.C., Graybiel, A.M. & Agid, Y. (1989) Selective vulnerability of pigmented dopaminergic neurons in Parkinson's disease. *Acta Neurol Scand Suppl*, **126**, 19-22.

Holderith, N., Lorincz, A., Katona, G., Rozsa, B., Kulik, A., Watanabe, M. & Nusser, Z. (2012) Release probability of hippocampal glutamatergic terminals scales with the size of the active zone. *Nat Neurosci*, **15**, 988-997.

Holt, A.B. & Netoff, T.I. (2014) Origins and suppression of oscillations in a computational model of Parkinson's disease. *J Comput Neurosci*, Advance online publication. doi: 10.1007/s10827-10014-10523-10827.

Hopkins, D.A. & Niessen, L.W. (1976) Substantia nigra projections to the reticular formation, superior colliculus and central gray in the rat, cat and monkey. *Neurosci Lett*, **2**, 253-259.

Hornykiewicz, O. (1973) Dopamine in the basal ganglia. Its role and therapeutic implications (including the clinical use of L-DOPA). *Br Med Bull*, **29**, 172-178.

Ibanez-Sandoval, O., Tecuapetla, F., Unal, B., Shah, F., Koos, T. & Tepper, J.M. (2011) A novel functionally distinct subtype of striatal neuropeptide Y interneuron. *J Neurosci*, **31**, 16757-16769.

Inglis, W.L., Olmstead, M.C. & Robbins, T.W. (2000) Pedunculopontine tegmental nucleus lesions impair stimulus--reward learning in autoshaping and conditioned reinforcement paradigms. *Behav Neurosci*, **114**, 285-294.

Jackson, A. & Crossman, A.R. (1983) Nucleus tegmenti pedunculopontinus: efferent connections with special reference to the basal ganglia, studied in the rat by anterograde and retrograde transport of horseradish peroxidase. *Neuroscience*, **10**, 725-765.

Jaeger, D. & Kita, H. (2011) Functional connectivity and integrative properties of globus pallidus neurons. *Neuroscience*, **198**, 44-53.

Joel, D. & Weiner, I. (1997) The connections of the primate subthalamic nucleus: indirect pathways and the open-interconnected scheme of basal ganglia-thalamocortical circuitry. *Brain Res Brain Res Rev*, **23**, 62-78.

Juraska, J.M., Wilson, C.J. & Groves, P.M. (1977) The substantia nigra of the rat: a Golgi study. *J Comp Neurol*, **172**, 585-600.

Kanazawa, I., Marshall, G.R. & Kelly, J.S. (1976) Afferents to the rat substantia nigra studied with horseradish peroxidase, with special reference to fibres from the subthalamic nucleus. *Brain Res*, **115**, 485-491.

Kanbar, R., Depuy, S.D., West, G.H., Stornetta, R.L. & Guyenet, P.G. (2011) Regulation of visceral sympathetic tone by A5 noradrenergic neurons in rodents. *J Physiol*, **589**, 903-917.

Kaneko, T. & Fujiyama, F. (2002) Complementary distribution of vesicular glutamate transporters in the central nervous system. *Neurosci Res*, **42**, 243-250.

Kapur, S. & Mann, J.J. (1992) Role of the dopaminergic system in depression. *Biol Psychiatry*, **32**, 1-17.

Kenny, P.J., Voren, G. & Johnson, P.M. (2013) Dopamine D2 receptors and striatopallidal transmission in addiction and obesity. *Curr Opin Neurobiol*, **23**, 535-538.

Kim, B.G., Shin, D.H., Jeon, G.S., Seo, J.H., Kim, Y.W., Jeon, B.S. & Cho, S.S. (2000) Relative sparing of calretinin containing neurons in the substantia nigra of 6-OHDA treated rat parkinsonian model. *Brain Res*, **855**, 162-165.

Kita, H., Chang, H.T. & Kitai, S.T. (1983) The morphology of intracellularly labeled rat subthalamic neurons: a light microscopic analysis. *J Comp Neurol*, **215**, 245-257.

Kita, H. & Kitai, S.T. (1987) Efferent projections of the subthalamic nucleus in the rat: light and electron microscopic analysis with the PHA-L method. *J Comp Neurol*, **260**, 435-452.

Kita, H. & Kitai, S.T. (1994) The morphology of globus pallidus projection neurons in the rat: an intracellular staining study. *Brain Res*, **636**, 308-319.

Kita, H., Kosaka, T. & Heizmann, C.W. (1990) Parvalbumin-immunoreactive neurons in the rat neostriatum: a light and electron microscopic study. *Brain Res*, **536**, 1-15.

Kitai, S.T. & Kita, H. (1987) *Anatomy and Physiology of the Subthalamic Nucleus: a driving force of the basal ganglia*. NY: Plenum, New York.

Kontis, D. & Theochari, E. (2012) Dopamine in anorexia nervosa: a systematic review. *Behav Pharmacol*, **23**, 496-515.

Kornhuber, J., Kim, J.S., Kornhuber, M.E. & Kornhuber, H.H. (1984) The cortico-nigral projection: reduced glutamate content in the substantia nigra following frontal cortex ablation in the rat. *Brain Res*, **322**, 124-126.

Koshimizu, Y., Fujiyama, F., Nakamura, K.C., Furuta, T. & Kaneko, T. (2013) Quantitative analysis of axon bouton distribution of subthalamic nucleus neurons in the rat by single neuron visualization with a viral vector. *J Comp Neurol*, **521**, 2125-2146.

Kubota, Y., Inagaki, S., Kito, S., Shimada, S., Okayama, T., Hatanaka, H., Pelletier, G., Takagi, H. & Tohyama, M. (1988) Neuropeptide Y-immunoreactive neurons receive synaptic inputs from dopaminergic axon terminals in the rat neostriatum. *Brain Res*, **458**, 389-393.

Kumar, A., Cardanobile, S., Rotter, S. & Aertsen, A. (2011) The role of inhibition in generating and controlling Parkinson's disease oscillations in the basal ganglia. *Front Syst Neurosci*, **5**, 86.

Lapper, S.R. & Bolam, J.P. (1992) Input from the frontal cortex and the parafascicular nucleus to cholinergic interneurons in the dorsal striatum of the rat. *Neuroscience*, **51**, 533-545.

Lee, C.R. & Tepper, J.M. (2007) Morphological and physiological properties of parvalbumin- and calretinin-containing gamma-aminobutyric acidergic neurons in the substantia nigra. *J Comp Neurol*, **500**, 958-972.

Leisman, G., Braun-Benjamin, O. & Melillo, R. (2014) Cognitive-motor interactions of the basal ganglia in development. *Front Syst Neurosci*, **8**, 16.

Levesque, J.C. & Parent, A. (2005) GABAergic interneurons in human subthalamic nucleus. *Mov Disord*, **20**, 574-584.

Liang, C.L., Sinton, C.M. & German, D.C. (1996) Midbrain dopaminergic neurons in the mouse: co-localization with calbindin-D28K and calretinin. *Neuroscience*, **75**, 523-533.

Little, S. & Brown, P. (2014) The functional role of beta oscillations in Parkinson's disease. *Parkinsonism Relat Disord*, **20 Suppl 1**, S44-48.

Lovinger, D.M. (2010) Neurotransmitter roles in synaptic modulation, plasticity and learning in the dorsal striatum. *Neuropharmacology*, **58**, 951-961.

Magee, J.C. (2000) Dendritic integration of excitatory synaptic input. *Nat Rev Neurosci*, **1**, 181-190.

Mallet, N., Micklem, B.R., Henny, P., Brown, M.T., Williams, C., Bolam, J.P., Nakamura, K.C. & Magill, P.J. (2012) Dichotomous organization of the external globus pallidus. *Neuron*, **74**, 1075-1086.

Mallet, N., Pogosyan, A., Marton, L.F., Bolam, J.P., Brown, P. & Magill, P.J. (2008) Parkinsonian beta oscillations in the external globus pallidus and their relationship with subthalamic nucleus activity. *J Neurosci*, **28**, 14245-14258.

Marani, E., Heida, T., Lakke, E.A. & Usunoff, K.G. (2008) The subthalamic nucleus. Part I: development, cytology, topography and connections. *Adv Anat Embryol Cell Biol*, **198**, 1-113, vii.

Marceglia, S., Fumagalli, M. & Priori, A. (2011) What neurophysiological recordings tell us about cognitive and behavioral functions of the human subthalamic nucleus. *Expert Rev Neurother*, **11**, 139-149.

Marinelli, M. & McCutcheon, J.E. (2014) Heterogeneity of dopamine neuron activity across traits and states. *Neuroscience*, Advance online publication. doi: 10.1016/j.neuroscience.2014.1007.1034.

Mastro, K.J., Bouchard, R.S., Holt, H.A. & Gittis, A.H. (2014) Transgenic mouse lines subdivide external segment of the globus pallidus (GPe) neurons and reveal distinct GPe output pathways. *J Neurosci*, **34**, 2087-2099.

Matsuda, W., Furuta, T., Nakamura, K.C., Hioki, H., Fujiyama, F., Arai, R. & Kaneko, T. (2009) Single nigrostriatal dopaminergic neurons form widely spread and highly dense axonal arborizations in the neostriatum. *J Neurosci*, **29**, 444-453.

McConnell, G.C., So, R.Q., Hilliard, J.D., Lopomo, P. & Grill, W.M. (2012) Effective deep brain stimulation suppresses low-frequency network oscillations in the basal ganglia by regularizing neural firing patterns. *J Neurosci*, **32**, 15657-15668.

McIntyre, C.C., Savasta, M., Kerkerian-Le Goff, L. & Vitek, J.L. (2004) Uncovering the mechanism(s) of action of deep brain stimulation: activation, inhibition, or both. *Clin Neurophysiol*, **115**, 1239-1248.

Mena-Segovia, J., Sims, H.M., Magill, P.J. & Bolam, J.P. (2008) Cholinergic brainstem neurons modulate cortical gamma activity during slow oscillations. *J Physiol*, **586**, 2947-2960.

Meyer, D., Bonhoeffer, T. & Scheuss, V. (2014) Balance and stability of synaptic structures during synaptic plasticity. *Neuron*, **82**, 430-443.

Mink, J.W. (1996) The basal ganglia: focused selection and inhibition of competing motor programs. *Prog Neurobiol*, **50**, 381-425.

Mirenowicz, J. & Schultz, W. (1996) Preferential activation of midbrain dopamine neurons by appetitive rather than aversive stimuli. *Nature*, **379**, 449-451.

Moechars, D., Weston, M.C., Leo, S., Callaerts-Vegh, Z., Goris, I., Daneels, G., Buist, A., Cik, M., van der Spek, P., Kass, S., Meert, T., D'Hooge, R., Rosenmund, C. & Hampson, R.M. (2006) Vesicular glutamate transporter VGLUT2 expression levels control quantal size and neuropathic pain. *J Neurosci*, **26**, 12055-12066.

Mori, S., Takino, T., Yamada, H. & Sano, Y. (1985) Immunohistochemical demonstration of serotonin nerve fibers in the subthalamic nucleus of the rat, cat and monkey. *Neurosci Lett*, **62**, 305-309.

Moss, J. & Bolam, J.P. (2008) A dopaminergic axon lattice in the striatum and its relationship with cortical and thalamic terminals. *J Neurosci*, **28**, 11221-11230.

Mouroux, M., Hassani, O.K. & Feger, J. (1995) Electrophysiological study of the excitatory parafascicular projection to the subthalamic nucleus and evidence for ipsi- and contralateral controls. *Neuroscience*, **67**, 399-407.

Murthy, V.N., Schikorski, T., Stevens, C.F. & Zhu, Y. (2001) Inactivity produces increases in neurotransmitter release and synapse size. *Neuron*, **32**, 673-682.

Nair-Roberts, R.G., Chatelain-Badie, S.D., Benson, E., White-Cooper, H., Bolam, J.P. & Ungless, M.A. (2008) Stereological estimates of dopaminergic, GABAergic and glutamatergic neurons in the ventral tegmental area, substantia nigra and retrorubral field in the rat. *Neuroscience*, **152**, 1024-1031.

Naito, A. & Kita, H. (1994) The cortico-nigral projection in the rat: an anterograde tracing study with biotinylated dextran amine. *Brain Res*, **637**, 317-322.

Nakamura, Y., Otake, K. & Tokuno, H. (2006) The parafascicular nucleus relays spinal inputs to the striatum: an electron microscope study in the rat. *Neurosci Res*, **56**, 73-79.

Nambu, A., Tokuno, H., Hamada, I., Kita, H., Imanishi, M., Akazawa, T., Ikeuchi, Y. & Hasegawa, N. (2000) Excitatory cortical inputs to pallidal neurons via the subthalamic nucleus in the monkey. *J Neurophysiol*, **84**, 289-300.

Nambu, A., Tokuno, H. & Takada, M. (2002) Functional significance of the cortico-subthalamo-pallidal 'hyperdirect' pathway. *Neurosci Res*, **43**, 111-117.

Nelson, A.B., Hammack, N., Yang, C.F., Shah, N.M., Seal, R.P. & Kreitzer, A.C. (2014) Striatal cholinergic interneurons drive GABA release from dopamine terminals. *Neuron*, **82**, 63-70.

Neuhoff, H., Neu, A., Liss, B. & Roeper, J. (2002) I(h) channels contribute to the different functional properties of identified dopaminergic subpopulations in the midbrain. *J Neurosci*, **22**, 1290-1302.

Nevado-Holgado, A.J., Mallet, N., Magill, P.J. & Bogacz, R. (2014) Effective connectivity of the subthalamic nucleus-globus pallidus network during Parkinsonian oscillations. *J Physiol*, **592**, 1429-1455.

Nikolaus, S., Antke, C., Beu, M. & Muller, H.W. (2010) Cortical GABA, striatal dopamine and midbrain serotonin as the key players in compulsive and anxiety disorders--results from in vivo imaging studies. *Rev Neurosci*, **21**, 119-139.

Nisell, M., Nomikos, G.G. & Svensson, T.H. (1995) Nicotine dependence, midbrain dopamine systems and psychiatric disorders. *Pharmacol Toxicol*, **76**, 157-162.

Nitsch, C., Mews, K., Wagner, A. & Hassler, R. (1984) Effects of frontal motor cortex ablation on the ultrastructure of cat substantia nigra. *Acta Anat (Basel)*, **119**, 193-202.

Omelchenko, N. & Sesack, S.R. (2006) Cholinergic axons in the rat ventral tegmental area synapse preferentially onto mesoaccumbens dopamine neurons. *J Comp Neurol*, **494**, 863-875.

Oorschot, D.E. (1996) Total number of neurons in the neostriatal, pallidal, subthalamic, and substantia nigral nuclei of the rat basal ganglia: a stereological study using the cavalieri and optical disector methods. *J Comp Neurol*, **366**, 580-599.

Pan, W.X. & Hyland, B.I. (2005) Pedunculopontine tegmental nucleus controls conditioned responses of midbrain dopamine neurons in behaving rats. *J Neurosci*, **25**, 4725-4732.

Parent, A. & De Bellefeuille, L. (1982) Organization of efferent projections from the internal segment of globus pallidus in primate as revealed by fluorescence retrograde labeling method. *Brain Res*, **245**, 201-213.

Parent, M., Wallman, M.J. & Descarries, L. (2010) Distribution and ultrastructural features of the serotonin innervation in rat and squirrel monkey subthalamic nucleus. *Eur J Neurosci*, **31**, 1233-1242.

Parent, M., Wallman, M.J., Gagnon, D. & Parent, A. (2011) Serotonin innervation of basal ganglia in monkeys and humans. *J Chem Neuroanat*, **41**, 256-265.

Pauls, D.L., Abramovitch, A., Rauch, S.L. & Geller, D.A. (2014) Obsessive-compulsive disorder: an integrative genetic and neurobiological perspective. *Nat Rev Neurosci*, **15**, 410-424.

Paxinos, G. & Watson, C. (2007) *The rat brain in stereotaxic coordinates*. Academic Press/Elsevier, Amsterdam ; Boston ;.

Pearson, J.C., Norris, J.R. & Phelps, C.H. (1985) Subclassification of neurons in the subthalamic nucleus of the lesser bushbaby (Galago senegalensis): a quantitative Golgi study using principal components analysis. *J Comp Neurol*, **238**, 323-339.

Petryszyn, S., Beaulieu, J.M., Parent, A. & Parent, M. (2014) Distribution and morphological characteristics of striatal interneurons expressing calretinin in mice: A comparison with human and nonhuman primates. *J Chem Neuroanat*, **59-60C**, 51-61.

Phelps, P.E., Houser, C.R. & Vaughn, J.E. (1985) Immunocytochemical localization of choline acetyltransferase within the rat neostriatum: a correlated light and electron microscopic study of cholinergic neurons and synapses. *J Comp Neurol*, **238**, 286-307.

Plenz, D. & Kital, S.T. (1999) A basal ganglia pacemaker formed by the subthalamic nucleus and external globus pallidus. *Nature*, **400**, 677-682.

Politis, M., Wu, K., Loane, C., Brooks, D.J., Kiferle, L., Turkheimer, F.E., Bain, P., Molloy, S. & Piccini, P. (2014) Serotonergic mechanisms responsible for levodopa-induced dyskinesias in Parkinson's disease patients. *J Clin Invest*, **124**, 1340-1349.

Prensa, L. & Parent, A. (2001) The nigrostriatal pathway in the rat: A single-axon study of the relationship between dorsal and ventral tier nigral neurons and the striosome/matrix striatal compartments. *J Neurosci*, **21**, 7247-7260.

Pringsheim, T., Jette, N., Frolkis, A. & Steeves, T.D. (2014) The prevalence of Parkinson's disease: A systematic review and meta-analysis. *Mov Disord*.

Rafols, J.A. & Fox, C.A. (1976) The neurons in the primate subthalamic nucleus: a Golgi and electron microscopic study. *J Comp Neurol*, **168**, 75-111.

Raju, D.V., Shah, D.J., Wright, T.M., Hall, R.A. & Smith, Y. (2006) Differential synaptology of vGluT2-containing thalamostriatal afferents between the patch and matrix compartments in rats. *J Comp Neurol*, **499**, 231-243.

Ramanathan, S., Hanley, J.J., Deniau, J.M. & Bolam, J.P. (2002) Synaptic convergence of motor and somatosensory cortical afferents onto GABAergic interneurons in the rat striatum. *J Neurosci*, **22**, 8158-8169.

Retailleau, A., Etienne, S., Guthrie, M. & Boraud, T. (2012) Where is my reward and how do I get it? Interaction between the hippocampus and the basal ganglia during spatial learning. *J Physiol Paris*, **106**, 72-80.

Ricardo, J.A. (1980) Efferent connections of the subthalamic region in the rat. I. The subthalamic nucleus of Luys. *Brain Res*, **202**, 257-271.

Rico, A.J., Barroso-Chinea, P., Conte-Perales, L., Roda, E., Gomez-Bautista, V., Gendive, M., Obeso, J.A. & Lanciego, J.L. (2010) A direct projection from the subthalamic nucleus to the ventral thalamus in monkeys. *Neurobiol Dis*, **39**, 381-392.

Sadek, A.R., Magill, P.J. & Bolam, J.P. (2007) A single-cell analysis of intrinsic connectivity in the rat globus pallidus. *J Neurosci*, **27**, 6352-6362.

Sadikot, A.F., Parent, A. & Francois, C. (1992) Efferent connections of the centromedian and parafascicular thalamic nuclei in the squirrel monkey: a PHA-L study of subcortical projections. *J Comp Neurol*, **315**, 137-159.

Sakai, S.T. (1988) Corticonigral projections from area 6 in the raccoon. *Exp Brain Res*, **73**, 498-504.

Sammut, S., Park, D.J. & West, A.R. (2007) Frontal cortical afferents facilitate striatal nitric oxide transmission in vivo via a NMDA receptor and neuronal NOS-dependent mechanism. *J Neurochem*, **103**, 1145-1156.

Schikorski, T. & Stevens, C.F. (1997) Quantitative ultrastructural analysis of hippocampal excitatory synapses. *J Neurosci*, **17**, 5858-5867.

Schikorski, T. & Stevens, C.F. (1999) Quantitative fine-structural analysis of olfactory cortical synapses. *Proc Natl Acad Sci U S A*, **96**, 4107-4112.

Schultz, W. (1998) Predictive reward signal of dopamine neurons. *J Neurophysiol*, **80**, 1-27.

Schultz, W. (2007a) Behavioral dopamine signals. *Trends Neurosci*, **30**, 203-210.

Schultz, W. (2007b) Multiple dopamine functions at different time courses. *Annu Rev Neurosci*, **30**, 259-288.

Schultz, W. (2013) Updating dopamine reward signals. *Curr Opin Neurobiol*, **23**, 229-238.

Seguela, P., Watkins, K.C., Geffard, M. & Descarries, L. (1990) Noradrenaline axon terminals in adult rat neocortex: an immunocytochemical analysis in serial thin sections. *Neuroscience*, **35**, 249-264.

Sharott, A., Doig, N.M., Mallet, N. & Magill, P.J. (2012) Relationships between the firing of identified striatal interneurons and spontaneous and driven cortical activities in vivo. *J Neurosci*, **32**, 13221-13236.

Shink, E., Bevan, M.D., Bolam, J.P. & Smith, Y. (1996) The subthalamic nucleus and the external pallidum: two tightly interconnected structures that control the output of the basal ganglia in the monkey. *Neuroscience*, **73**, 335-357.

Sidibe, M., Bevan, M.D., Bolam, J.P. & Smith, Y. (1997) Efferent connections of the internal globus pallidus in the squirrel monkey: I. Topography and synaptic organization of the pallidothalamic projection. *J Comp Neurol*, **382**, 323-347.

Sidibe, M. & Smith, Y. (1999) Thalamic inputs to striatal interneurons in monkeys: synaptic organization and co-localization of calcium binding proteins. *Neuroscience*, **89**, 1189-1208.

Siksou, L., Silm, K., Biesemann, C., Nehring, R.B., Wojcik, S.M., Triller, A., El Mestikawy, S., Marty, S. & Herzog, E. (2013) A role for vesicular glutamate transporter 1 in synaptic vesicle clustering and mobility. *Eur J Neurosci*, **37**, 1631-1642.

Smith, Y., Bevan, M.D., Shink, E. & Bolam, J.P. (1998) Microcircuitry of the direct and indirect pathways of the basal ganglia. *Neuroscience*, **86**, 353-387.

Smith, Y. & Bolam, J.P. (1989) Neurons of the substantia nigra reticulata receive a dense GABA-containing input from the globus pallidus in the rat. *Brain Res*, **493**, 160-167.

Smith, Y. & Bolam, J.P. (1990) The output neurones and the dopaminergic neurones of the substantia nigra receive a GABA-containing input from the globus pallidus in the rat. *J Comp Neurol*, **296**, 47-64.

Smith, Y. & Bolam, J.P. (1991) Convergence of synaptic inputs from the striatum and the globus pallidus onto identified nigrocollicular cells in the rat: a double anterograde labelling study. *Neuroscience*, **44**, 45-73.

Smith, Y., Bolam, J.P. & Von Krosigk, M. (1990a) Topographical and Synaptic Organization of the GABA-Containing Pallidosubthalamic Projection in the Rat. *Eur J Neurosci*, **2**, 500-511.

Smith, Y., Galvan, A., Ellender, T.J., Doig, N., Villalba, R.M., Huerta-Ocampo, I., Wichmann, T. & Bolam, J.P. (2014) The thalamostriatal system in normal and diseased states. *Front Syst Neurosci*, **8**, 5.

Smith, Y., Hazrati, L.N. & Parent, A. (1990b) Efferent projections of the subthalamic nucleus in the squirrel monkey as studied by the PHA-L anterograde tracing method. *J Comp Neurol*, **294**, 306-323.

Smith, Y. & Parent, A. (1988) Neurons of the subthalamic nucleus in primates display glutamate but not GABA immunoreactivity. *Brain Res*, **453**, 353-356.

Smith, Y., Raju, D.V., Pare, J.F. & Sidibe, M. (2004) The thalamostriatal system: a highly specific network of the basal ganglia circuitry. *Trends Neurosci*, **27**, 520-527.

Squire, L.R. (2009) *Encyclopedia of neuroscience*. Elsevier/Academic Press, Amsterdam ; Boston.

Sudhof, T.C. (2012) The presynaptic active zone. *Neuron*, **75**, 11-25.

Sugimoto, T., Hattori, T., Mizuno, N., Itoh, K. & Sato, M. (1983) Direct projections from the centre median-parafascicular complex to the subthalamic nucleus in the cat and rat. *J Comp Neurol*, **214**, 209-216.

Surmeier, D.J., Plotkin, J. & Shen, W. (2009) Dopamine and synaptic plasticity in dorsal striatal circuits controlling action selection. *Curr Opin Neurobiol*, **19**, 621-628.

Tachibana, Y., Iwamuro, H., Kita, H., Takada, M. & Nambu, A. (2011) Subthalamo-pallidal interactions underlying parkinsonian neuronal oscillations in the primate basal ganglia. *Eur J Neurosci*, **34**, 1470-1484.

Takakusaki, K., Habaguchi, T., Ohtinata-Sugimoto, J., Saitoh, K. & Sakamoto, T. (2003) Basal ganglia efferents to the brainstem centers controlling postural muscle tone and locomotion: a new concept for understanding motor disorders in basal ganglia dysfunction. *Neuroscience*, **119**, 293-308.

Takamori, S. (2006) VGLUTs: 'exciting' times for glutamatergic research? *Neurosci Res*, **55**, 343-351.

Takamori, S., Rhee, J.S., Rosenmund, C. & Jahn, R. (2000) Identification of a vesicular glutamate transporter that defines a glutamatergic phenotype in neurons. *Nature*, **407**, 189-194.

Takamori, S., Rhee, J.S., Rosenmund, C. & Jahn, R. (2001) Identification of differentiation-associated brain-specific phosphate transporter as a second vesicular glutamate transporter (VGLUT2). *J Neurosci*, **21**, RC182.

Tattersall, T.L., Stratton, P.G., Coyne, T.J., Cook, R., Silberstein, P., Silburn, P.A., Windels, F. & Sah, P. (2014) Imagined gait modulates neuronal network dynamics in the human pedunculopontine nucleus. *Nat Neurosci*, **17**, 449-454.

Tepper, J.M., Tecuapetla, F., Koos, T. & Ibanez-Sandoval, O. (2010) Heterogeneity and diversity of striatal GABAergic interneurons. *Front Neuroanat*, **4**, 150.

Threlfell, S. & Cragg, S.J. (2011) Dopamine signaling in dorsal versus ventral striatum: the dynamic role of cholinergic interneurons. *Front Syst Neurosci*, **5**, 11.

Threlfell, S., Lalic, T., Platt, N.J., Jennings, K.A., Deisseroth, K. & Cragg, S.J. (2012) Striatal dopamine release is triggered by synchronized activity in cholinergic interneurons. *Neuron*, **75**, 58-64.

Trifilieff, P. & Martinez, D. (2014) Imaging addiction: D2 receptors and dopamine signaling in the striatum as biomarkers for impulsivity. *Neuropharmacology*, **76 Pt B**, 498-509.

Tritsch, N.X., Oh, W.J., Gu, C. & Sabatini, B.L. (2014) Midbrain dopamine neurons sustain inhibitory transmission using plasma membrane uptake of GABA, not synthesis. *Elife*, **3**, e01936.

Tseng, H.M., Su, P.C., Liu, H.M., Liou, H.H. & Yen, R.F. (2007) Bilateral subthalamotomy for advanced Parkinson disease. *Surg Neurol*, **68 Suppl 1**, S43-50; discussion S50-41.

Turjanski, N., Lees, A.J. & Brooks, D.J. (1999) Striatal dopaminergic function in restless legs syndrome: 18F-dopa and 11C-raclopride PET studies. *Neurology*, **52**, 932-937.

Unal, B., Ibanez-Sandoval, O., Shah, F., Abercrombie, E.D. & Tepper, J.M. (2011) Distribution of tyrosine hydroxylase-expressing interneurons with respect to anatomical organization of the neostriatum. *Front Syst Neurosci*, **5**, 41.

van der Kooy, D. & Hattori, T. (1980a) Dorsal raphe cells with collateral projections to the caudate-putamen and substantia nigra: a fluorescent retrograde double labeling study in the rat. *Brain Res*, **186**, 1-7.

Van Der Kooy, D. & Hattori, T. (1980b) Single subthalamic nucleus neurons project to both the globus pallidus and substantia nigra in rat. *J Comp Neurol*, **192**, 751-768.

van Schouwenburg, M.R., den Ouden, H.E. & Cools, R. (2013) Selective attentional enhancement and inhibition of fronto-posterior connectivity by the basal ganglia during attention switching. *Cereb. Cortex*, Advance online publication. doi: 10.1093/cercor/bht1345.

Villalba, R.M. & Smith, Y. (2011) Differential structural plasticity of corticostriatal and thalamostriatal axo-spinous synapses in MPTP-treated Parkinsonian monkeys. *J Comp Neurol*, **519**, 989-1005.

Vuillet, J., Dimova, R., Nieoullon, A. & Kerkerian-Le Goff, L. (1992) Ultrastructural relationships between choline acetyltransferase- and neuropeptide y-containing neurons in the rat striatum. *Neuroscience*, **46**, 351-360.

Watabe-Uchida, M., Zhu, L., Ogawa, S.K., Vamanrao, A. & Uchida, N. (2012) Whole-brain mapping of direct inputs to midbrain dopamine neurons. *Neuron*, **74**, 858-873.

Wei, P., Smeyne, R.J., Bao, D., Parris, J. & Morgan, J.I. (2007) Mapping of Cbln1-like immunoreactivity in adult and developing mouse brain and its localization to the endolysosomal compartment of neurons. *Eur J Neurosci*, **26**, 2962-2978.

Wichmann, T., Kliem, M.A. & Soares, J. (2002) Slow oscillatory discharge in the primate basal ganglia. *J Neurophysiol*, **87**, 1145-1148.

Williams, D., Kuhn, A., Kupsch, A., Tijssen, M., van Bruggen, G., Speelman, H., Hotton, G., Loukas, C. & Brown, P. (2005) The relationship between oscillatory activity and motor reaction time in the parkinsonian subthalamic nucleus. *Eur J Neurosci*, **21**, 249-258.

Wilson, C.J. (1988) Cellular mechanisms controlling the strength of synapses. *J Electron Microsc Tech*, **10**, 293-313.

Wilson, C.J. & Bevan, M.D. (2011) Intrinsic dynamics and synaptic inputs control the activity patterns of subthalamic nucleus neurons in health and in Parkinson's disease. *Neuroscience*, **198**, 54-68.

Wilson, C.L., Puntis, M. & Lacey, M.G. (2004) Overwhelmingly asynchronous firing of rat subthalamic nucleus neurones in brain slices provides little evidence for intrinsic interconnectivity. *Neuroscience*, **123**, 187-200.

Wise, R.A. (2004) Dopamine, learning and motivation. *Nat Rev Neurosci*, **5**, 483-494.

Wise, R.A. (2009) Roles for nigrostriatal--not just mesocorticolimbic--dopamine in reward and addiction. *Trends Neurosci*, **32**, 517-524.

Wu, Y. & Parent, A. (2000) Striatal interneurons expressing calretinin, parvalbumin or NADPH-diaphorase: a comparative study in the rat, monkey and human. *Brain Res*, **863**, 182-191.

Yetnikoff, L., Lavezzi, H.N., Reichard, R.A. & Zahm, D.S. (2014) An update on the connections of the ventral mesencephalic dopaminergic complex. *Neuroscience*.

Yung, K.K., Tse, Y.C., Gao, Z.G., Choi, S.Y. & Kwok, F.S. (1998) Localization of GABA transaminase immunoreactivity in the rat substantia nigra pars reticulata. *Neurosci Lett*, **253**, 57-60.

Zavala, B.A., Tan, H., Little, S., Ashkan, K., Hariz, M., Foltynie, T., Zrinzo, L., Zaghloul, K.A. & Brown, P. (2014) Midline frontal cortex low-frequency activity drives subthalamic nucleus oscillations during conflict. *J Neurosci*, **34**, 7322-7333.

Zhang, L., Doyon, W.M., Clark, J.J., Phillips, P.E. & Dani, J.A. (2009) Controls of tonic and phasic dopamine transmission in the dorsal and ventral striatum. *Mol Pharmacol*, **76**, 396-404.

Zigmond, M.J. & Stricker, E.M. (1984) Parkinson's disease: studies with an animal model. *Life Sci*, **35**, 5-18.

Zold, C.L., Kasanetz, F., Pomata, P.E., Belluscio, M.A., Escande, M.V., Galinanes, G.L., Riquelme, L.A. & Murer, M.G. (2012) Striatal gating through up states and oscillations in the basal ganglia: Implications for Parkinson's disease. *J Physiol Paris*, **106**, 40-46.

Zucca, F.A., Basso, E., Cupaioli, F.A., Ferrari, E., Sulzer, D., Casella, L. & Zecca, L. (2014) Neuromelanin of the human substantia nigra: an update. *Neurotox Res*, **25**, 13-23.